Vol. 87, Number 4, Pp. 249–289 31 December 2022

CT STUDY OF THE CRANIAL OSTEOLOGY OF THE GRAY SHORT-TAILED OPOSSUM MONODELPHIS DOMESTICA (WAGNER, 1842) (MARSUPIALIA, DIDELPHIDAE) AND COMMENTS ON THE INTERNAL NASAL SKELETON FLOOR

JOHN R. WIBLE

Curator, Section of Mammals, Carnegie Museum of Natural History 5800 Baum Boulevard, Pittsburgh, Pennsylvania 15206 wiblej@carnegiemnh.org

ABSTRACT

The individual bones of the adult cranium of the gray short-tailed opossum, *Monodelphis domestica* (Wagner, 1842) are described and illustrated in multiple views based on CT scans. The author previously reported on the outer bony surfaces of the skull of *Monodelphis* Burnett, 1830, and the current contribution is a companion piece, paying particular attention to the inner bony surfaces (within the endocranium and nasal cavity) and the facets between individual cranial elements, including the ethmo- and frontoturbinals.

Comments are provided on the internal nasal floor skeleton, which in *M. domestica* includes a fused conglomerate formed by the medial palatine processes of the premaxillae, the vomer, the ethmoid, the presphenoid, and the orbitosphenoids. This conglomerate includes horizontal shelves just dorsal to the hard palate, and occurs widely in marsupials but is currently unknown in monotremes and placentals.

KEY WORDS: ala vomeris, Didelphis marsupialis, Dromiciops, Erinaceus, medial palatine process of premaxilla, Tachyglossus, vomer

INTRODUCTION

In 2003, this author published a bone-by-bone description of the exterior of the skull of the didelphid marsupial Monodelphis Burnett, 1830, based on the Carnegie Museum of Natural History (CM) holdings of the genus. The primary specimen illustrated was CM 52729, which was identified as Monodelphis brevicaudata (Erxleben, 1777). Comparisons were made between M. brevicaudata and other species represented in the CM collection, namely, Monodelphis dimidiata (Wagner, 1847), Monodelphis domestica (Wagner, 1842), and Monodelphis osgoodi Doutt, 1938. The only bone whose internal surface was described was the petrosal, based on isolated elements from Monodelphis sp., CM 5024, and M. brevicaudata, CM 5061. Subsequent revisions of the M. brevicaudata complex (Pavan et al. 2012; Pavan and Voss 2016; Pavan 2019) resulted in the re-identification of some CM Monodelphis. Of the 16 specimens of M. brevicaudata reported by Wible (2003), Pavan and Voss (2016) assigned seven to Monodelphis arlindoi Pavan et al., 2012, including CM 52729, two to Monodelphs glirina (Wagner, 1842), including CM 5061, and two to Monodelphis touan (Shaw, 1800).

Since the publication of Wible (2003), the most substantive additions to our understanding of the cranial morphology of *Monodelphis* are with regard to the nasal cavity, brain endocast, bony labyrinth, and middle-ear structures. Rowe et al. (2005) described the internal nasal skeleton based on a growth series of *M. domestica*, including serially sectioned, cleared and stained, and CT scanned specimens. Theirs represents the definitive work on the adult anatomy and ontogeny of this anatomical region. Freyer (1999), a thesis unknown to Wible (2003), included detail on the ontogeny of the nasal cartilages in *M. domestica*. The results of Rowe et al. (2005) were placed in a broader comparative perspective by Macrini (2012) who

studied the internal nasal skeleton in representatives from 19 of the 20 marsupial families recognized in Wilson and Reeder (2005). Macrini et al. (2007) reported on aspects of the brain, digital endocasts, and the endocranial space in a growth series of *M. domestica* that included dissected frozen and ethanol preserved as well as CT scanned specimens. Sanchéz-Villagra (2002) described the ontogeny of the cerebellar paraflocculus (petrosal lobule) and subarcuate fossa in *M. domestica*. Ekdale (2010) studied the ontogeny of the bony labyrinth in the CT scanned specimens from the growth series reported by Macrini et al. (2007). Lastly, Nummela et al. (2022) reported on the ontogenetic growth trajectories for the middle-ear ossicles, tympanic membrane, and oval window for crania from an aged growth series of *M. domestica*.

Regarding the cranial morphology of other didelphids, as part of his dissertation, Maga (2008) described the cranial osteology of *Didelphis virginiana* Kerr, 1792, from CT scans, segmenting out individual cranial elements. Voss and Jansa (2003, 2009) included numerous cranial characters in their phylogenetic studies of Didelphidae. Regarding the cranial morphology of marsupials more broadly, Beck et al. (2022) have compared craniodental features across a vast array of extinct and extant taxa. Their illustrations and discussions of anatomy are a major new comparative resource.

The current report, a follow-up to Wible (2003), resulted from work conditions imposed during the COVID-19 pandemic, when working from home was mandated. The inspiration was the discovery of an available CT scanned cranium of *M. domestica*, American Museum of Natural History (AMNH) 261241, on MorphoSource.org. The author segmented the bones of the cranium from the CT scans, illustrates them individually, and presents bone-by-bone descriptions. Emphasis is on the surfaces not addressed in Wible (2003), that is, the internal surfaces and

surfaces hidden by other bones. Unusual findings of the internal nasal skeleton in *M. domestica* inspired a broader treatment of this topic in a separate section. This contribution represents a companion piece to Wible (2003). The few extant mammals that have been described in this fashion are primarily from the ranks of domesticated forms, such as cats (Jayne 1898) and dogs (Evans and Christensen 1993).

MATERIALS AND METHODS

The following CT scans were studied:

Monodelphis domestica, AMNH 261241, adult male, collected 14 July 1985 in Porvenir, Luis Calvo, Chiquisaca, Bolivia. The cranium was scanned on the General Electric phoenix v|tome|x s240 at the American Museum of Natural History (AMNH) Microscopy and Imaging Facility (MIF). Eric Delson and the AMNH Department of Mammalogy provided access to these data, the collection of which was funded by AMNH and NYCEP. The files were downloaded from www.MorphoSource.org, Duke University. The CT image series included 1,586 tiff images [https://www.morphosource.org/concern/biological_specimens/0000S5433]. X, Y, and Z spacing is 0.024336 mm.

Didelphis marsupialis Linnaeus, 1758, DU BAA 0164, adult of unreported sex, collected 31 May 1993. The cranium was scanned on the Nikon Metrology XT H 225 ST at the Duke University Shared Materials Instrumentation Facility. Funding was provided by National Science Foundation grants: BCS 1552848 (to D.M. Boyer) and DBI 1458192 (to G.F. Gunnell). The files were downloaded from www. Morphosource.org, Duke University. The CT image series included 1,910 tiff images [https://www.morphosource.org/concern/biological_specimens/0000S5277]. X, Y, and Z spacing is 0.069078 mm.

Dromiciops bozinovici Quintero-Galvis et al., 2022, CM 40621, adult female, collected 16 Feb. 1961 in Parque Nacional, 27 km WNW Angol, Malleco Province, Chile. The cranium was scanned on the 300 kV microfocus directional tube of the GE v|tome|x L300 X-ray CT Scanner at the Center for Quantitative Imaging, The Pennsylvania State University. The CT image series included 1,684 tiff images. X, Y, and Z spacing is 0.017 mm.

Tachyglossus aculeatus (Shaw, 1792), AMNH 154457, adult male, collected 23 June 1948 in Cape York, Queensland, Australia. The cranium was scanned on the Varian Medical Systems (Bio-Imaging Research, Inc) ACTIS CT scanner with FeinFocus X-ray source, The University of Texas High-Resolution X-ray Computed Tomography Facility. The files were downloaded from www. Morphosource.org, Duke University. The CT image series included 693 tiff images [https://www.morphosource.org/media/000167386]. X, Y, and Z spacing is reported at 0.046000 mm, but this is in error as the Z spacing should be different from the X and Y for these scans.

Erinaceus europaeus Linnaeus, 1758, LACM mammals:058376, adult male, collected 18 April 1978 in Alvor Algarve, Alvov, Portugal. The cranium was scanned on the General Electric phoenix nanotom s, General Electric Inspection Technology California. The files were downloaded from www.Morphosource.org, Duke University. The CT image series included 821 tiff images [https://www.morphosource.org/media/000044782]. X, Y, and Z spacing is 0.007885 mm.

Individual cranial bones of *M. domestica*, AMNH 261241, were identified by their sutures with neighboring bones and segmented in Avizo 2020.3 (© FEI SAS a part of Thermo Fisher Scientific). The sole exception concerned some bony structures of the nasal cavity where the premaxillae, ethmoid, ossified nasal septum, presphenoid, and orbitosphenoids comprise a single unit. Segmentation within this unit followed the report on the internal nasal skeleton of *M. domestica* by Rowe et al. (2005) and the CT scans of *D. marsupialis*, DU BAA 0164.

Terminology follows prior works by the author (e.g., Wible 2003, 2008; Wible and Spaulding 2013) with the exception of the internal nasal skeleton. A variety of terms have been applied to the structures of the nasal cavity. Here, I follow Maier (1993) and Smith and Rossie (2008), which are not in total agreement with prior describers of these structures in *M. domestica* (i.e., Rowe et al. 2005; Macrini 2012). Where appropriate, terms are used from the Nomina Anatomica Veterinaria (2017) (abbreviated NAV here).

Institutional Abbreviations

AMNH—Department of Mammalogy, American Museum of Natural History, New York, New York, USA.

CM—Section of Mammals, Carnegie Museum of Natural History, Pittsburgh, Pennsylvania, USA.

DU BAA—Department of Biological Anthropology and Anatomy, Duke University, Durham, North Carolina, USA.

LACM—Natural History Museum, Los Angeles County, Los Angeles, California, USA.

DESCRIPTIONS Overview

Colorized bones of the hemi-cranium of *M. domestica*, AMNH 261241, are shown in various views in Figures 1 to 3. In the medial view (Fig. 1B), most of the internal nasal skeleton (ossified nasal septum, nasoturbinal, maxilloturbinal, five ethmoturbinals, and two frontoturbinals) has been omitted to show the bones forming the walls of the nasal cavity; the exception is the central part of the vomer, which holds the base of the ossified nasal septum and therefore spans the midline. In Figure 3, the jugal has been removed and the zygomatic process of the squamosal has been cut to expose the orbit. Missing from the cranium of AMNH 261241 are the left and right ectotympanics and

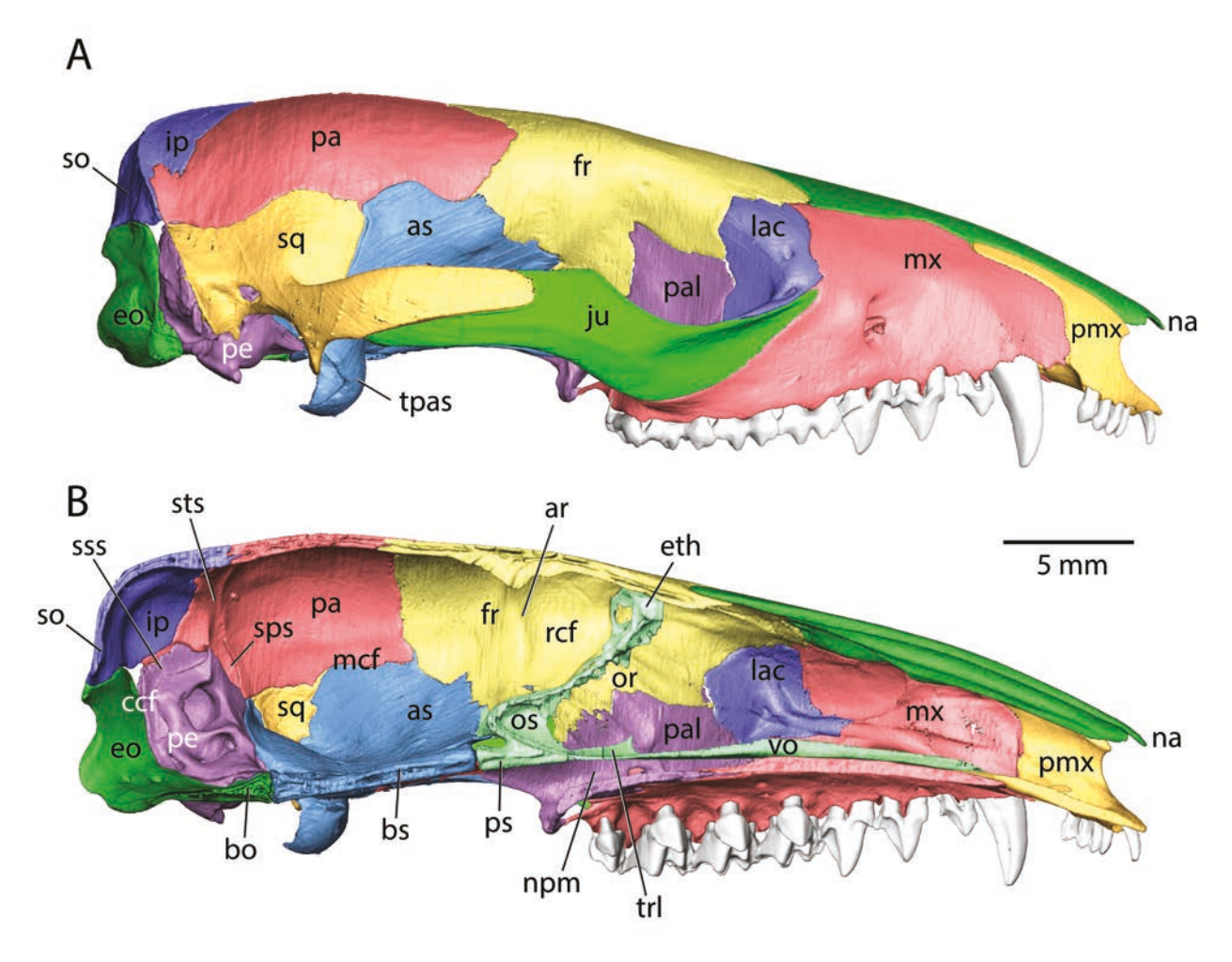


Fig. 1.—Monodelphis domestica, AMNH 261241, isosurface of hemi-cranium rendered from CT scans; anterior to the right. A, right lateral view (left side of specimen reversed); B, left medial view. Turbinals omitted in B. Abbreviations: ar, annular ridge; as, alisphenoid; bo, basioccipital; bs, basisphenoid; ccf, caudal cranial fossa; eo, exoccipital; ethm, ethmoid; fr, frontal; ip, interparietal; ju, jugal; lac, lacrimal; mcf, middle cranial fossa; mx, maxilla; na, nasal; npm, nasopharyngeal meatus; or, olfactory recess; os, orbitosphenoid; pa, parietal; pal, palatine; pe, petrosal; pmx, premaxilla; ps, presphenoid; rcf, rostral cranial fossa; so, supraoccipital; sq, squamosal; sss, sulcus for sigmoid sinus; sts, sulcus for transverse sinus; tpas, tympanic process of alisphenoid; trl, transverse lamina; vo, vomer.

the left malleus; the remaining auditory ossicles have been omitted from these overview figures and are not treated here (see Wible 2003 for comments and references on the ectotympanic and auditory ossicles in *Monodelphis*). Major damage to the specimen concerns the left and right pterygoids, which preserve only their horizontal portion on the basicranium; missing are the entopterygoid crests, which contribute to the lateral walls of the basipharyngeal passage. In the descriptions of the individual bones, the reader will be directed to Figures 1–3 in order to place those bones in their broader context. Accompanying the bone descriptions are illustrations of the isolated bones in various views. In these illustrations, facets and crests for neighboring bones are delineated by white lines.

As this report emphasizes the inner aspects of the cranial bones, I point out terms used here for common spaces within the cranium. There are two large spaces, the cranial cavity housing the brain and the nasal cavity housing the internal nasal skeleton. The cranial cavity is divided into three parts (Fig. 1B): rostral, middle, and caudal cranial fossae, roughly corresponding to fore-, mid-, and hindbrains. The rostral and middle cranial fossae are delimited by the annular ridge on the frontal, and the middle and caudal cranial fossae are delimited by the sulcus for the transverse sinus. The nasal cavity includes an olfactory recess (recessus ethmoturbinalis of Maier 1993; recessus cupularis of Rossie 2006) anterior to the ethmoid, which houses the turbinals. Following the terminology of Maier

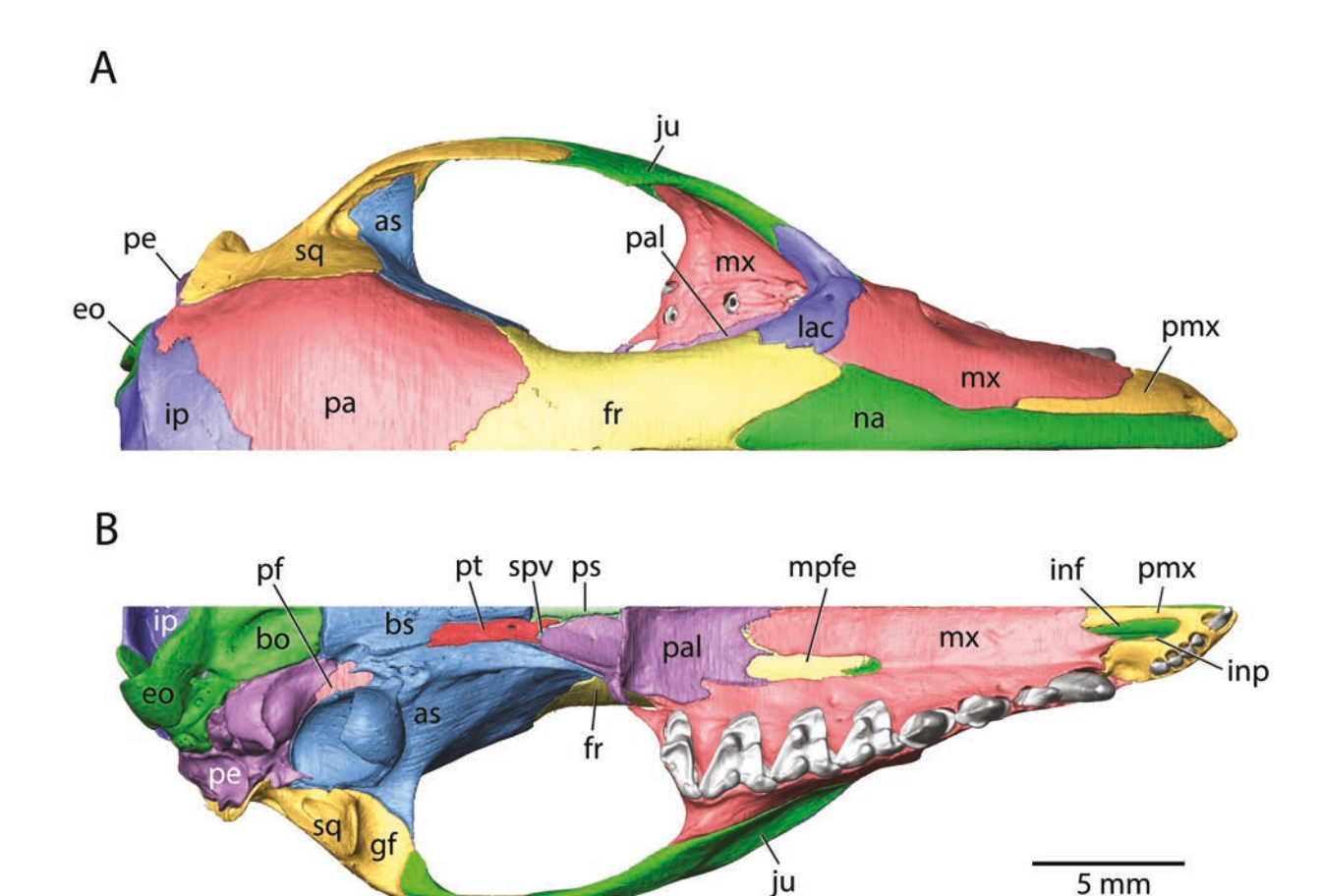


Fig. 2.—Monodelphis domestica, AMNH 261241, isosurface of left hemi-cranium rendered from CT scans; anterior to the right. A, dorsal view; B, ventral view. Abbreviations: as, alisphenoid; bo, basioccipital; bs, basisphenoid; eo, exoccipital; fr, frontal; gf, glenoid fossa; inf, incisive foramen; inp, incisive process of premaxilla; ju, interparietal; ju, jugal; lac, lacrimal; mpfe, maxillopalatine fenestra; mx, maxilla; na, nasal; pa, parietal; pal, palatine; pe, petrosal; pf, piriform fenestra; pmx, premaxilla; ps, presphenoid; pt, pterygoid; spv, sphenopterygoid vacuity; sq, squamosal.

(1993), *M. domestica* has five ethmoturbinals (endoturbinals of Rowe et al. 2005; Macrini 2012) and two frontoturbinals (ectoturbinals of Rowe et al. 2005; Macrini 2012). Anterior to the olfactory recess is the broad lateral recess (Maier 1993; Rossie 2006), which is further subdivided into anterolateral and posterolateral recesses (Smith and Rossie 2008; Smith et al. 2011; Fig. 4A). The anterolateral recess is delimited by the crista semicircularis to which the nasoturbinal is attached (Figs. 4A, 5C–D). The posterolateral recess is further subdivided into the frontal recess above and the maxillary recess below (Smith and Rossie

2008; Smith et al. 2011) by the lateral root of ethmoturbinal I, also referred to as the frontomaxillary septum (Figs. 4A, D, 5D). The frontal recess houses the two frontoturbinals (Figs. 4B, 5D).

Nasal

The nasal is shown in the hemi-cranium of AMNH 261241 in Figures 1A, 2, and 3 ("na"), and the isolated left nasal is shown in dorsal, lateral, and ventral views in Figure 6. In Figures 6A–B, most of the lateral border of the nasal

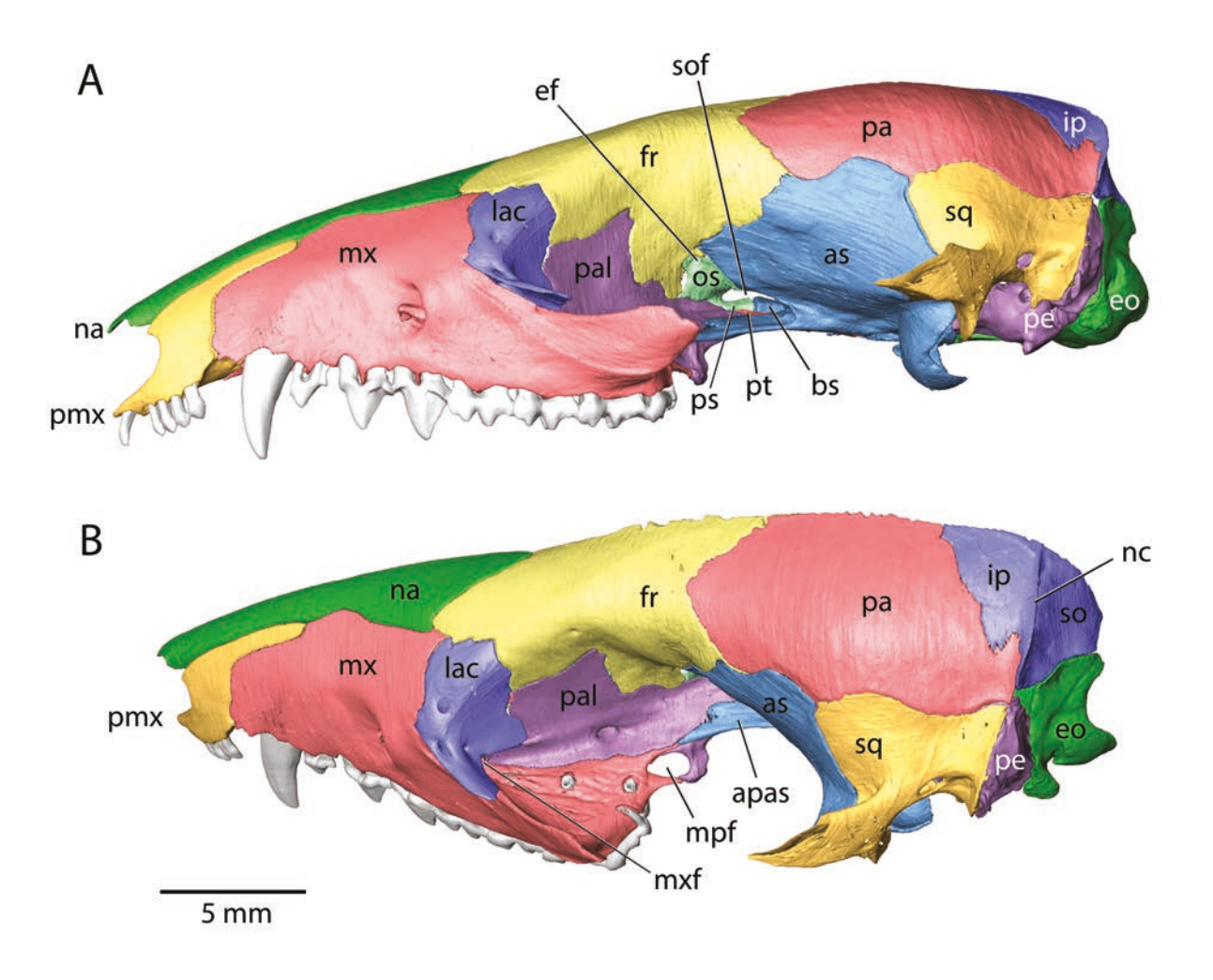


Fig. 3.—Monodelphis domestica, AMNH 261241, isosurface of left hemi-cranium rendered from CT scans; anterior to the left; jugal removed and zygomatic process of squamosal cut. **A,** lateral view; **B,** oblique posteroventrolateral view. Abbreviations: **apas,** anterior process of alisphenoid; **as,** alisphenoid; **bs,** basisphenoid; **ef,** ethmoidal foramen; **eo,** exoccipital; **fr,** frontal; **ip,** interparietal; **lac,** lacrimal; **mpf,** minor palatine foramen; **mx,** maxilla; **mxf,** maxillary foramen; **na,** nasal; **nc,** nuchal crest; **os,** orbitosphenoid; **pa,** parietal; **pal,** palatine; **pe,** petrosal; **pmx,** premaxilla; **ps,** presphenoid; **pt,** pterygoid; **so,** supraorbital; **sof,** sphenorbital fissure; **sq,** squamosal.

consists of facets for the premaxilla and maxilla that are roughly subequal in length. The facet for the premaxilla is cigar-shaped and that for the maxilla is irregular, concavoconvex from anterior to posterior. The ventral view (Fig. 6C) shows the complex morphology of the nasal in the roof of the nasal cavity. Medial and lateral longitudinal crests run from the anterior end of the nasal to near its posterior limit. The medial crest, the septal process, lies on the midline and abuts the septal process of the right nasal medially and the nasal septum ventrally. Ventral to the septal process, the nasal septum is cartilaginous anteriorly and ossified posteriorly, the latter segment slightly

longer than the former. The lateral longitudinal crest is the crista ethmoidalis of NAV, which is termed here the nasoturbinal crest, because it represents a point of attachment for the nasoturbinal. In a comparative study of the internal nasal skeleton in marsupials, Macrini (2012) identified two portions of the nasoturbinal, rostral and caudal, and noted that *M. domestica* lacks the rostral portion. This explains why only the posterior third of the nasoturbinal crest of *M. domestica* has nasoturbinal contacting it. Between the medial and lateral longitudinal crests is a concavity, the roof of the dorsal nasal meatus, the space between the nasal and the dorsal surface of ethmoturbinal I. A second shorter

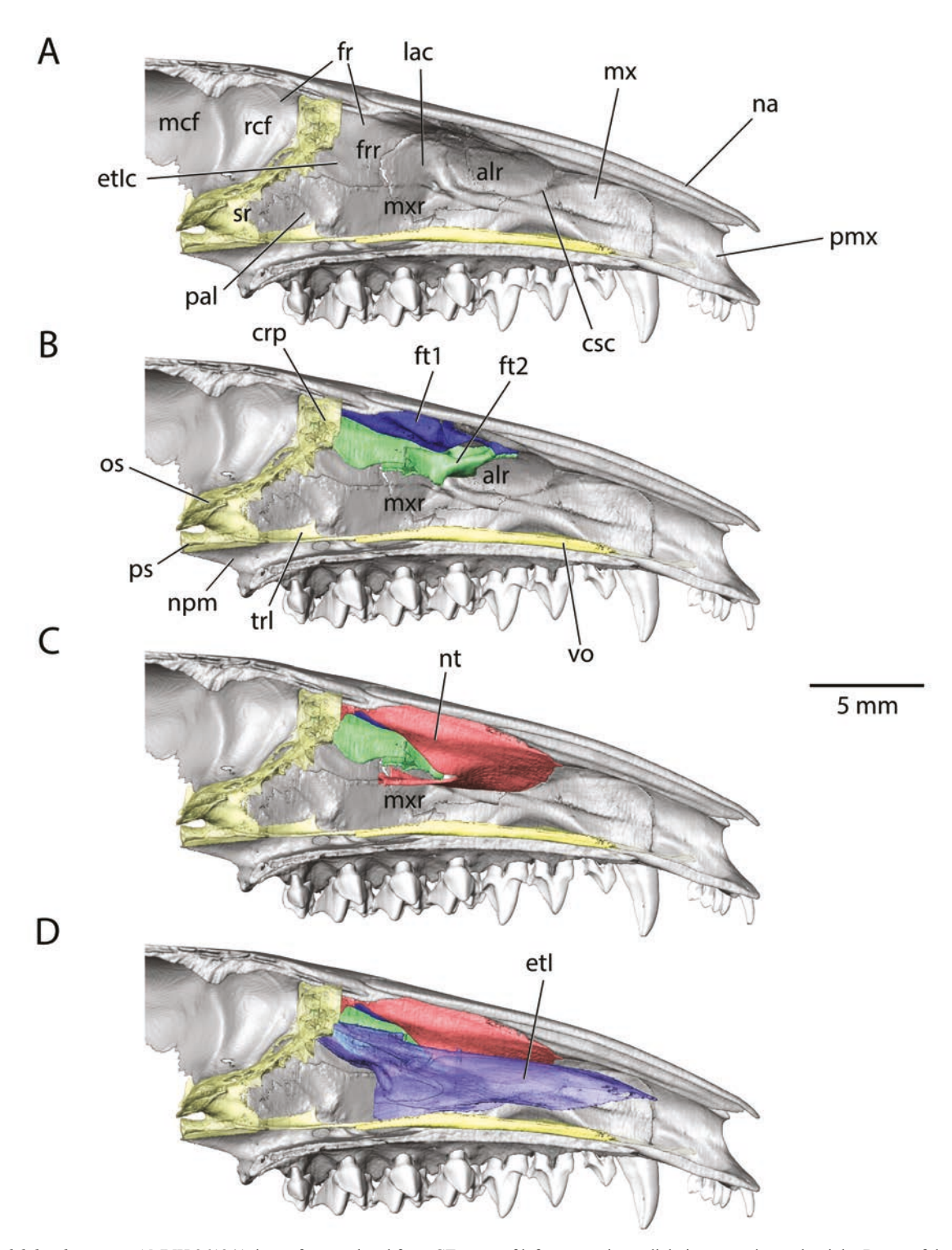


Fig. 4.—Monodelphis domestica, AMNH 261241, isosurface rendered from CT scans of left rostrum in medial view; anterior to the right. Bones of the lateral wall are in gray; unpaired bones of the internal nasal skeleton are in yellow. Vomer is cut parasagittally to the right of the midline. A, all turbinals are removed; the lateral recess consists of the anterolateral, frontal, and maxillary recesses; B, the two frontoturinals occupy the frontal recess; C, the nasoturbinal walls the anterolateral recess; D, ethmoturbinal I delimits the frontal and maxillary recesses. Abbreviations: alr, anterolateral recess; crp, cribriform plate of ethmoid; csc, crista semicircularis; etl, ethmoturbinal I; etlc, ethmoturbinal I crest; eth, ethmoid; fr, frontal; frr, frontal recess; ft1, frontoturbinal 1; ft2, frontoturbinal 2; lac, lacrimal; mcf, middle cranial fossa; mx, maxilla; mxr, maxillary recess; na, nasal; npm, nasopharyngeal meatus; nt, nasoturbinal; os, orbitosphenoid; pal, palatine; pmx, premaxilla; ps, presphenoid; rcf, rostral cranial fossa; sr, sphenoidal recess; trl, transverse lamina; vo, vomer.

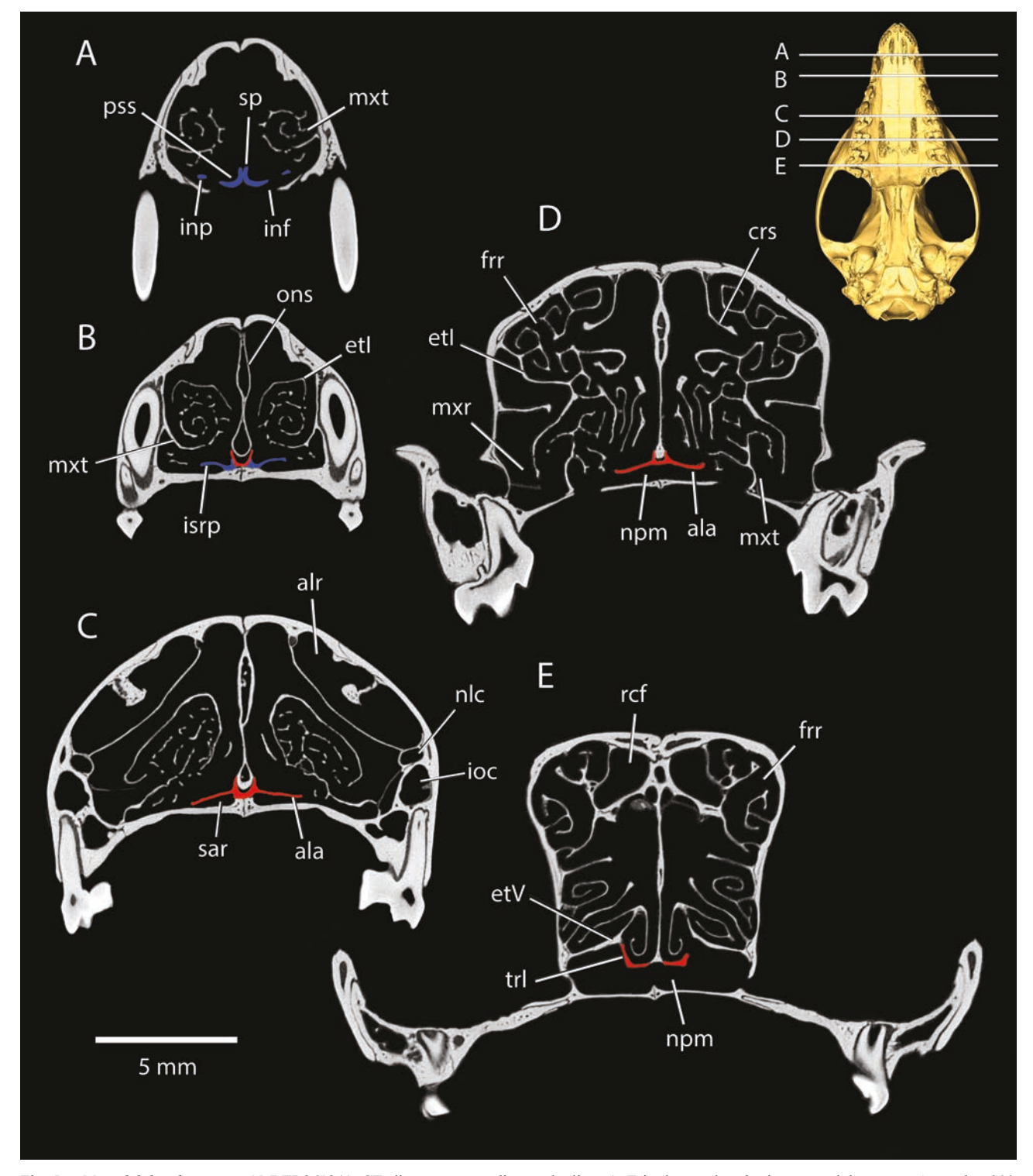


Fig. 5.—Monodelphis domestica, AMNH 261241, CT slices corresponding to the lines A–E in the cranium in the upper right corner. A, section 200, across incisive foramina; B, section 295, just posterior to incisive foramina; C, section 499, just anterior to the maxillopalatine fenestrae; D, section 616, across the maxillopalatine fenestrae; E, section 751, across the rear of the palate. The medial palatine processes of the premaxilla are in blue (A and B); the vomer (B–D) and transverse laminae (E) are in red. Abbreviations: ala, ala vomeris; alr, anterolateral recess; etI, ethmoturbinal I; etV, ethmoturbinal V; frr, frontal recess; inf, incisive foramen; inp, incisive process of premaxilla; ioc, infraorbital canal; isrp, inferior septal ridge process; mxr, maxillary recess; mxt, maxilloturbinal; nlc, nasolacrimal canal; npm, nasopharyngeal meatus; nt, nasoturbinal; ons, ossified nasal septum; pss, paraseptal shelf of premaxilla; rcf, rostral cranial fossa; sar, sub-alar recess; sp, septal process of premaxilla; trl, transverse lamina.

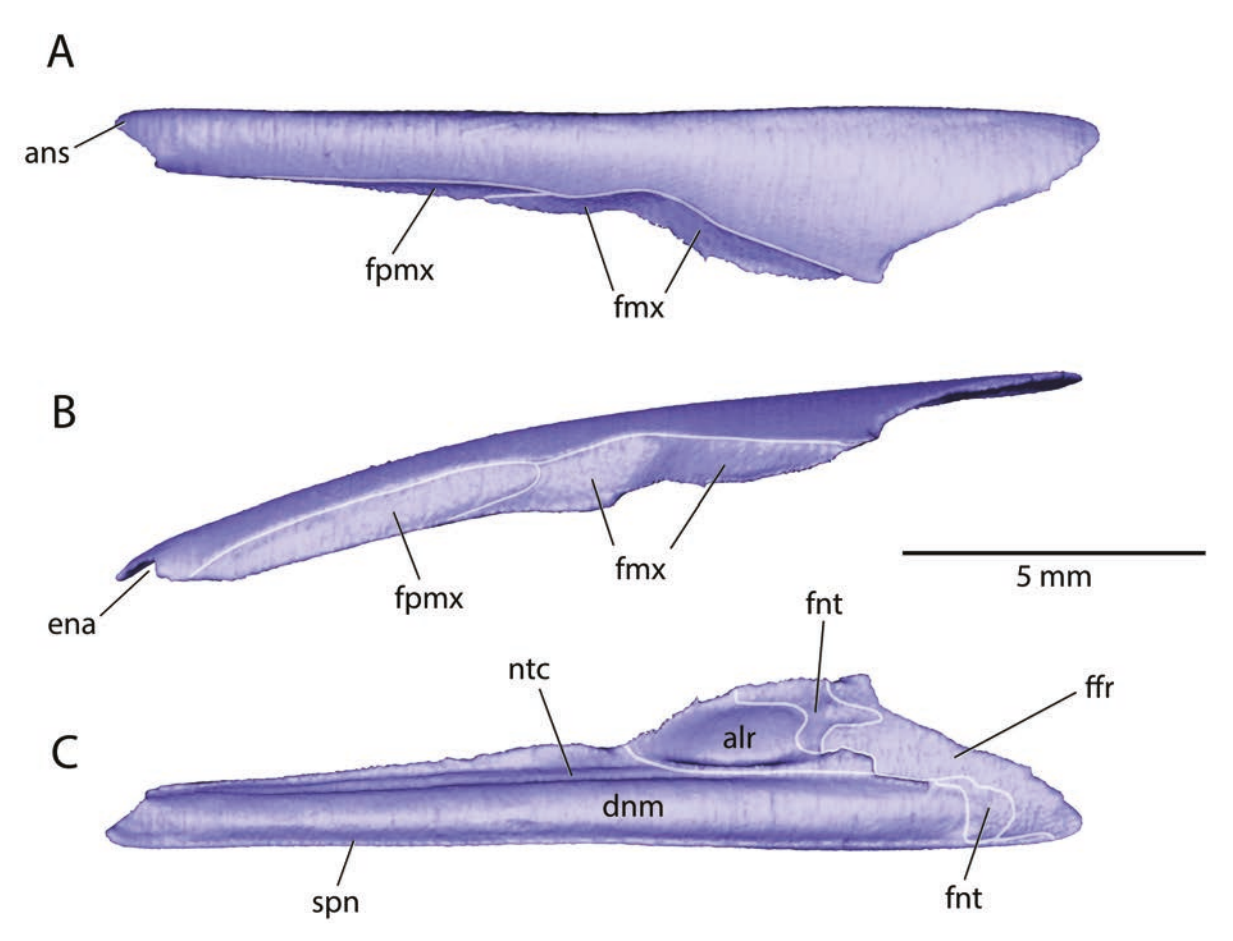


Fig. 6.—Monodelphis domestica, AMNH 261241, left nasal isosurface rendered from CT scans; anterior to the left. A, dorsal view; B, lateral view; C, ventral view. Abbreviations: alr, anterolateral recess; ans, anterior nasal spine; dnm, dorsal nasal meatus; ena, external nasal aperture; ffr, facet for frontal; fmx, facet for maxilla; fnt, facet for nasoturbinal; fpmx, facet for premaxilla; ntc, nasoturbinal crest; spn, septal process of nasal.

concavity in the nasal lies lateral to the posterior third of the nasoturbinal crest. This is the nasal's small contribution to the roof of the anterolateral recess (recessus maxillaris of NAV; superior recess of maxillary sinus of Rowe et al. 2005; frontal recess of Macrini 2012). The posterior aspect of the nasal is dominated by facets for contacting other elements. The largest and most posterior is for the frontal and spans the width of the nasal; anterior to this are two smaller facets for the nasoturbinal. The discovery of the facet for the frontal reveals an error in the description of the nasal in Wible (2003:139) who stated the "frontals overlap the nasals" but the reverse is the case.

Premaxilla

The premaxilla is shown in the hemi-cranium of AMNH 261241 in Figures 1–3 ("pmx"). In this specimen, the posterior margin of the premaxilla inside the nasal cavity is fused with a lateral shelf of the vomer. Moreover, the CM

Monodelphis sample, which includes young juveniles, did not have specimens showing clear evidence of a suture distinguishing the two bones, although not all specimens could be studied as this area is not easily accessible and often obscured by tissue. In describing and illustrating the isolated left premaxilla (Fig. 7), I relied on the CT scans of D. marsupialis, DU BAA 0164, where the premaxilla and vomer are separated by a narrow gap (Wible 2022: fig. 8f); I also found a similar gap in a pouch young D. virginiana, CM 33655. The position of this gap in DU BAA 0164 corresponds to an indentation in AMNH 261241 that I have accepted as the border between the two bones.

The lateral view of the isolated left premaxilla (Fig. 7A) is dominated by the facial process and its finger-like posterodorsal process. The posterior surface of the facial process has a facet for the overlapping maxilla. In the posteroventral aspect of the maxillary facet is a small foramen directed anteriorly into the premaxilla, which represents an opening into the incisivomaxillary canal (see Maxilla

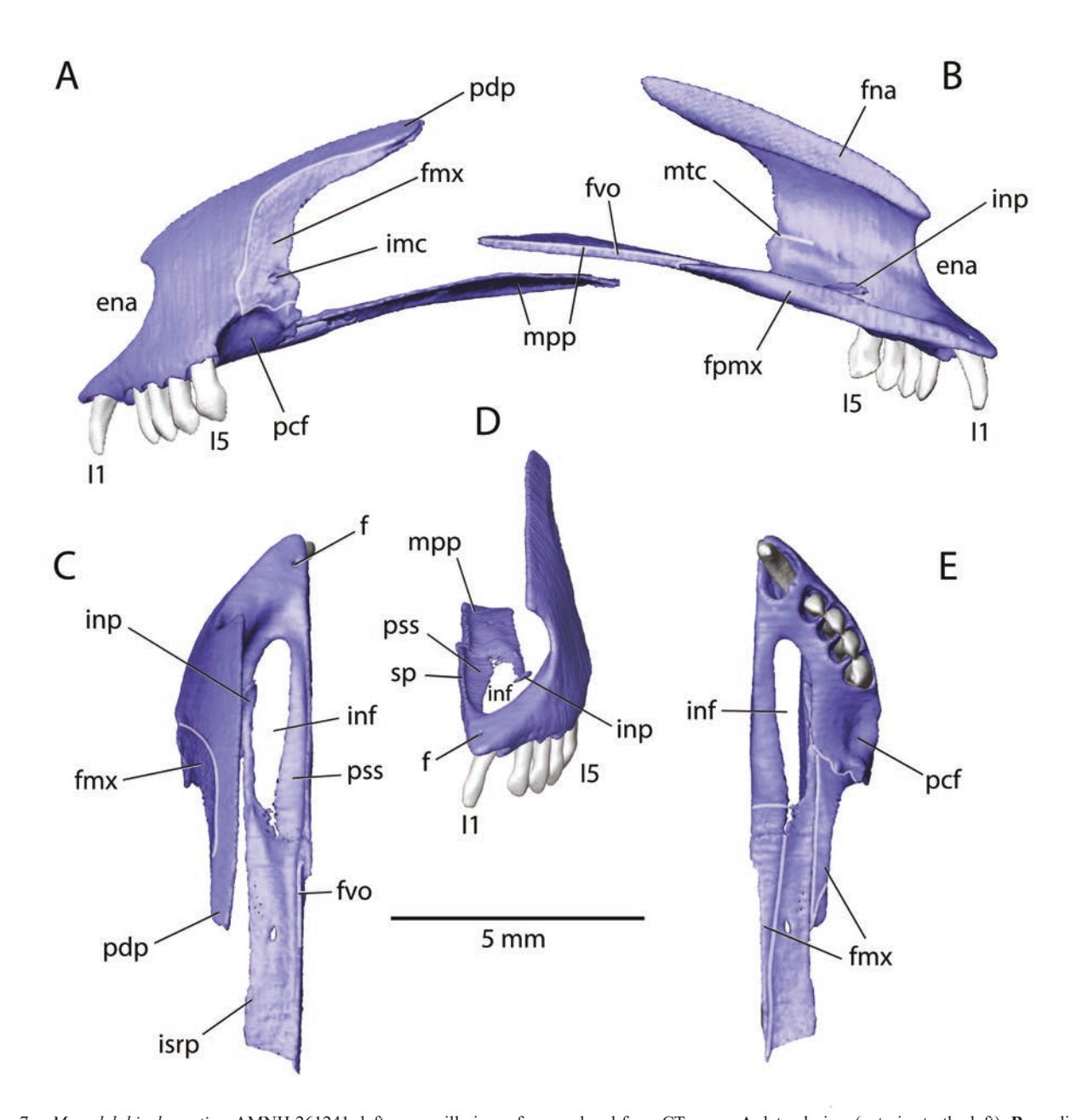


Fig. 7.—Monodelphis domestica, AMNH 261241, left premaxilla isosurface rendered from CT scans. A, lateral view (anterior to the left); B, medial view (anterior to the right) C, dorsal view (anterior to the top); D, anterior view (medial to the left); E, ventral view (anterior to the top). Abbreviations: ena, external nasal aperture; f, foramen; fmx, facet for maxilla; fna, facet for nasal; fpmx, facet for opposite premaxilla; fvo, facet for vomer; I1, upper first incisor; I5, upper fifth incisor; imc, incisivomaxillary canal; inf, location of incisive foramen; inp, incisive process of premaxilla; isp, inferior septal ridge process; mpp, medial palatine process; mtc, maxilloturbinal crest; pcf, paracanine fossa; pdp, posterodorsal process; pss, paraseptal shelf of premaxilla; sp, septal process of premaxilla.

below). Ventral to the maxillary facet is a deep concavity that accommodates the tip of the lower canine, the paracanine fossa (Fig. 7E; Voss and Jansa 2009), which has a small contribution posterolaterally from the maxilla (Fig. 2B). Posterior to this, the premaxilla has a long, narrow facet for the maxilla (Fig. 7E).

In medial view (Fig. 7B), the left premaxilla is dominated by the smooth, concave lateral wall of the anterior nasal cavity. About a third of the way up the lateral wall along the posterior margin is a low eminence that marks the anteriormost contact of the maxilloturbinal. Dorsal to the lateral wall of the nasal cavity is a facet on the inner surface

of the posterodorsal process of the premaxilla for contact with the left nasal. In dorsal view (Fig. 7C), there is a small foramen over the alveolus for the first upper incisor. This foramen opens ventrally in the medial aspect of the alveolus but is hidden in ventral view by the tooth.

The CT scans reveal details of the elongate medial palatine process (Fig. 7) not accessible to Wible (2003). This structure is treated in three parts, anteromedial, anterolateral, and posterior. The anteromedial part is distinguished by its midline contact with its fellow of the opposite side, sporting a broad premaxillary facet on its medial face (Figs. 5A, 7B). Also, it has a raised medial lip, the septal process, that contacted the cartilaginous nasal septum in the intact head, and a concave dorsal aspect (Figs. 5A, 7D), which in pouch young M. domestica accommodates the vomeronasal organ and paraseptal cartilage (Freyer 1999; Sánchez-Villagra and Forasiepi 2017). In adult M. domestica, according to Poran (1988), the vomeronasal organ lies at the level between the ultimate incisor and canine; this is precisely in the domain of the anteromedial part of the medial palatine process (Fig. 2B). Rowe et al. (2005) referred to the surface housing the vomeronasal organ in M. domestica as the paraseptal shelf of the premaxilla (and vomer, see below). I accept this term as appropriate for the premaxilla (Figs. 5A, 7C–D), given the relationship to the paraseptal cartilage. Most of the ventral surface of the anteromedial part of the medial palatine process is visible on the palate where it forms the medial border of the incisive foramen (Fig. 2B). The remaining, short anteromedial part lies dorsal to the maxilla in the nasal cavity floor with a facet for that bone on its ventral surface (Fig. 7E).

The posterior part of the medial palatine process is roughly equal in length to the anteromedial part. It has a thicker medial body and a substantial lateral shelf (Fig. 5B). The body lies off the midline, in contact with the maxilla ventrally, and its slightly upturned medial surface contacts the vomer (Figs. 5B, 7B). The lateral shelf is convex dorsally, concave ventrally, and separated from the maxilla by a narrow space that opens into the nasal cavity laterally (Fig. 5B). This shelf is continuous posteriorly with the ala of the vomer (Fig. 5C; see below). Penetrating the posterior part of the medial palatine process is a small opening of unknown function, bilaterally present (Figs. 7C, E). The posterior part contributes to the formation of a mucosal fold identified in pouch young marsupials as the inferior septal ridge by Broom (1896), which also includes the paraseptal cartilage (see also Freyer 1999). To distinguish the mucosal fold from the bone within it, I use the term inferior septal ridge process for the posterior part of the medial palatine process (Figs. 5B, 7C).

The anterolateral part projects forward from the inferior septal ridge process (Figs. 7C–E). It is a long, slender, finger-like process that tapers distally and extends into a plane dorsal to the incisive foramen (Fig. 5B). The tip of this process is visible in ventral view in the lateral margin of the incisive foramen (Fig. 2B). To my knowledge, such a structure on the mammalian premaxilla has not been

identified; it is visible, but not labelled in cross sections of *D. virginiana* in Maga (2008: fig. 3.8, sections 105 and 113). A survey of marsupials in the CM collection reveals this structure to be ubiquitous in didelphids but absent in the Australian taxa. Given the unique nature of this feature and its relation to the incisive foramen, I have termed it here the incisive process.

Maxilla

The maxilla in AMNH 261241 is visible in all views of the hemi-cranium in Figures 1–3 ("mx"). The lateral view of the isolated element (Fig. 8A) is dominated by the infraorbital foramen, which has a slight difference in position between the two sides: on the left it is dorsal to the distal root of the upper ultimate premolar, whereas on the right it is between the mesial and distal roots of that tooth. In the 25 adult *M. domestica* reported by Wible (2003), 23 have the condition of the left side and two have the condition of the right. Just anterior to the infraorbital foramen is the posterior opening into the incisivomaxillary canal (see below). Facets for two bones are visible on the anterior and ventral orbital rim: a small facet for the facial process of the lacrimal and a large facet for the jugal extending the length and height of the zygomatic process of the maxilla.

The medial view (Fig. 8B) is complicated by the numerous bones contacting the inner surface of the maxilla. Anteriorly is the sickle-shaped facet for the premaxilla, including its posterodorsal process. In the posteroventral aspect of this facet is a small foramen, which is the anterior opening of the incisivomaxillary canal (see below). Most of the dorsal margin of the maxilla has a facet for the nasal, but the posteriormost corner has a small facet where the maxilla overlies the frontal. Ventral to these facets for neighboring intramembranous bones, the facial process of the maxilla forms the lateral wall of the nasal cavity (Figs. 1B, 4A). A broad groove for the nasolacrimal duct runs nearly the length of the inner surface of the maxilla (Fig. 8B). The posterior third of the groove is transformed into a canal by the underlying lacrimal, which has a large, roughly triangular facet on the maxilla. The middle third is also transformed into a canal by the underlying maxilloturbinal (Fig. 5C), which contacts both the dorsal and ventral edges of the groove. However, in the anterior third, the maxilloturbinal only attaches to the dorsal edge of the groove and so it is open ventrally. In addition to its attachment along the nasolacrimal groove, the maxilloturbinal runs posteroventrally along another eminence into the floor of the nasal cavity, ending at the lateral edge of the maxillopalatine fenestra of Voss and Jansa (2009) (major palatine foramen of Wible 2003) (Fig. 8C). The posterior half of the inner facial process of the maxilla dorsal to the nasolacrimal groove has a large depression housing the anterolateral recess, which also has contributions from the nasal and lacrimal (Figs. 1B, 4A). The margin of the anterior half of the anterolateral recess on the maxilla is formed by

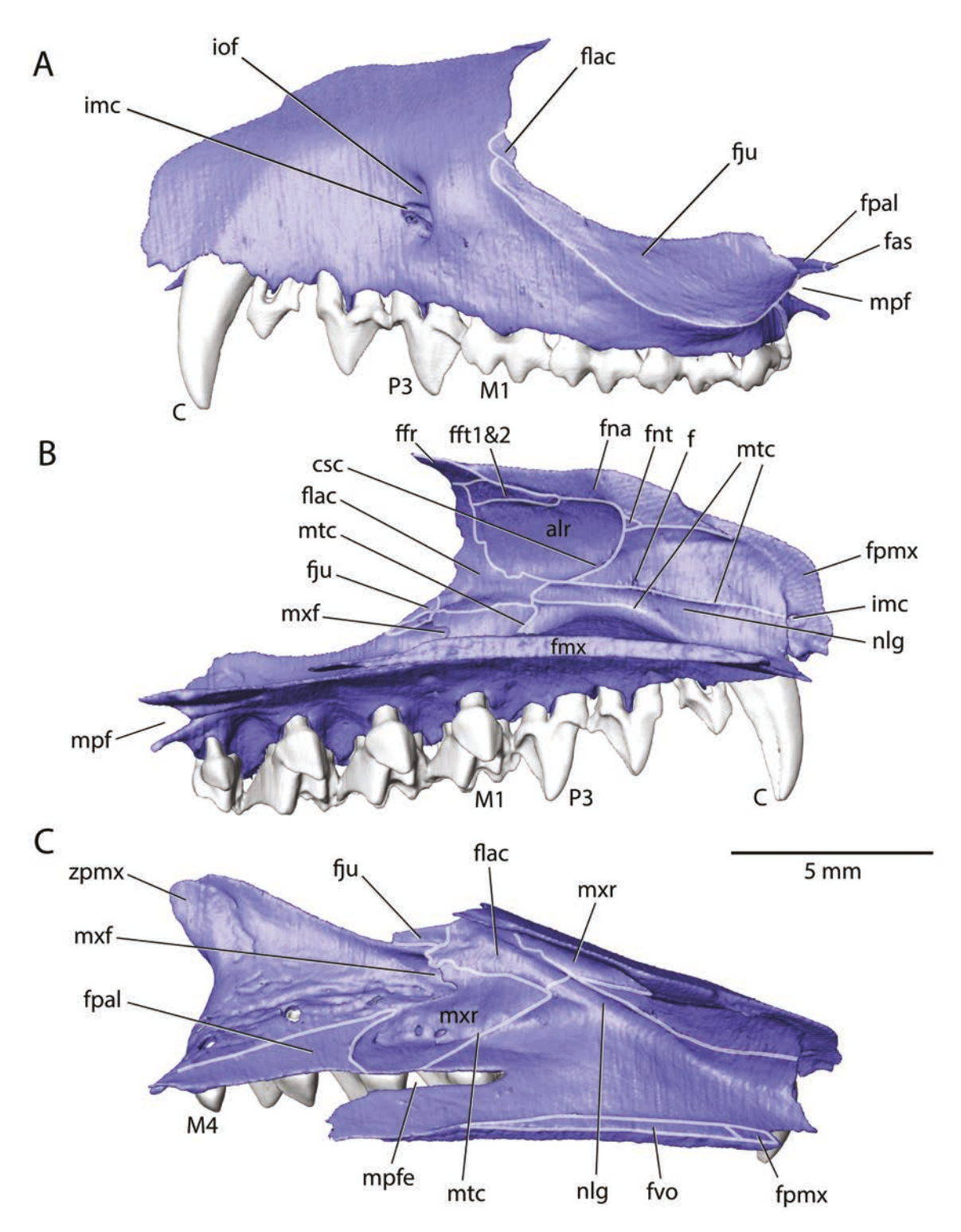


Fig. 8.—Monodelphis domestica, AMNH 261241, left maxilla isosurface rendered from CT scans. A, lateral view (anterior to the left); B, medial view (anterior to the right); C, oblique dorsomedial view (anterior to the right). Abbreviations: alr, anterolateral recess; C, upper canine; csc, crista semicirculatis; f, foramen; fas, facet for alisphenoid; ffr, facet for frontal; fft1&2, facet for frontoturbinal 1 and 2; fju, facet for jugal; flac, facet for lacrimal; fmx, facet for opposite maxilla; fna, facet for nasal; fnt, facet for nasoturbinal; fpal, facet for palatine; fpmx, facet for premaxilla; fvo, facet for vomer; imc, incisivomaxillary canal; iof, infraorbital foramen; M1, upper first molar; M4, upper fourth molar; mpf, location of minor palatine foramen; mpfe, location of maxillopalatine fenestra; mtc, maxilloturbinal crest; mxr, maxillary recess; nlg, nasolacrimal groove; P3, upper third premolar; zpmx, zygomatic process of maxilla.

a sharp, curved crest, the crista semicircularis (Fig. 8B), to which is attached the nasoturbinal (Fig. 4C). In the posterior half of the dorsal margin of the anterolateral recess on the maxilla is a facet for frontoturbinal 1 and 2 (Fig. 8B). The last facet visible in medial view is the midline facet on the palatal process of the maxilla that abuts the same structure on the opposite side.

The oblique dorsomedial view of the maxilla (Fig. 8C) shows several structures in the floor of the nasal cavity. The medial edge of the palatal process is thickened, and on its dorsal surface is a short facet for the medial palatine process of the premaxilla anteriorly and a long facet for the vomer posteriorly. Lateral to the maxillopalatine fenestra, behind the attachment of the maxilloturbinal in the floor of the maxillary recess are three small foramina; the anterior one opens into the maxilla medial to the roots of the first upper molar, and the posterior two into the maxilla medial to the roots of the second upper molar. Posterior to these foramina is a three-sided flat surface that contacts the lateral aspect of the horizontal process of the palatine. On the posterior tip of that surface is a small contact for the anterior process of the alisphenoid (Fig. 8A). Lateral to the facet for the palatine in the floor of the orbit are openings in the maxilla associated with the distal and lingual roots of the upper ultimate molar and with the lingual roots of the upper second and third molars (Fig. 8C). Posterior to the openings with the upper ultimate molar is a deep incisure in the maxilla that represents the anterior half of the minor palatine foramen, which is closed posterior by the palatine (Fig. 3B). A narrow sulcus runs forward from the minor palatine foramen on the palatal surface of the maxilla. At the level of the mesial root of the upper second molar is the position of the maxillary foramen, the posterior opening of the infraorbital canal. The maxilla forms the floor and lateral border of the maxillary foramen, which is completed by the lacrimal and palatine (Fig. 3B). The infraorbital canal within the maxilla runs from the level of the distal root of the upper first molar to the infraorbital foramen.

The last feature on the maxilla to address is the incisivomaxillary canal. In the dog (Evans and Christensen 1993:141), this canal "carries the nerves and blood vessels to the first three premolars and the canine and incisor teeth. It leaves the medial wall of the infraorbital canal within the infraorbital foramen, passes dorsal to the apex of the canine alveolus with which it communicates, and enters the incisive bone" (= premaxilla). The incisivomaxillary canal in AMNH 261241 is remarkably like that in the dog. It runs through the facial process of the maxilla roughly parallel but dorsal to the nasolacrimal groove and communicates with the alveoli of the three premolars and canine before entering the premaxilla to communicate with the incisor alveoli. However, the canal has three small openings into the nasal cavity not described for the dog. One foramen is just dorsal to the midpoint of the nasolacrimal groove (Fig. 8B), and the other two are in the anterior aspect of the anterolateral recess (not visible in the figures). Wible (2003) did not report on the incisivomaxillary canal in the CM holdings of *Monodelphis*, because it was a structure he was not aware of at the time. The specimen illustrated in Wible (2003), *M. arlindoi*, CM 52729, has an incisivomaxillary canal but it is positioned more posteriorly than in AMNH 261241 and is hidden within the infraorbital canal in direct lateral view.

Palatine

The palatine is visible in all views of the hemi-cranium of AMNH 261241 in Figures 1–3 ("pal"). The horizontal and perpendicular parts of the palatine are most readily visualized in oblique anteromedial view of the isolated bone (Fig. 9E). The dorsal surface of the horizontal part forms the floor of the nasopharyngeal meatus and choanae, and its ventral surface forms the roof of the rear of the palate. The lateral surface of the perpendicular part contributes to the medial orbital wall, and its medial surface contributes to the rear of the nasal cavity and forms the lateral wall of the nasopharyngeal meatus and choanae.

Most of what is visible in lateral view of the left palatine is the perpendicular part in the medial orbital wall (Fig. 9A). The perpendicular part is tallest in its middle and short at both its anterior and posterior ends. The anterior end reaches into the infraorbital canal, forming with the maxilla and lacrimal the borders of the maxillary foramen (Fig. 3B); the posterior end nearly reaches the sphenorbital fissure (Fig. 3A). At the base of the perpendicular part, near the anteroposterior midpoint, is the large sphenopalatine foramen (Fig. 9A). Ventral to the foramen is a horizontal shelf that runs the length of the perpendicular part and contributes to the floor of the orbit. This shelf is broadest in the vicinity of and posterior to the sphenopalatine foramen and tapers both anteriorly and posteriorly. At the sphenopalatine foramen, this shelf has a distinct concavity that indicates the pterygopalatine fossa. There are three small nutrient foramina just posterior to the sphenopalatine foramen, and two more substantial ones that penetrate through the palatine more posteriorly. The more anterior of these two opens medially into the nasopharyngeal meatus ventral to ethmoturbinal V, whereas the posterior one opens ventrally into the roof of the nasopharynx, posterior to the choanae. The dorsal aspect of the perpendicular part has a facet anteriorly for the lacrimal and two more posteriorly for the orbital process of the frontal. The posterior half of the ventrolateral aspect of the perpendicular part has a grooved facet holding the palatal process of the maxilla and a flat facet for the anterior process of the alisphenoid.

The medial surface of the perpendicular part has a complex of facets and crests for the attachment of neighboring bones (Figs. 9D), including elements of the internal nasal skeleton (some of which are shown in situ in Fig. 9B). Across the dorsal margin of the medial surface is a facet for the underlying orbital process of the frontal. Ventral to the anteriormost extent of the frontal facet is a small facet that

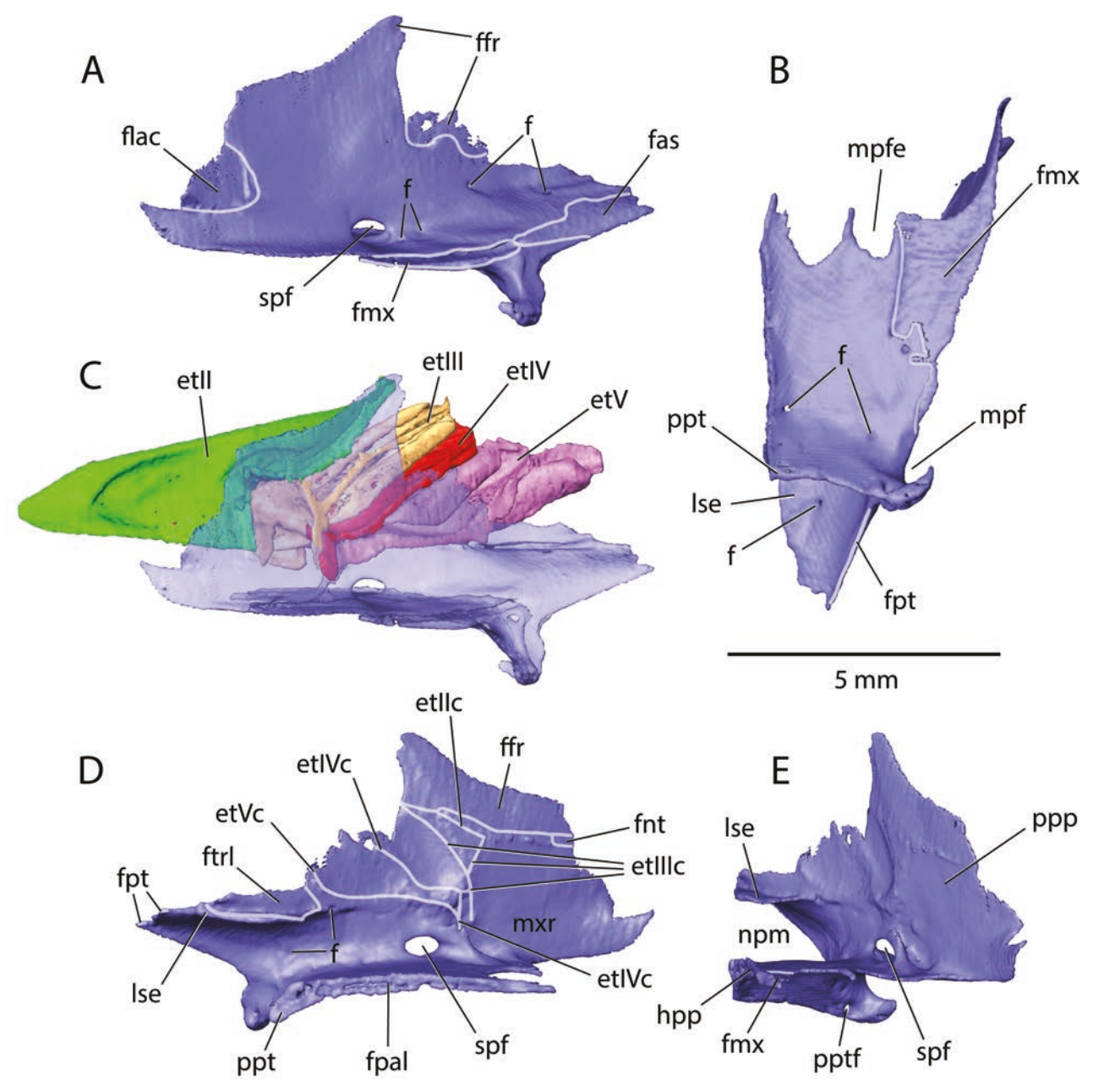


Fig. 9.—Monodelphis domestica, AMNH 261241, left palatine isosurface rendered from CT scans. A, lateral view (anterior to the left); B, ventral view (anterior to the top); C, lateral transparent view (anterior to the left) with ethmoturbinals II—V; D, medial view (anterior to the right); E, oblique anteromedial view (medial to the left). Abbreviations: etII, ethmoturbinal II; etIIC, ethmoturbinal III crest; etIII, ethmoturbinal III; etIIIC, ethmoturbinal IV crest; etIV, ethmoturbinal IV crest; etVe, ethmoturbinal V crest; f, foramen; fas, facet for alisphenoid; ffr, facet for frontal; flac, facet for lacrimal; fmx, facet for maxilla; fnt, facet for nasoturbinal; fpal, facet for opposite palatine; fpt, facet for pterygoid; hpp, horizontal part of palatine; lse, lamina sphenoethmoidalis; mpf, location of minor palatine foramen; mpfe, location of maxillopalatine fenestra; npm, nasopharyngeal meatus; ppp, perpendicular part of palatine; ppt, postpalatine torus; pptf, postpalatine torus foramen; spf, sphenopalatine foramen.

contacts the rear of the nasoturbinal. Ventral to the frontal facet and posterior to the nasoturbinal facet is a raised crest that is the attachment for ethmoturbinal II. Lying ventral to that is a V-shaped crest, the attachment for ethmotur-

binal III, and posteroventral to that are two more crests, the attachments for ethmoturbinals IV and V. Ventral to the posterior end of the attachment for ethmoturbinal V is the medial side of the foramen mentioned above opening into the nasopharyngeal meatus. Posterior to that foramen is a narrow horizontal shelf, the lamina sphenoethmoidalis of NAV, that contributes to the roof of the nasopharyngeal meatus and nasopharynx behind the choanae (Fig. 9E shows the extent of this shelf in the horizontal plane). The dorsal surface of this shelf is overlain by the presphenoid and transverse lamina (see Internal Nasal Skeleton below). At the posterior end of the lamina sphenoethmoidalis is a small contact with the anteromedial aspect of the pterygoid and posterolateral to that is a second small contact more laterally on the pterygoid (Fig. 9D), visible on the cranial surface just anterior to the sphenorbital fissure (Fig. 3A). The midline of the palatine is the medial face of the horizontal part; its length has a facet that contacts the right palatine.

In ventral view (Fig. 9B), the horizontal part is the palatal process of the palatine, which has a facet for the maxilla along most of its lateral border. Its anterior border is Wshaped, with the lateral part of the W forming the posterior border of the maxillopalatine fenestra between the palatine and maxilla (Fig. 2B). The fenestra serves as the exit for the major palatine nerve and vessels. The medial part of the W is largely filled by maxilla; along the anterior midline, the horizontal part underlies the maxilla and there is a small facet on the dorsal surface of the palatine for the maxilla (Fig. 9E). The midline in ventral view has a low, raised crest and the entire posterior border is thickened, forming a postpalatine torus. The medial view shows that the postpalatine torus is angled posteroventrally and, unlike the rest of the horizontal part is not in a horizontal plane (Fig. 9D). At the lateral end of the postpalatine torus is a beak-shaped process directed anterolaterally (Fig. 9B) that contributes to the minor palatine foramen between the palatine and maxilla (Fig. 3B).

Lacrimal

The lacrimal is visible on the hemi-cranium of AMNH 261241 in all views in Figures 1-3 ("lac") except the ventral one (Fig. 2B). In lateral view of the isolated left element (Fig. 10A), the three parts of the lacrimal exposed on the cranial surface are visible: the facial, orbital, and zygomatic processes. The small, irregular facial process is dominated by the dorsal of the two lacrimal foramina, which lies close to the anterior orbital rim; the ventral foramen is positioned near the juncture of the facial and zygomatic processes. Anterior to the facial process is a triangular shaped process of lacrimal that is covered by the facial process of the maxilla in the intact cranium. Running to the apex of this triangle is the open nasolacrimal canal, which is initially within the lacrimal where the two lacrimal foramina meet, then between the lacrimal and maxilla, and more anteriorly between the maxilla and maxilloturbinal. At the posterior base of the nasolacrimal canal is a foramen ("nlcf" in Fig. 10A) that allows communication between the nasolacrimal and infraorbital canals (see below).

The posterior view of the lacrimal (Fig. 10C) shows the

large, smooth orbital process and the small, tongue-shaped zygomatic process. At the juncture of these two processes is a foramen of uncertain function. It connects with two smaller foramina on the ventral surface of the lacrimal (Fig. 10D: "f"). The anterior of these two opens into a large facet on the zygomatic process for the jugal bone, whereas the posterior one opens into posteriormost part of the infraorbital canal, between the lacrimal, maxilla, and palatine. A small groove runs anteriorly from the posterior foramen to the foramen in the nasolacrimal canal. Consequently, these structures constitute a pathway, which is likely vascular in nature, from the orbit to the infraorbital canal and then to the nasolacrimal canal. Beck et al. (2022: 40) noted that in the didelphid Lestodelphys Tate, 1934, "one or two much smaller foramina are also present within the orbital fossa; the presence of dried blood within the lumina of the latter perforations in some specimens...suggests that these are vascular pores." Most of the remaining surface of the lacrimal in AMNH 261241 in ventral view is a facet for the maxilla.

The quadrangular medial surface of the lacrimal contributes to the lateral wall of the nasal cavity (Figs. 1B, 4A, 10B). Running the length of the dorsal margin of the medial lacrimal is a facet for the underlying frontal (Fig. 10B). Ventral to the anterior half of the frontal facet is a facet for frontoturbinal 2. Lastly, the posteroventral corner has a facet for the underlying perpendicular part of the palatine. Dominating the medial surface of the lacrimal is a rounded prominence that begins at the anteroventral corner and runs posteriorly and slightly dorsally a short distance before bifurcating into dorsal and ventral branches. The main prominence is the lacrimal's contribution to the nasolacrimal canal, and its dorsal and ventral branches reflect the location of the two lacrimal foramina on the lateral surface. The main prominence and dorsal branch circumscribe a depression along the anterior aspect of the lacrimal that contributes to the rear of the anterolateral recess, the bulk of which is on the maxilla with a small portion on the nasal (Figs. 1B, 4A, 6C, 8B). Running on the dorsal aspect of the main prominence and across the length of the lacrimal is a low crest for the attachment of the nasoturbinal (Fig. 10B).

Jugal

The jugal is the principal element of the zygomatic arch (Figs. 1A, 2: "ju"). The isolated left jugal, has a facet posteriorly on its lateral surface for the zygomatic process of the squamosal (Fig. 11A), and anteriorly on its medial surface for the zygomatic process of the maxilla (Fig. 11B). The facet for the zygomatic process of the lacrimal is primarily on the anterodorsal surface of the jugal but is visible in both lateral and medial views (Fig. 11). The final facet of note is the glenoid facet on the posteromedial aspect of the glenoid process of the jugal (Fig. 11B), which articulates with the condylar process of the dentary.

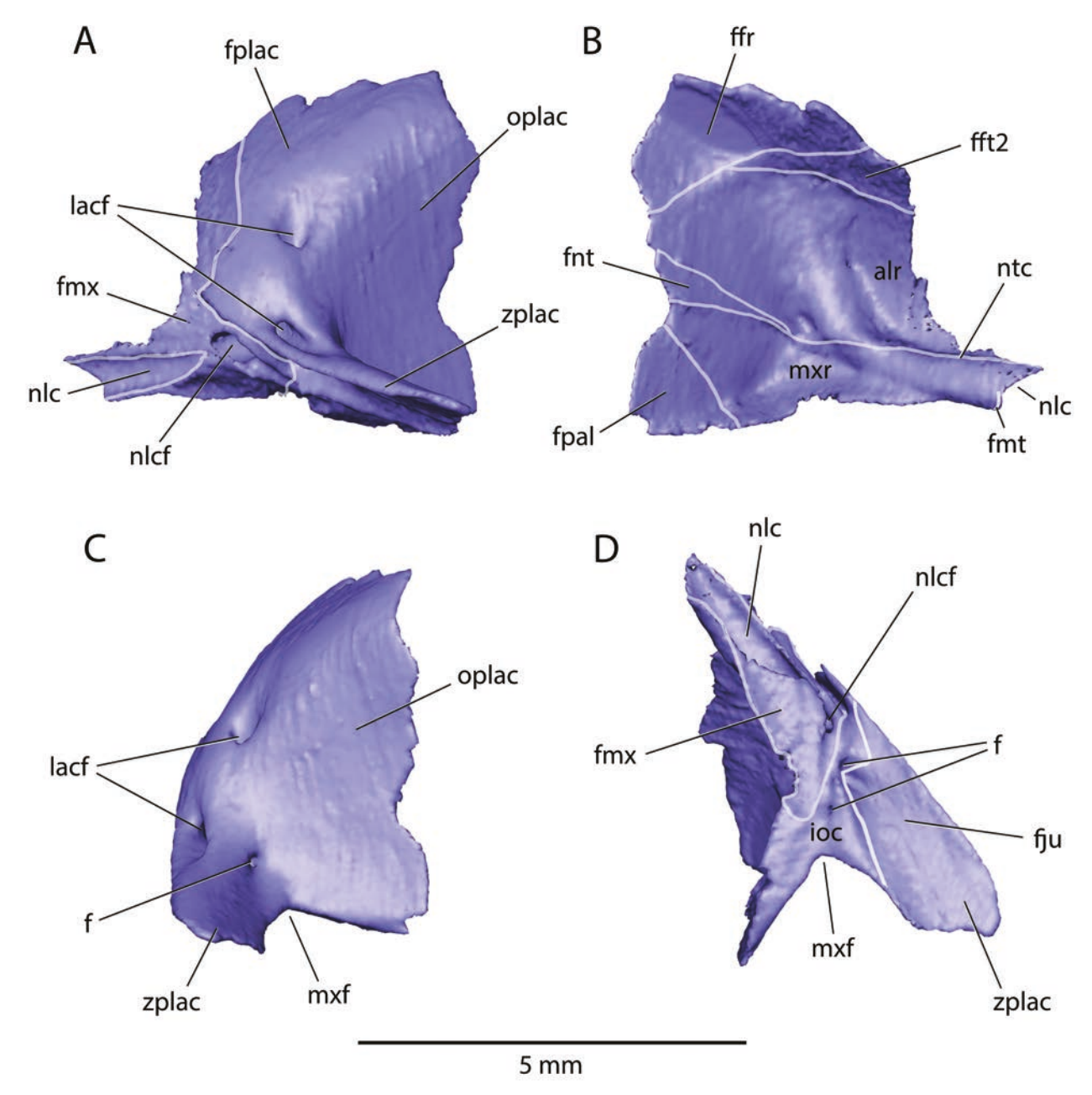


Fig. 10.—Monodelphis domestica, AMNH 261241, left lacrimal isosurface rendered from CT scans. A, lateral view (anterior to the left), B, medial view (anterior to the right); C, posterior view (lateral to the left); D, ventral view (anterior to the top). Abbreviations: alr, anterolateral recess; f, foramen; ffr, facet for frontal; fft2, facet for frontoturbinal 2; fju, facet for jugal; fmx, facet for maxilla; fpal, facet for palatine; fplac, facial process of lacrimal; ioc, roof of infraorbital canal; lacf, lacrimal foramen; mxf, location of maxillary foramen; nlacf, nasolacrimal canal foramen; nlc, nasolacrimal canal; ntc, nasoturbinal crest; oplac, orbital process of lacrimal; zplac, zygomatic process of lacrimal.

As reported for *M. arlindoi*, CM 52729, by Wible (2003), *M. domestica*, AMNH 261241, has two muscular depressions on the jugal's lateral surface (Fig. 11A). Based on *D. marsupialis*, the anterior depression is for the zygomaticus and levator labii muscles (Turnbull 1970), and the posterior one is for the superficial and deep masseters (Hiiemae and Jenkins 1969; Turnbull 1970). There is also

a weak frontal process for the attachment of the postorbital ligament.

Frontal

The frontal is visible in all views of the hemi-cranium of AMNH 261241 in Figures 1–3 ("fr"). Although the frontal

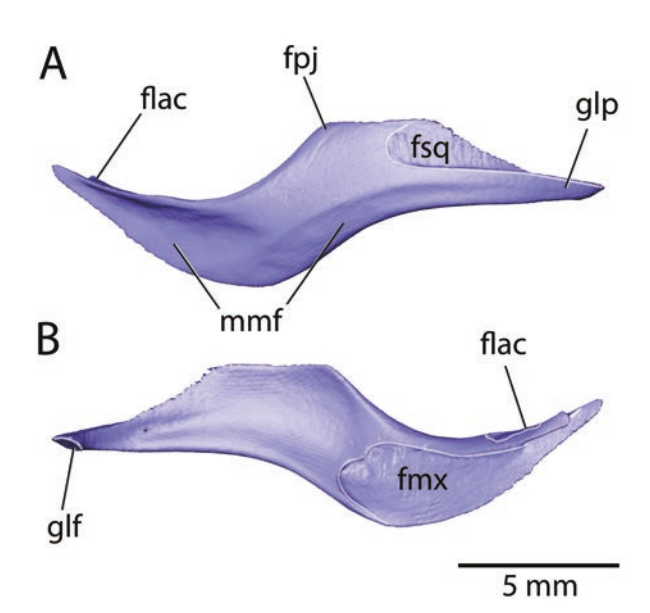


Fig. 11.—Monodelphis domestica, AMNH 261241, left jugal isosurface rendered from CT scans. A, lateral view (anterior to the left); B, medial view (anterior to the right). Abbreviations: flac, facet for zygomatic process of lacrimal; fmx, facet for zygomatic process of maxilla; fpj, frontal process of jugal; fsq, facet for zygomatic process of squamosal; glf, glenoid facet; glp, glenoid process of jugal; mmf, muscular facet.

has a relatively simple morphology (C-shaped in cross section), it has complex relationships with a great number of neighboring elements. The external surface of the frontal has two faces: the squama frontalis in the cranial roof, and the facies temporalis in the orbitotemporal region (Fig. 12A). The anterior aspect of the squama has facets for the nasal, maxilla, and lacrimal, from medial to lateral (Fig. 12C); the anterior aspect of the temporal face has facets for the lacrimal and palatine, from dorsal to ventral (Fig. 12A). The posterior aspect of the frontal has a large, prominent facet for the parietal on both the squama and temporal face; anteroventral to that is a barely perceptible facet for the alisphenoid and a small facet for the orbitosphenoid, which is a tiny element in M. domestica. The left and right squamae have weak temporal lines that start at the supraorbital margin and converge on each other at the very rear of the frontals (Fig. 12C). A postorbital process is absent. Ventral to the origin of the temporal line at the supraorbital margin is a small foramen in the temporal face for the frontal diploic vein directed posteriorly into the frontal (Fig. 12A). The only other foramen associated with the frontal in lateral view is the ethmoidal foramen, which is between the frontal and orbitosphenoid; the contribution from the frontal is in the bone's ventral margin immediately anterior to the facet for the orbitosphenoid (Fig. 12A).

Figure 12D is an oblique dorsomedial view of the inner surface of the frontal. The bone can be roughly divided

into thirds: the anterior third is in the roof of the nasal cavity, the middle third in the roof of the rostral cranial fossa, which houses the olfactory bulbs, and the posterior third in the anterior roof of the middle cranial fossa, which houses the cerebral hemispheres (Figs. 1B, 12D). Separating the nasal cavity and rostral cranial fossa is a sharp ridge that begins dorsally off the midline and extends the height of the frontal (Fig. 12D). On the anterior face of this ridge is a facet for the cribriform plate of the ethmoid bone. Extending rostrally from this ridge are a series of facets and crests that abut elements of the internal nasal skeleton, from anterodorsal to posteroventral, the nasoturbinal, frontoturbinals 1 and 2, and ethmoturbinals I to V; these elements are shown in place in lateral view with the frontal transparent in Figure 12B. The maxilloturbinal is the only turbinal that does not contact the frontal. In the anteroventral corner of the frontal is a facet for the perpendicular part of the palatine opposite the attachments of ethmoturbinals III to V.

Separating the rostral and middle cranial fossae on the frontal is another sharp ridge, the annular ridge (Figs. 1B, 12D), which abuts the brain's circular fissure separating the olfactory bulbs and cerebral hemispheres (Macrini et al. 2007). At the ventral margin of the rostral cranial fossa is a facet on the frontal for the orbitosphenoid and anterior to it a notch marking the frontal's contribution to the ethmoidal foramen. There is a weak groove running anterodorsally from the ethmoidal foramen parallel to and behind the crest for the cribriform plate of the ethmoid. In the anterior roof of the rostral cranial fossa are two small foramina that communicate with the frontal diploic vein foramen on the lateral surface. The transparent frontal in Figure 12B shows the diploic space anterior and dorsal to the frontal diploic vein foramen; this space approaches but does not cross the midline. Additionally, it is continuous with another large diploic space within the dorsal half of the annular ridge. The dorsal midline includes a facet for the frontal of the opposite side (Fig. 12D), which is of uniform height except at the annular ridge where it is considerably thicker. The roof of the rostral cranial fossa has a sharp midline ridge that separates the olfactory bulbs in the endocast (Macrini et al. 2007: fig. 2B) and houses the dorsal sagittal sinus, based on D. virginiana (Dom et al. 1970). The frontal's contribution to the roof of the middle cranial fossa has a low eminence that forms the median sulcus on the endocast (Macrini et al. 2007: fig. 2B), for the continuation of the dorsal sagittal sinus. As seen in the medial view of the hemi-cranium (Fig. 1B), the frontal is only a minor contributor to the middle cranial fossa, which has larger contributions from the parietal and alisphenoid.

Parietal

The parietal is visible in all the views of the hemi-cranium in Figures 1–3 ("pa"). The isolated left parietal in lateral view has facets along its ventral border for the overlying alisphenoid and squamosal (Fig. 13A); the remainder of

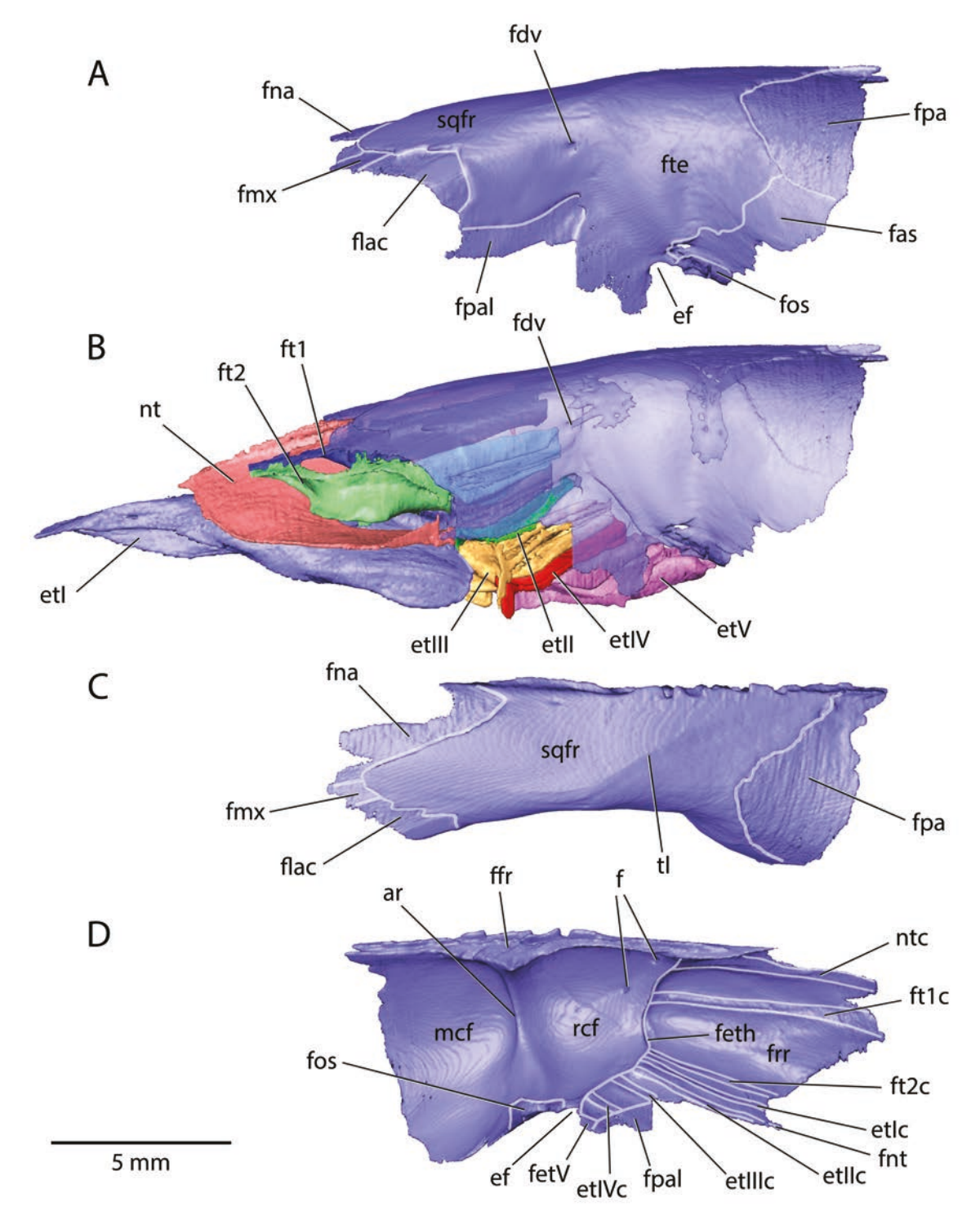


Fig. 12.—Monodelphis domestica, AMNH 261241, left frontal isosurface rendered from CT scans. A, lateral view (anterior to the left); B, lateral transparent view (anterior to the left) with turbinals that contact frontal; C, dorsal view (anterior to the left); D, oblique dorsoventral view (anterior to the right). Abbreviations: ar, annular ridge; ef, location of ethmoidal foramen; etl, ethmoturbinal I; etlc, ethmoturbinal I crest; etll, ethmoturbinal II; etllc, ethmoturbinal III; etllc, ethmoturbinal III; etllc, ethmoturbinal IV; etlVc, ethmoturbinal IV crest; etV, ethmoturbinal IV crest; etV, foramen; fas, facet for alisphenoid; fdv, foramen for frontal diploic vein; fetV, facet for ethmoturbinal V; feth, facet for ethmoid (cribriform plate); ffr, facet for opposite frontal; flac, facet for lacrimal; fmx, facet for maxilla; fos, facet for orbitosphenoid; fpa, facet for parietal; fpal, facet for palatine; ft, facet semporalis; ft1, frontoturbinal 1; ft1c, frontoturbinal 1 crest; ft2, frontoturbinal 2; ft2c, frontoturbinal 2 crest; mcf, middle cranial fossa; nt, nasoturbinal; ntc, nasoturbinal crest; rcf, rostral cranial fossa; sqfr, squama frontalis; tl, temporal line.

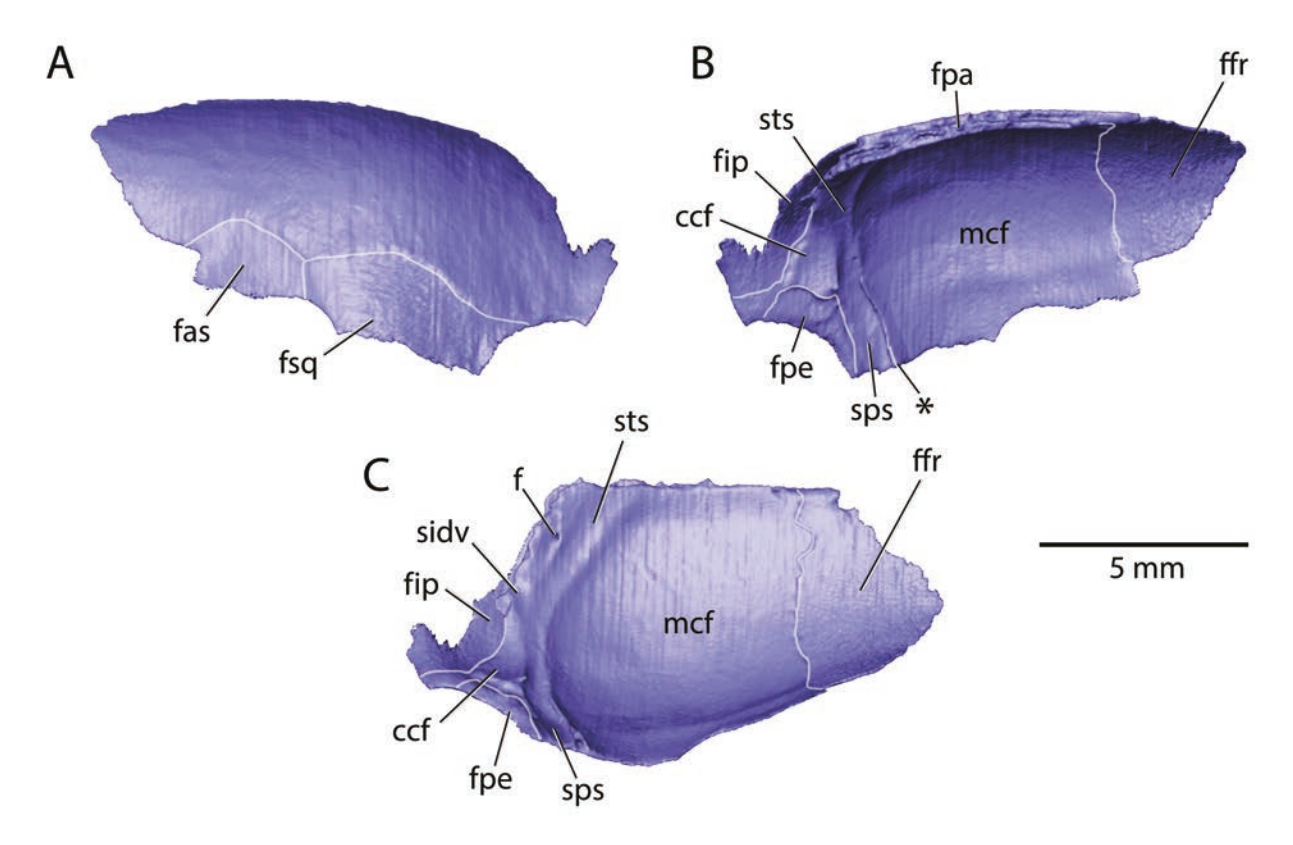


Fig. 13.—Monodelphis domestica, AMNH 261241, left parietal isosurface rendered from CT scans. A, lateral view (anterior to the left); B, medial view (anterior to the right); C, ventral view (anterior to the right). "*" is location of contact with petrosal enclosing the prootic sinus in a canal. Abbreviations: ccf, caudal cranial fossa; f, foramen; fas, facet for alisphenoid; ffr, facet for frontal; fip, facet for interparietal; fpa, facet for opposite parietal; fpe, facet for petrosal; mcf, middle cranial fossa; sidv, sulcus for interparietal diploic vein; sps, sulcus for prootic sinus; sts, sulcus for transverse sinus.

the external surface provides attachment for the temporalis muscle, based on *D. marsupialis* (Hiiemae and Jenkins 1969; Turnbull 1970). AMNH 261241 has a very weak sagittal crest running the length of the parietal midline.

The bulk of the inner surface of the parietal lies in the middle cranial fossa (Figs. 1B, 13B-C). On its anterior aspect is a large facet for the underlying frontal. In the smaller caudal cranial fossa, running nearly the breadth of the parietal surface is the facet for the interparietal; ventrolateral to it and separated by a small exposure of parietal is the facet for the underlying pars canalicularis of the petrosal. Marking the border between the middle and caudal cranial fossae is a prominent venous sulcus. From the midline to the level of the dorsal margin of the facet for the petrosal, this sulcus houses the transverse sinus; however, ventrolateral to that it continues as the sulcus for the prootic sinus (see Wible 2003; Rougier and Wible 2006). The ventralmost extent of the sulcus for the prootic sinus is enclosed in a canal by a small contact between the parietal and pars canalicularis of the petrosal ("*" in Fig. 13C). Off the midline, posterior to the sulcus for the transverse sinus is a small foramen directed anteriorly into the parietal (Fig. 13C); it opens into a diploic space that parallels the transverse sinus sulcus. Lateral to this foramen is a short sulcus directed posteriorly from the transverse sinus sulcus (Fig. 13C); it leads to a foramen into the diploic space of the interparietal (see below).

Interparietal

The interparietal is fused seamlessly with the supraoccipital in AMNH 261241 (Figs. 1, 3B) and is considered with that bone below.

Internal Nasal Skeleton

In the last two decades, the osseous elements of the nasal cavity have been described based on study of CT scans for several marsupials. The most relevant contribution is that of Rowe et al. (2005), which reported on adult *M. domestica* as well as on a series of postnatal specimens. The same specimens used by Rowe et al. (2005) were included in Macrini (2012, 2014), which considered a broader array of marsupials. As these accounts are comprehensive, the reader should consult them for more detail on the internal

nasal skeleton than is provided here for the one adult studied. My intention is to document aspects of the morphology not addressed by Rowe et al. (2005) and Macrini (2012, 2014), and any variations. Identifications and terminology for the internal nasal skeleton differ considerably from author to author, including between Rowe et al. (2005) and Macrini (2012, 2014). These authors used the terms endo-and ectoturbinal, whereas I follow Maier (1993) and Smith and Rossie (2008) among others in using ethmo- and frontoturbinal.

Rowe et al. (2005) reported nine paired turbinals (nasoturbinal, maxilloturbinal, five endoturbinals [here ethmoturbinals], and two ectoturbinals [here frontoturbinals]) for *M. domestica*, which along with the ossified nasal septum, ethmoid, and vomer are essentially a single unit in the adult AMNH 261241. Additionally, the medial palatine processes of the left and right premaxillae of AMNH 261241 are fused to the lateral shelf of the vomer, and the presphenoid and orbitosphenoids are fused to the ossified nasal septum, ethmoid, and vomer. The nasal cavity is roofed, walled laterally, and floored by the paired intramembranous bones of the rostrum described above: nasal, premaxilla, maxilla, palatine, lacrimal, and frontal (Figs. 1B, 4A). Each of these bones in turn has some contact with the main constituents of the internal nasal skeleton.

Ossified nasal septum.—The ossified nasal septum (= mesethmoid of Rowe et al. 2005; Figs. 5B–E, 14A–C, E) occupies the midline from the cribriform plate of the ethmoid posteriorly, where it forms the low crista galli (Fig. 14D), to the level of the mesial root of the upper first premolar; the cartilaginous nasal septum forms the midline anterior to this (Rowe et al. 2005). Roughly the anterior two-thirds of the ossified nasal septum lies in a U-shaped trough on the dorsal aspect of the underlying vomer (Figs. 5B-D, 14E), from which it remains separate, as noted by Rowe et al. (2005). Roughly, the posterior one-third is fused with the surrounding elements, which include the ethmoid, orbitosphenoids, and presphenoid, but the exact boundaries between these structures are not possible to define. Dorsally, the ossified nasal septum contacts the septal processes of the nasals anteriorly (Fig. 14A) and contributes to the nasal tectum (roof) posteriorly where it is continuous with the nasoturbinals (Fig. 15A). Rowe et al. (2005: 310) noted "In adults it may coossify with the frontal and nasal above the olfactory recess" but this is not the case in AMNH 261241. There are three faint sulci that run from posterodorsal to anteroventral on the lateral surface of the ossified nasal septum (Fig. 14B); the two dorsal sulci are more than twice as long as the ventral one. These sulci are in the same position as the vomeronasal nerves are in the dog (Evans and Christensen 1993: fig. 15-1), suggesting that would be their contents in AMNH 261241.

Ethmoid.—Following Rowe et al. (2005), the nine paired turbinals are considered to be components of the ethmoid (Fig. 15). The turbinals coalesce posteriorly at the obliquely oriented cribriform plate, also part of the ethmoid, which separates the nasal cavity from the rostral

cranial fossa (Figs. 1B, 4A). The last part of the ethmoid is more horizontal, ventral to the cribriform plate, and contributes along with the vomer to the transverse lamina (= posterior transverse lamina of Macrini 2012; Figs. 14C, E), which forms the floor of the sphenoidal recess and the roof of the nasopharyngeal meatus. Because the ethmoid forms from multiple bilateral ossification centers in *M. domestica*, Rowe et al. (2005) and Macrini (2012) considered it to be paired. In contrast, in their study of cranial osteogenesis in *M. domestica*, Clark and Smith (1993) reported no separate ethmoid ossification. I follow the standard usage (e.g., NAV) in treating the ethmoid as a single bone, albeit fused to its neighbors. The cribriform plate is treated here, the transverse lamina with the vomer, and the turbinals individually below.

Contacting the dorsal and lateral surfaces of the cribriform plate is the frontal (Figs. 12D), and the posteroventral aspect of the plate is seamlessly fused with the presphenoid and orbitosphenoids (Fig. 14). The midline of the cribriform plate is relatively flat except dorsally where the crista galli is slightly raised (Fig. 14D). There are approximately 50 foramina of various sizes on each side of the cribriform plate. The largest foramen is in the dorsomedial corner of the cribriform plate and leads to the nasoturbinal. Those along the lateral aspect of the plate lead into successively, from dorsal to ventral, frontoturbinal 1 and 2, and then ethmoturbinal I through V. Those on the medial aspect of the plate lead into the common nasal meatus (= septoturbinal space of Macrini 2012).

Vomer.—Rowe et al. (2005) reported the vomer as paired in M. domestica, arising from paired bilateral ossifications that fuse early in ontogeny, whereas Clark and Smith (1993) noted only one center of ossification. I follow the standard usage (e.g., NAV) in treating the vomer as unpaired, albeit fused to other bones. Rowe et al. (2005) described the vomer as having rostral and choanal processes, but the bone is treated here as having midline and bilateral components. The midline component is the U-shaped element that holds the base of the ossified nasal septum (Figs. 5B-D, 14B-C, E); the sides of the U are the lateral laminae, the base is the body, and the dorsal surface of the body is the sulcus septi nasi. Anteriorly, the midline component begins at the level of the mesial root of the upper first premolar and extends posteriorly to the level of the embrasure between the upper second and third (= penultimate) molars. The ventral surface of the midline component abuts the dorsal surface of the left and right maxillae along the midline (Figs. 5B-C, 8C) between the levels of the mesial root of the upper first premolar and the lingual root of the upper second molar. Posterior to this level, a space separates the midline component of the vomer and maxillae and behind that the vomer and palatine; this space is the nasopharyngeal meatus connecting the nasal fossa and nasopharynx at the choanae (Figs. 1B, 5D-E). In ventral view (Fig. 14C), the midline component has paired prongs at its anterior and posterior ends, the former much shorter than the latter. The anterior prongs

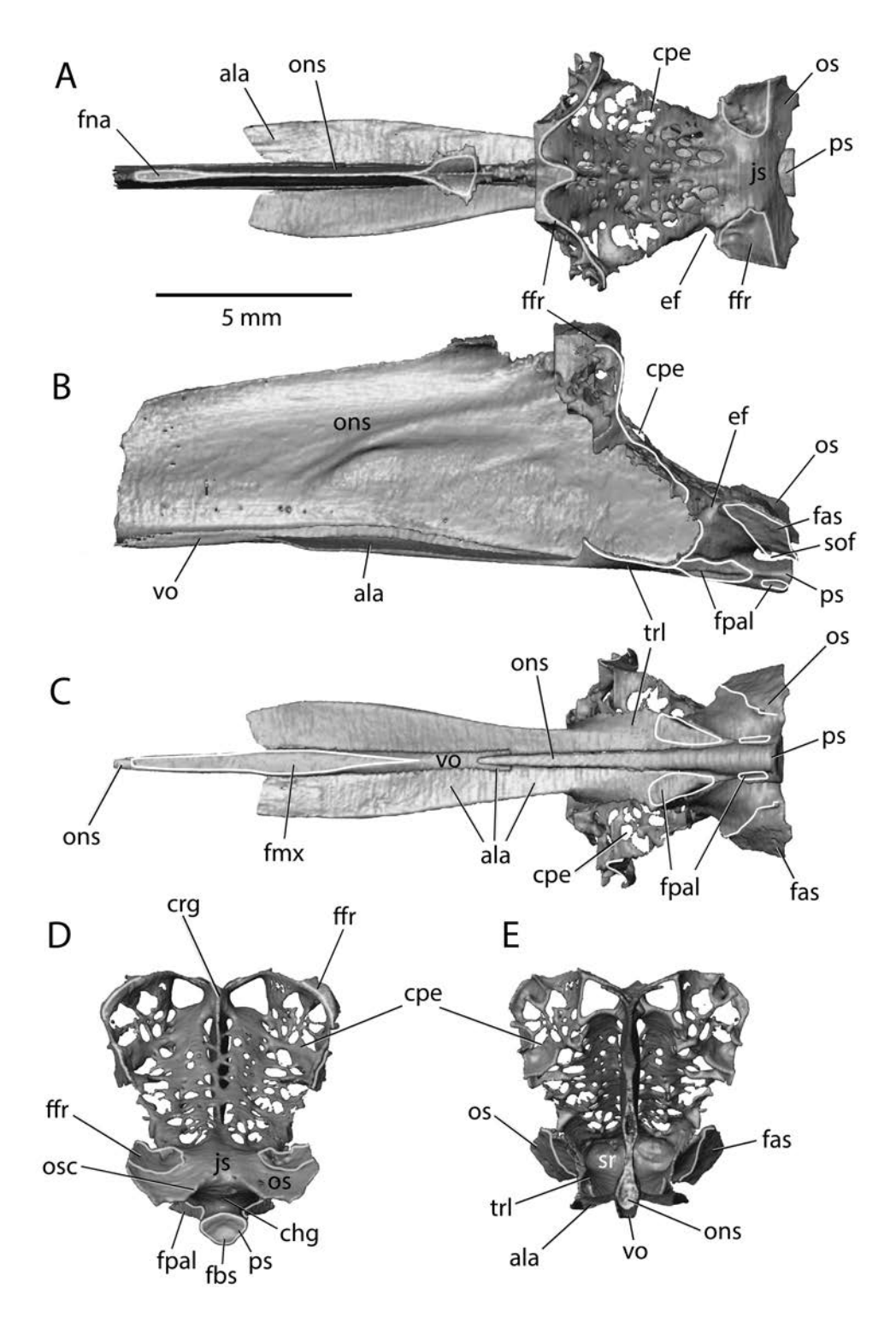


Fig. 14—Monodelphis domestica, AMNH 261241, isosurface of internal nasal skeleton without turbinals rendered from CT scans. A, dorsal view (anterior to the left); B, left lateral view (anterior to the left); C, ventral view (anterior to the left); D, posterior view; E, anterior view. The posterior part of the medial palatine process of the premaxilla, which is fused to the ala vomeris, has been separated from the rest of the premaxilla (see Fig. 5). The lateral edge of the transverse lamina, which is continuous with ethmoturbinal V (see Fig. 15B), has been separated from that structure. Abbreviations: ala, ala vomeris; chg, chiasmatic groove; cpe, cribriform plate of ethmoid; crg, crista galli; ef, location of ethmoidal foramen; fas, facet for alisphenoid; ffr, facet for frontal; fmx, facet for maxilla; fna, facet for nasal; fpal, facet for palatine; js, jugum sphenoidale; ons, ossified nasal septum; os, orbitosphenoid; osc, orbitosphenoid; crest; ps, presphenoid; sof, location of sphenorbital fissure; sr, sphenoidal recess; trl, transverse lamina; vo, vomer.

cradle the osseous nasal septum and contact the medial palatine processes of the premaxillae; the posterior prongs are the base of the vomerine alae or wings (see below).

The bilateral component is a paired shelf that arises anteriorly in the second third of the midline component and then extends posteriorly well behind the midline component (Fig. 14C). As noted above with the premaxilla, this shelf at its anterior origin is continuous with the inferior septal ridge process of the medial palatine process (Figs. 7C, E). In the region where the vomer shelf attaches to the midline component, it arises from the ventrolateral aspect of the lateral lamina (Figs. 5B-C). Rowe et al. (2005) applied two names to this shelf on the vomer: the wider anterior part on the midline component is the paraseptal shelf and the narrower posterior part extending beyond the midline component is the choanal process, which fuses with the ethmoid to form the transverse lamina (Figs. 5D-E). For reasons enumerated in the Discussion, I prefer to call this entire shelf the vomerine wing or ala vomeris (NAV).

The orientation of the vomerine wing is not uniform. It is horizontal anteriorly, slanted ventrolaterally in the middle (Fig. 5C), and with an upturned lateral margin posteriorly (Fig. 5D). The slanted middle section nearly seals off a recess, termed here the sub-alar recess, that ultimately extends from the incisive foramen to the nasopharyngeal meatus (Fig. 5C). Although fused, the vomerine wing is distinguished from the transverse lamina because its lateral edges are upturned to an even greater extent (Figs. 1B, 4B, 5E, 14C) and are continuous with ethmoturbinal V (Figs. 5E, 15B). As noted with the palatine (Fig. 9D), the transverse lamina contacts the lamina sphenoethmoidalis to form the roof of the nasopharyngeal meatus and the floor of the sphenoidal recess (Figs. 4A–B).

Maxilloturbinal.—The cigar-shaped maxilloturbinal (Fig. 15) extends from just behind the upper anterior incisors to the level of the embrasure between the upper second and third molars; it is visible through the external nasal aperture, the incisive foramen, and the maxillopalatine fenestra. The basal lamina of the maxilloturbinal contacts crests on the maxilla (Fig. 8B) and premaxilla (Fig. 7B) between the levels of the upper ultimate premolar and the diastema between the upper canine and upper ultimate incisor. There is a short segment of the posterior contact on the maxilla where the basal lamina and maxilla enclose a nasolacrimal canal; anterior to this, the basal lamina defines the roof of a nasolacrimal groove (Fig. 8B). The posterior surface of the basal lamina has a tiny contact with the lacrimal (Fig. 10B) and nasoturbinal.

Nasoturbinal.—In his comparative study across marsupials, Macrini (2012) divided the nasoturbinal into rostral and caudal parts. He noted that *M. domestica* has only the caudal part. In contrast, Rowe et al. (2005) called the element in *M. domestica* the nasoturbinal, which is the usage followed here. The nasoturbinal is roughly U-shaped with a medial arm on the dorsomedial cribriform plate and a lateral arm on ethmoturbinal I (Fig. 15). It extends rostrally to the level of the upper second premolar, overlying

ethmoturbinal I and in turn overlain by frontoturbinal 1 and 2. The relatively flat dorsal surface of the nasoturbinal forms the medial wall of the anterolateral recess (= superior recess of maxillary sinus of Rowe et al. 2005; Figs. 4A, C, 5C). The nasoturbinal has contacts with more bones of the rostrum than any turbinal. Starting at the cribriform plate, the nasoturbinal abuts a facet on the frontal (Fig. 12D), a crest and facet on the nasal (Fig. 6C), a crest on the maxilla (Fig. 8B) and lacrimal (Fig. 10B), and lastly has a small contact with the palatine (Fig. 9D).

Ethmoturbinal I.—Ethmoturbinal I (Fig. 15) extends from the cribriform plate at the level of the lingual root of the upper ultimate molar to the level of the anterior margin of the upper canine. It is visible through the maxillopalatine fenestra posterior to the maxilloturbinal and through the external nasal aperture where it forms a scroll on the dorsal and medial aspects of the maxilloturbinal (Fig. 5B) Anterior to the cribriform plate, ethmoturbinal I has a broad contact with a facet on the frontal (Fig. 12D), the only bone of the rostrum exterior that it contacts.

Ethmoturbinal II.—Ethmoturbinal II (Fig. 15) extends from the cribriform plate just ventral to ethmoturbinal I to the level of the distal root of the upper ultimate premolar. It contacts a crest and facet on the frontal rostral to the cribriform plate (Fig. 12D) and then abuts a crest on the palatine (Fig. 8D).

Ethmoturbinal III.—Ethmoturbinal III (Fig. 15) extends from the cribriform plate just ventral to ethmoturbinal II to the level of the distal root of the upper second molar. It has a tiny exposure behind ethmoturbinal I at the maxillopalatine fenestra and contacts crests on the frontal (Fig. 12D) and palatine (Fig. 9D) rostral to the cribriform plate.

Ethmoturbinal IV.—Ethmoturbinal IV (Fig. 15) extends from the cribriform plate just ventral to ethmoturbinal III to the level of the embrasure between the upper first and second molars. Rostral to the cribriform plate, it contacts faint crests on the frontal (Fig. 12D) and palatine (Fig. 9D).

Ethmoturbinal V.—Ethmoturbinal V (Fig. 15) extends from the cribriform plate just ventral to ethmoturbinal IV within the sphenoidal recess (sphenethmoid recess of Rowe et al. 2005) to the level of the lingual root of the upper second molar. Rostral to the cribriform plate, it contacts faint crests on the frontal (Fig. 12D) and palatine (Fig. 9D) and is continuous with the transverse lamina (Figs. 5E, 14B, 15B).

Frontoturbinal 1.—Frontoturbinal 1 (Fig. 15) extends from the dorsolateral corner of the cribriform plate to the level of the mesial root of the upper ultimate premolar. Rostral to the cribriform plate, it contacts a sulcus and facet on the frontal (Fig. 12D) and then a facet on the maxilla (Fig. 8B).

Frontoturbinal 2.— Frontoturbinal 2 (Fig. 15) extends from the cribriform plate between frontoturbinal 1 and ethmoturbinal I to the level of the mesial root of the upper ultimate premolar. Rostral to the cribriform plate, it contacts

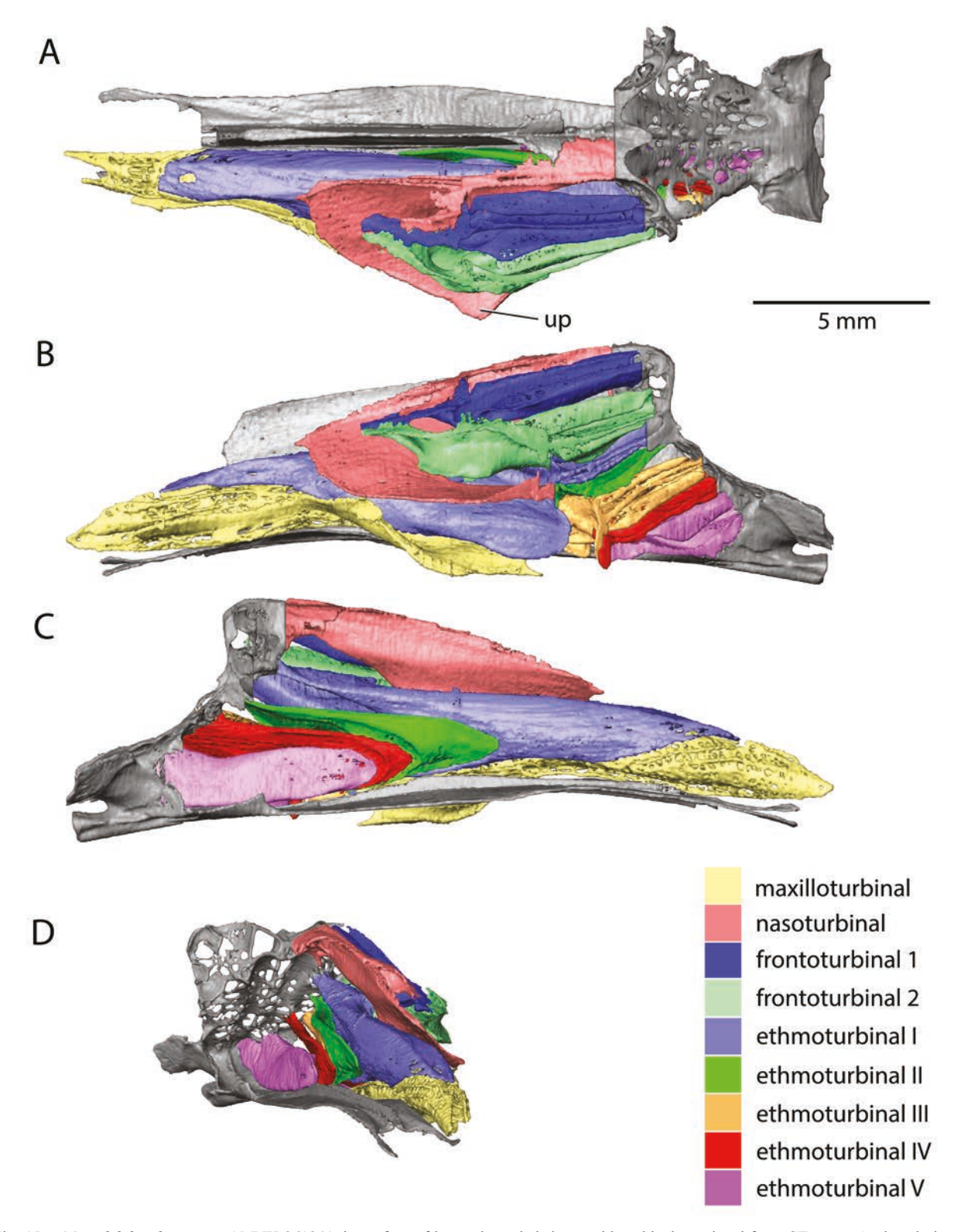


Fig. 15.—Monodelphis domestica, AMNH 261241, isosurface of internal nasal skeleton with turbinals rendered from CT scans. A, dorsal view (anterior to the left); B, left lateral view (anterior to the left); C, left medial view with ossified nasal septum removed (anterior to the right); D, oblique anteromedial view. With the exception of the maxilloturbinal, the other turbinals are continuous with the cribriform plate of the ethmoid, but have been individually segmented and colorized from the cribriform plate following Rowe et al. (2005) and Macrini (2012) in order to visualize them. Abbreviation: up, uncinate process.

facets on the frontal (Fig. 12D), lacrimal (Fig. 10B), and maxilla (Fig. 8B).

Sphenoid Complex

Following Clark and Smith (1993), the sphenoid complex of *M. domestica* is composed of anterior and posterior parts, each of which includes a midline component and paired wings. The anterior part is the midline presphenoid and the winged orbitosphenoids; the posterior part is the midline basisphenoid and the winged alisphenoids. AMNH 261241 shows this pattern but is complicated by the fusion of the anterior part of the sphenoid complex with the internal nasal skeleton noted above (Fig. 14). It appears likely that Rowe et al. (2005: 312) found the same situation in their *M. domestica* specimens, as they wrote "The mesethmoid [= ossified nasal septum here] ends caudally inside the nose, at the back of the sphenethmoid recess, where it joins the orbitosphenoid at a point near the optic chiasm."

As the sphenoid complex is such an integral component of the cranium, I have illustrated it in two views in Figure 16 along with the closely associated pterygoids. This figure shows that the anterior part is dwarfed by the massive posterior part. These two parts of the sphenoid complex are considered separately below.

Presphenoid and Orbitosphenoids

The presphenoid ("ps") and paired orbitosphenoids ("os") contribute to the floor of the rostral cranial fossa (Fig. 1B), but have little exposure on the cranial exterior, best seen in lateral view with the jugal removed in the vicinity of the sphenorbital fissure (Fig. 3A); the presphenoid is also exposed on the ventral midline in the roof of the basipharyngeal canal (Fig. 2B). These bones are fused with each other and in turn with the internal nasal skeleton (Fig. 14); the boundaries delimiting the pre- and orbitosphenoid followed here conform to those in Evans and Christensen (1993) where the orbitosphenoids are referred to as the orbital wings or alae orbitalis (lesser wings). The pre- and orbitosphenoid are shown with the internal nasal skeleton in Figures 14 and 15 and with the sphenoid complex in Figure 16.

When isolated from the dermal bones around them, the presphenoid and orbitosphenoids show a complex morphology especially in light of their fusion to the internal nasal skeleton (Figs. 14–15). The presphenoid body is the rod-like central base, which in ventral view (Fig. 14C) tapers anteriorly into the ossified nasal septum and continues anterolaterally into a more horizontal shelf, the transverse lamina (see Vomer above). On the lateral side of the presphenoid body are paired facets for the palatine (Fig. 14B). The posterior face of the presphenoid is oval and contacts the basisphenoid in the basicranial central stem (Figs. 14D, 16).

The dorsal surface of the presphenoid body can be

treated in anterior and posterior halves. The posterior half does not contact other bones and is exposed in the anteriormost midline floor of the middle cranial fossa (Figs. 1B, 16B). The sphenorbital fissures lie lateral to the presphenoid body here, and the left and right fissures communicate across the posterior half of the dorsal surface of the presphenoid (Figs. 3A, 16B). The anterior half of the presphenoid serves as a pedestal for the orbitosphenoids. The posterior face of the pedestal is marked by the chiasmatic groove for the optic nerves (Fig. 14D), which leave the cranial cavity via the sphenorbital fissure.

The orbitosphenoids have the shape of an empty bin tilted such that the rim of the bin is attached to the presphenoid and the bin opening points anteriorly (Figs. 1B, 16A). The rear of the bin overhangs the gap connecting the sphenorbital fissures. The empty bin is divided by the ossified nasal septum into paired sphenoidal recesses (Fig. 14E), which house the posterior attachments of ethmoturbinal V (Fig. 15). The roof of the bin forms the floor of the rostral cranial fossa posterior to the cribriform plate of the ethmoid (Figs. 1B, 14A, D, 16B). The bin roof is flat along the midline and represents the voke or jugum sphenoidale (Figs. 14A, D, 16B). The orbitosphenoid wings fan out laterally and posterolaterally from the jugum. Laterally, the wings are overlaid by the frontals, and posterolaterally, the wings end at a sharp orbitosphenoidal crest (Figs. 14D, 16B), which contributes to the posterior boundary of the rostral cranial fossa. The lateral surface of each orbitosphenoid wing has anterior and posterior halves. The posterior half overhangs the gap between the sphenorbital fissures and is overlaid by the alisphenoid (Figs. 14B-C, E). The anterior half is the small quadrangular area of orbitosphenoid that is exposed in the orbit between the palatine, frontal, and alisphenoid (Figs. 3A, 16A). In the dorsal margin of this exposure is the ethmoidal foramen in the suture between the orbitosphenoid and frontal with a shallow groove on the orbitosphenoid leading into it from below (Fig. 16A).

Basisphenoid and Alisphenoids

The basisphenoid and paired alisphenoids are visible in all views of the hemi-cranium in Figures 1–3 ("bs" and "as," respectively) and are the primary elements of the floor of the middle cranial fossa (Fig. 1B) and anterior basicranium (Fig. 2B). The bones are fused to each other and the boundaries delimiting the basi- and alisphenoid followed here conform to those in Evans and Christensen (1993) where the alisphenoids are referred to as the temporal wings or alae temporalis (greater wings). The basi- and alisphenoid are shown with the sphenoid complex in Figure 16 and isolated in Figure 17.

The body of the basisphenoid is keystone shaped with the short transverse axis abutting the presphenoid anteriorly and the long transverse axis abutting the basioccipital posteriorly (Fig. 17). The anterior half of the body is rod-like

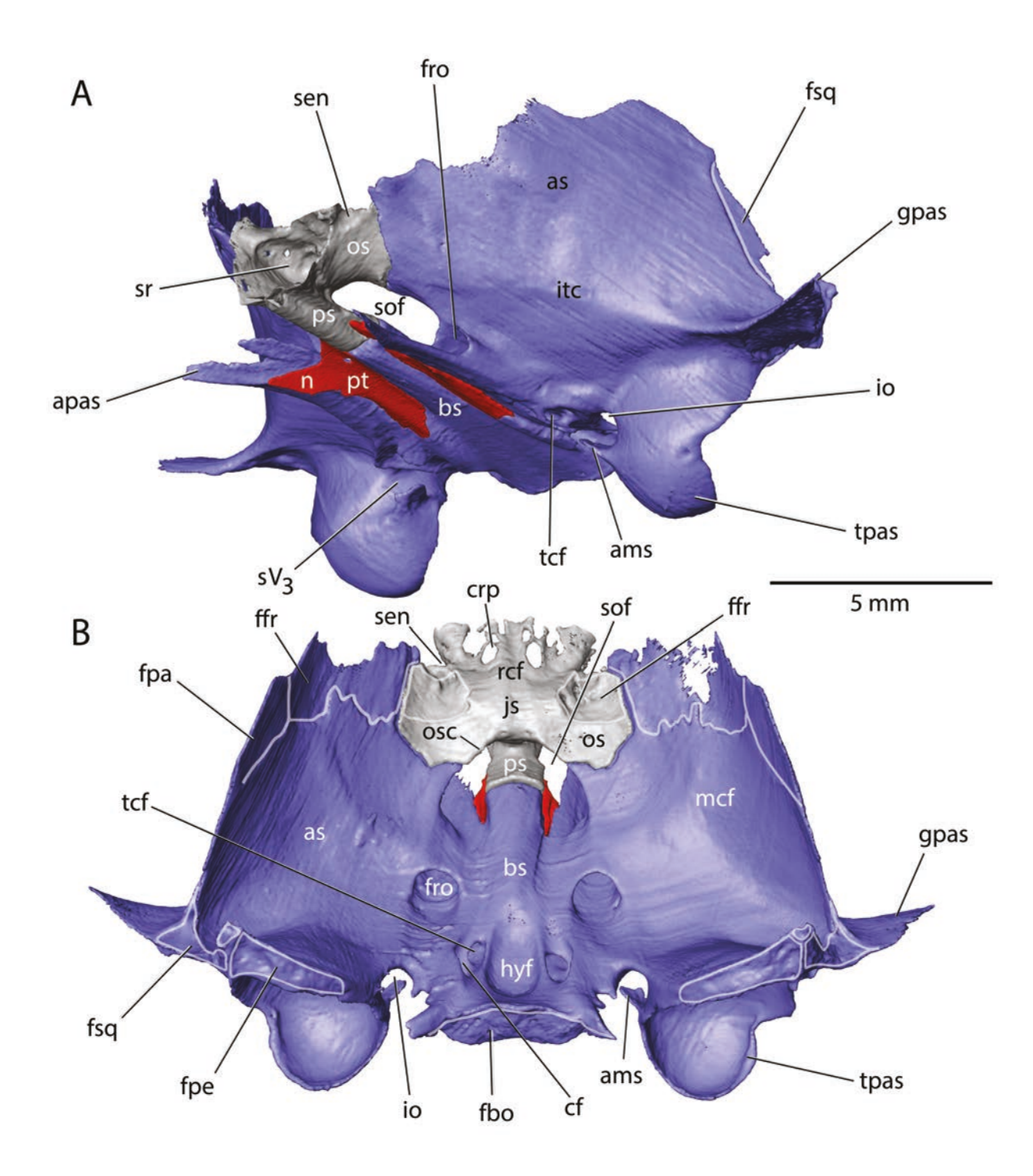


Fig. 16.—Monodelphis domestica, AMNH 261241, isosurface rendered from CT scans of sphenoid complex (pre- and orbitosphenoids in gray; basi- and alisphenoids in blue) plus pterygoid (in red). A, oblique anterolateral view (anterior to the left); B, oblique dorsal view (anterior to the top). The pre- and orbitosphenoids have been separated from the internal nasal skeleton in A but part of the cribriform plate of the ethmoid is preserved in B (see Fig. 14). Most of the vertical portion of the pterygoid is missing (see Fig. 18). Abbreviations: ams, anteromedial strut; apas, anterior process of alisphenoid; as, alisphenoid; bs, basisphenoid; cf, carotid foramen; fbo, facet for basioccipital; fpa, facet for parietal; fpal, facet for palatine; fpe, facet for petrosal; fro, foramen rotundum; fsq, facet for squamosal; gpas, glenoid process of alisphenoid; hyf, hypophyseal fossa; io, incisura ovalis; itc, infratemporal crest; mcf, middle cranial fossa; n, neck of pterygoid; pt, pterygoid; rcf, rostral cranial fossa; sen, sulcus for ethmoidal nerve; sof, sphenorbital fissure; sV₃, sulcus for mandibular nerve; tcf, transverse canal foramen; tpas, tympanic process of alisphenoid.

in both ventral and dorsal views, similar to the presphenoid body anterior to it. Along the ventrolateral aspect of the anterior half is a facet for the underlying pterygoid, which also extends laterally onto the alisphenoid (Fig. 17A). The posterior half of the basisphenoid is flat in ventral view except along its lateral margin where there is a rounded ridge at the rear of which is the anteriorly directed carotid foramen. Lateral to this rounded ridge is a narrow sulcus transmitting the nerve of the pterygoid canal, which in the anterior half of the basisphenoid occupies a canal between the basisphenoid, alisphenoid, and pterygoid. Lateral to the sulcus for the nerve of the pterygoid canal is a medially directed transverse canal foramen (Fig. 16A), largely hidden in ventral view (Fig. 17A), which serves as the boundary between the basi- and alisphenoid. Lateral to the transverse canal foramen is a small depression. In the dorsolateral aspect of this depression are two small foramina (Fig. 17A) that open into diploic spaces in the alisphenoid and presumably transmit diploic veins. Posterolateral to the carotid foramen is a notch in the basisphenoid indicating the position of the exit of the greater petrosal nerve from the cranial cavity; this notch is not enclosed as a foramen but is part of a larger opening between the petrosal and basi- and alisphenoid, the piriform fenestra (Fig. 2B). From this notch, the greater petrosal nerve with contribution from the internal carotid nerve runs forward as the nerve of the pterygoid canal. The posterolateral corners of the basisphenoid have sharp, posterolaterally directed prongs (Fig. 17); contacting these prongs are the basioccipital medially and the petrosal laterally.

The dorsal surface of the posterior half of the basisphenoid has an oval-shaped, midline depression, the hypophyseal fossa for the pituitary gland (Figs. 16B, 17B). The basisphenoid posterior to the hypophyseal fossa slopes gently ventrally to meet the basioccipital, but a dorsum sellae is not produced. Lateral to the posterior aspect of the hypophseal fossa is the endocranial aperture of the carotid foramen, which leads into a broad, anteromedially directed carotid groove (Fig. 17B). In the floor of the carotid groove opposite the anterior aspect of the hypophyseal fossa is a depression into which open three foramina that are largely hidden in dorsal view. The largest of the three is in the lateral wall of this depression and is the endocranial aperture of the transverse canal foramen. The other two ("f" in Fig. 17B) are smaller, medially directed, and positioned at the level of the anterior and posterior margins of the hypophyseal fossa. The CT scans reveal that these two foramina communicate across the midline, presumably transmitting transverse sinuses. The posterior of these also communicates with the hypophyseal fossa via tiny openings in the fossa floor.

The alisphenoid projects laterally from the basisphenoid and then curves dorsally into the braincase sidewall. Although the alisphenoid is longer than the basisphenoid, its connection is roughly three-quarters the length of the basisphenoid body (Fig. 17). Its posterior border is ballooned out to form a hemispherical tympanic process that

projects well below the basicranium (Fig. 1A) and partially shields the ectotympanic (Wible 2003). The inner concave surface of this hemisphere is a large hypotympanic sinus of the middle ear (Fig. 17A). According to Wible (2003), the anterior crus of the ectotympanic contacts the tympanic process, but this bone is absent in AMNH 261241 and there is no visible facet on the tympanic process to illustrate. Lateral to the hypotympanic sinus and tympanic process is a broad facet for the underlying part of the squamosal sporting the glenoid fossa. Medial to this facet is the glenoid process of the alisphenoid, which buttresses the glenoid fossa both ventrally (Fig. 17A) and dorsally (Fig. 17B). Extending anteromedially from the base of the glenoid process is a distinct infratemporal crest (Figs. 16A, 17A), delimiting the temporal and infratemporal fossae. Opposite the posterolateral corner of the tympanic process is the prominent postglenoid process of the squamosal (see below) and separating the two is a deep notch formed by both bones, the Glaserian fissure (Fig. 17A), transmitting the chorda tympani nerve. Projecting from the anteromedial aspect of the tympanic process is a short, flat, rounded protuberance, the anteromedial strut of Voss and Jansa (2003), which is associated with the course of the mandibular nerve (Figs. 16, 17A). This nerve exits the cranial cavity at the incisura ovalis in the alisphenoid (Figs. 16B, 17B), which is part of the larger piriform fenestra mentioned above (Fig. 2B). The nerve runs anteroventrally in a short groove on the alisphenoid before turning ventrolaterally across the tympanic process dorsal to the anteromedial strut (Fig. 17A). The strut contributes to the formation of a partial secondary foramen ovale for the mandibular nerve. At the opposite end of the alisphenoid is the elongate anterior process (Figs. 16A, 17), which lies in an oblique plane and overlies the perpendicular process of the palatine in the rear of the orbit (Fig. 3B).

In dorsal view (Fig. 16B, 17B), the inner dorsolateral margin of the alisphenoid has facets from anterior to posterior for the underlying orbitosphenoid, frontal, and parietal. At the lateral corner of the alisphenoid's posterior border (Fig. 16B, 17B) is a facet for the overlying squamosal. Medial to this is a small facet for the parietal (Fig. 16B), where these two bones contact posterior to the endocranial exposure of the squamosal in the rear of the middle cranial fossa (Fig. 1B). The dorsomedial surface of the alisphenoid has a broad longitudinal sulcus housing the trigeminal nerve. The sulcus is directed primarily at the large foramen rotundum (for V2), which opens anteriorly near the base of the anterior process of the alisphenoid, posterolateral to the sphenorbital fissure (Fig. 16A). Medial to the posterior opening of the foramen rotundum is a narrower, poorly defined longitudinal sulcus representing the floor of the sphenorbital fissure (Fig. 17B).

Pterygoid

As noted above, the pterygoids are damaged in AMNH 261241, preserving only the horizontal portion on the

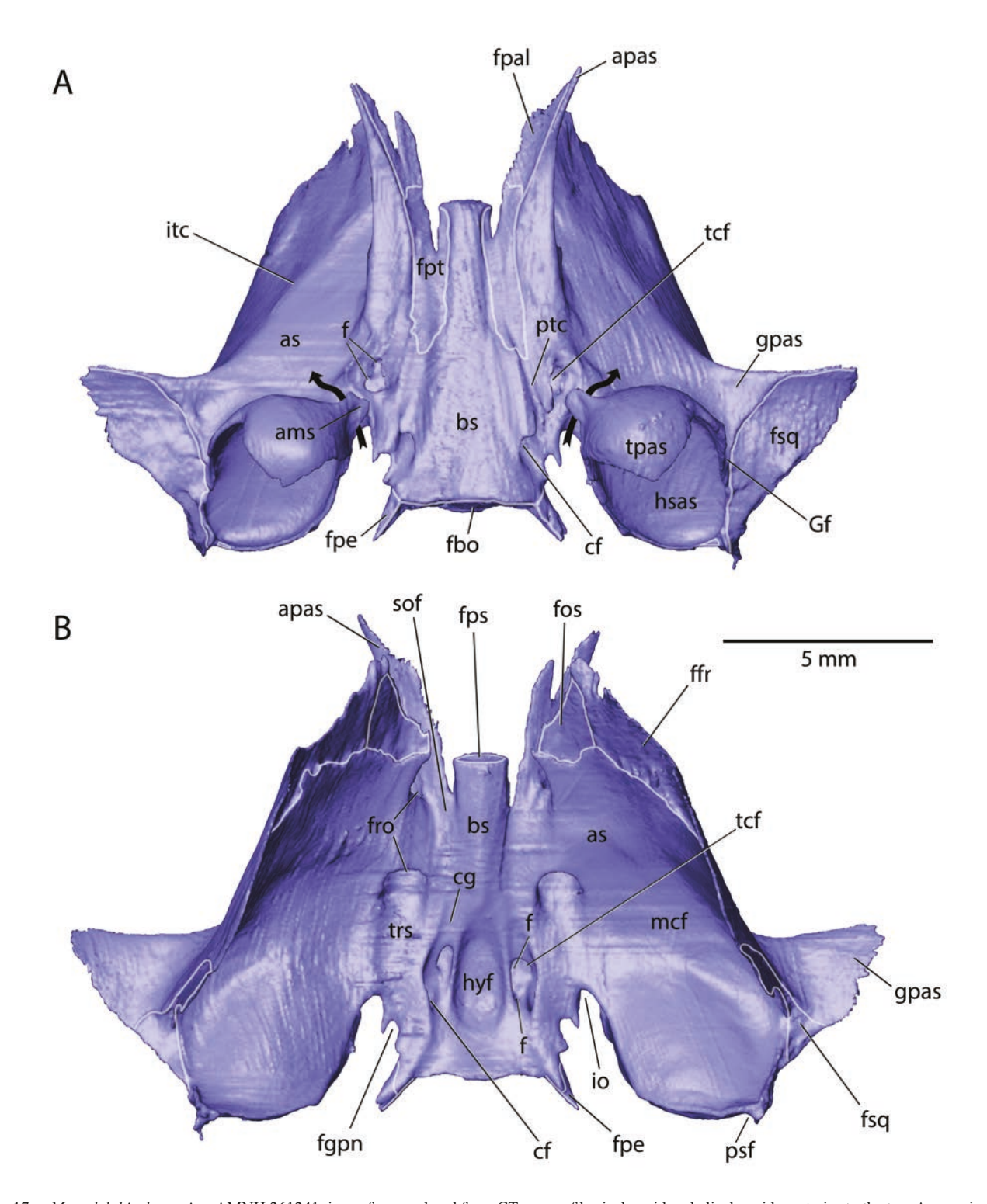


Fig. 17.—Monodelphis domestica, AMNH 261241, isosurface rendered from CT scans of basisphenoid and alisphenoids; anterior to the top. Arrows in A indicate the course of the mandibular nerve (cranial nerve V₃). A, ventral view; B, dorsal view. Abbreviations: ams, anteromedial strut; apas, anterior process of alisphenoid; as, alisphenoid; bs, basisphenoid; cf, carotid foramen; cg, carotid groove; f, foramen; fbo, facet for basioccipital; fgpn, foramen for greater petrosal nerve; fos, facet for orbitosphenoid; fpal, facet for palatine; fpe, facet for petrosal; fps, facet for presphenoid; fpt, facet for pterygoid; fro, foramen rotundum; fsq, facet for squamosal; Gf, Glaserian fissure; gpas, glenoid process of alisphenoid; hsas, hypotympanic sinus of alisphenoid; hyf, hypophyseal fossa; io, incisura ovalis; itc, infratemporal crest; mcf, middle cranial fossa; psf, contribution to foramen for prootic sinus; ptc, sulcus for nerve of pterygoid canal; sof, sphenorbital fissure; tcf. transverse canal foramen; tpas, tympanic process of alisphenoid; trs, trigeminal sulcus.

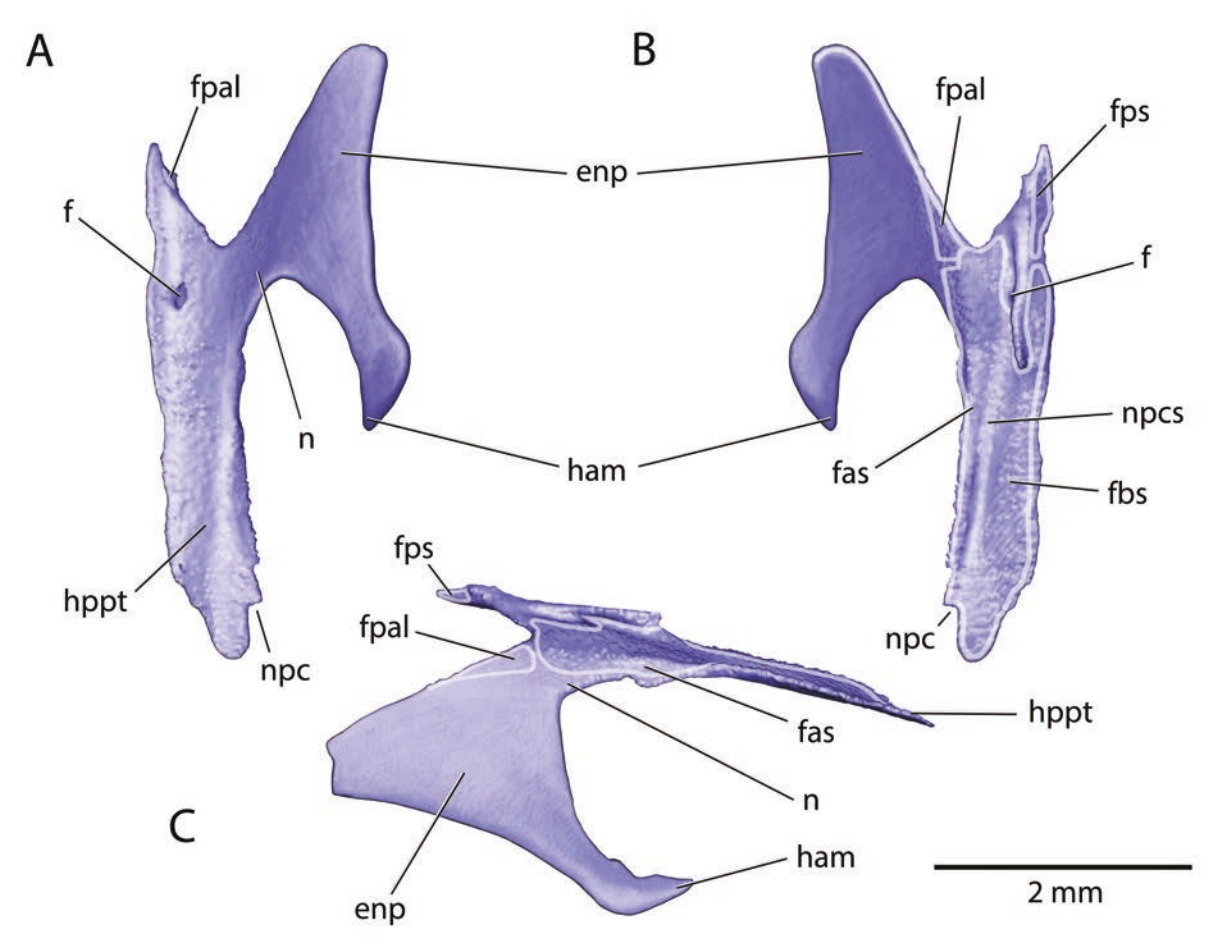


Fig. 18.—Monodelphis domestica, left pterygoid. A, ventral view (anterior to the top); B, dorsal (anterior to the top); C, lateral views (anterior to the left) Horizontal portion is isosurface rendered from CT scans of AMNH 261241; vertical portion (entopterygoid crest) is from CM 80031. Abbreviations: enp, entopterygoid crest; f, foramen; fas, facet for alisphenoid; fbs, facet for basisphenoid; fpal, facet for palatine; fps, facet for presphenoid; ham, hamulus; hppt, horizontal portion of pterygoid; n, neck; npc, notch indicating foramen for nerve of pterygoid canal; npcs, nerve of pterygoid canal sulcus.

basicranium and missing the vertical portion forming the entopterygoid crest except for the neck of the crest (see Figs. 2B, 16A). In illustrating the isolated left pterygoid of AMNH 261241 (Fig. 18), the vertical portion is restored based on intact elements in *M. domestica*, CM 80031.

The horizontal portion is roughly a flat parallelogram, with long medial and lateral sides and short anterior and posterior sides (Fig. 18A). It sits primarily on the basi- and alisphenoid but also at its anterior end on the presphenoid and palatine. These contacts are reflected in facets on the dorsal surface of the pterygoid (Fig. 18B). On the posterolateral aspect of the horizontal portion is a shallow indent indicating the position of a foramen for the nerve of the pterygoid canal, which is closed dorsally by the basi- and alisphenoid (Fig. 18A). A sulcus for the nerve runs anteromedially from this foramen on the dorsal surface of the horizontal portion (Fig. 18B). The sulcus is transformed into a canal by the overlying basi- and alisphenoid. Near the anterior end of the sulcus is a small foramen of uncertain

function that penetrates to the ventral surface (Fig. 18A). Similar foramina are variably present in the CM sample. Wible (2003) did not discuss this foramen, but it is figured on the right pterygoid of *M. arlindoi*, CM 52729, but is absent on the left (Wible 2003: fig. 5). As noted above, there is a small exposure of the horizontal portion visible through the sphenorbital fissure (Figs. 3A, 16B); it is lateral to this small piece of pterygoid that the nerve of the pterygoid canal leaves its canal between the pterygoid and alisphenoid to enter the orbit.

The vertical portion of the pterygoid is flat and roughly triangular (Fig. 18C); it is connected to the horizontal portion by a narrow neck. The dorsal side runs anteroventrally from the neck and is the only side in contact with another bone, in its case the palatine (Fig. 9B). A second side runs ventrally from the neck but curves posteriorly ending in a distinct hook-like hamulus (Fig. 18C). The third and longest side forms the ventral border of the entopterygoid crest. In *D. marsupialis*, the medial or internal pterygoid

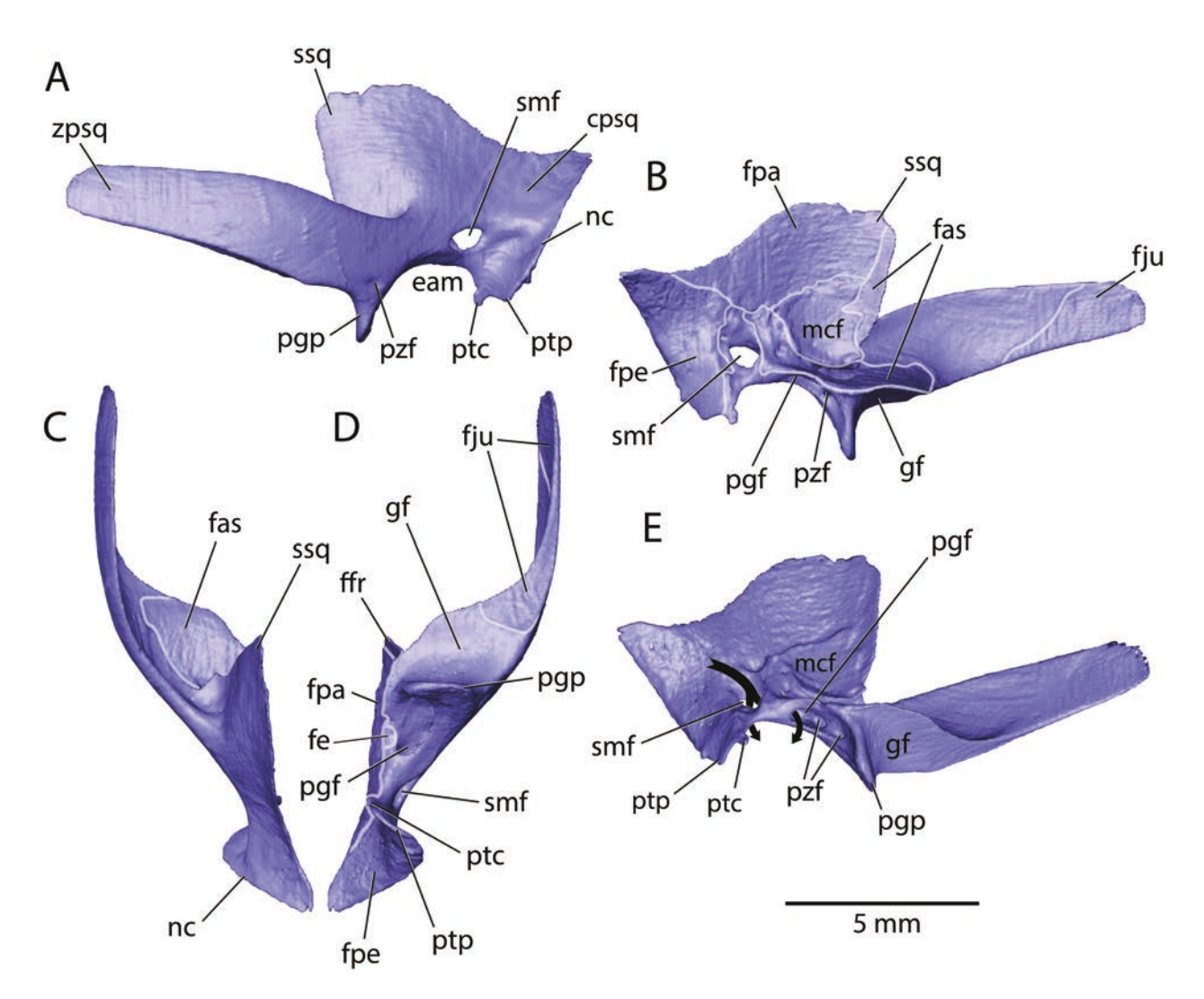


Fig. 19.—Monodelphis domestica, AMNH 261241, isosurface of left squamosal rendered from CT scans. A, lateral view (anterior to the left); B, medial view (anterior to the right); C, dorsal view (anterior to the top); D, ventral view (anterior to the top); E, oblique medial view (anterior to the right). Arrows in E indicate the course of the postglenoid and suprameatal veins. Abbreviations: cpsq, caudal process of squamosal; eam, external acoustic meatus; fas, facet for alisphenoid; fe, facet for ectotympanic; ffr, facet for frontal; fju, facet for jugal; fpa, facet for parietal; fpe, facet for petrosal; gf, glenoid fossa; mcf, middle cranial fossa; nc, nuchal crest; pgf, postglenoid foramen; ptc, posttympanic crest; ptp, posttympanic process; pzf, postzygomatic foramen; smf, suprameatal foramen; ssq, squama of squamosal; zpsq, zygomatic process of squamosal.

muscle attaches to the lateral surface of the vertical portion and adjacent parts of the palatine and alisphenoid (Hiiemae and Jenkins 1969; Turnbull 1970).

Squamosal

The squamosal is visible in all views of the hemi-cranium in Figures 1–3. The squamosal is primarily an element of the braincase and zygoma, and has only a small exposure in the posterolateral wall of the middle cranial fossa (Fig. 1B). The isolated left squamosal is shown in multiple views in Figure 19.

The squamosal can be divided into three parts: the zygo-

matic process, the squama, and the caudal process (Wible 2003 included the caudal process with the squama). The zygomatic process contributes to the posterior half of the zygoma (Fig. 1A) and includes the glenoid fossa, which lies entirely on the zygomatic root (Fig. 2B). The zygomatic process has facets on its anteromedial surface for the jugal and on its posterodorsal surface for the glenoid process of the alisphenoid (Fig. 19B). The squama, the portion on the braincase wall anterior to the level of the glenoid fossa, has facets for the underlying parietal and alisphenoid, with only a small exposure in the middle cranial fossa. The caudal process, which is posterior to the level of the glenoid, has no endocranial exposure but is excluded

by the underlying parietal, alisphenoid, and petrosal. It has a small area that does not contact another bone in the vicinity of the suprameatal foramen; this area transmits the prootic sinus (see below). On the ventral surface behind the glenoid fossa (Fig. 19D) are consecutively the postglenoid process, postglenoid foramen, posttympanic crest, and posttympanic process. Wible (2003) reported the anterior crus of the ectotympanic contacted the squamosal medial to the postglenoid foramen in *Monodelphis*. Although the ectotympanic is missing in AMNH 261241, this contact is included in Figure 19D because a small facet is present. The lateral surface of the squamosal has two more foramina, the large suprameatal foramen above the external acoustic meatus and the tiny postzygomatic foramen at the base of the postglenoid process. In the CT scans, I was able to trace the course of the major veins of the squamosal (see Wible 2003). As noted above (see Parietal), the prootic sinus (Fig. 1B) first runs in a groove on the parietal and then in a canal between the parietal and petrosal. This is followed by a short canal between the squamosal and petrosal before the prootic sinus becomes the sphenoparietal emissary vein (Gelderen 1924), also known as the postglenoid vein. The sphenoparietal emissary vein (Fig. 19E) has a branch out of the suprameatal foramen and then runs through a canal in the squamosal with the vein exiting ventrally at the postglenoid foramen. In the anterolateral aspect of the postglenoid foramen are two small postzygomatic foramina that communicate with the small foramen of the same name on the lateral base of the postglenoid process (Fig. 19A); these postzygomatic foramina are venous in nature. As noted by Wible (2003), the postglenoid foramen in M. domestica also transmits a small postglenoid artery that does not ramify further.

Petrosal

Wible (2003: figs. 7–8) illustrated an isolated left petrosal of *Monodelphis* sp., CM 5024, in three views and reconstructed the major veins and facial nerve. He described that bone along with an isolated right petrosal of *M. glirina*, CM 5061. The most substantive additions here to those descriptions concern changes in terminology, any varying features, and illustration of facets on the petrosal for neighboring bones. Although not well exposed on the cranial exterior, the petrosal is visible in all views of the hemi-cranium in Figures 1–3. The isolated left petrosal is shown in five views in Figure 20.

Ekdale (2010) reported various measurement of the bony labyrinth for an ontogenetic series of *M. domestica*. The two measurements that I repeat here for AMNH 261241 following Ekdale's (2010) methods are the cochlea coiling and stapedial ratio (length to width of the fenestra vestibuli). The cochlea coiling in Ekdale's (2010) sample ranged from 604° to 685° with the adult individual at 650°; AMNH 261241 is 630°. The stapedial ratio in Ekdale's (2010) sample ranged from the low of 1.3 in the adult to 1.7; the ratio for the left petrosal of AMNH 261241 is 1.36.

As with other didelphids, *M. domestica*, AMNH 261241, has a shelf directed anteromedially from the promontorium. Wible (2003) called this an anteromedial flange, but following Wible and Shelley (2020), I refer to this as the epitympanic wing (Figs. 20A–C). Additionally, there is a sharp crest running on the ventral surface of the epitympanic wing that represents an anterior septum (Figs. 20C–D); this is present in the CM *Monodelphis* sample but unnamed by Wible (2003).

AMNH 261241 has a long, delicate spinous process anterior to the epitympanic recess, identified here as the tip of the tegmen tympani (Fig. 20). Wible (2003: fig. 7) illustrated a short, blunt process in the comparable place in Monodelphis sp., CM 5024, and called it a tuberculum tympani, following Toeplitz (1920), but noted its homology with the placental tegmen tympani, following Kuhn and Zeller (1987). I revisited CM 5024 and discovered that the tip of this process is broken. In restudying the CM sample, I was unable to determine the condition of the tegmen tympani in the vast majority of specimens because the element was obscured by tissue and/or the ectotympanic. Of the instances where I could see the tegmen, I found it to be broken in eight specimens (five M. domestica, one M. arlindoi, one M. glirina, and one M. dimidiata). There were two M. domestica, CM 80031 and 80036, in which the tegmen was not broken and was not as prolonged a spine as in AMNH 261241. In light of this small M. domestica sample, it appears the length of the tegmen may be variable. An additional difference I noted concerned contact between the anterior crus of the ectotympanic and tegmen. These were close in the two M. domestica showing an unbroken tegmen, CM 80031 and 80036, but the ectotympanic overlaid and obscure the tegmen in two others, CM 80027 and 80032. The meaning of this variation is unclear as the difference in contact with the ectotympanic may result from preservational issues.

CM 5024 and 5061 preserved ossified cartilage of Paaw in the stapedius fossa (see Wible et al. 2021) but this element is absent in AMNH 261241. In light of its broad distribution in the CM *Monodelphis* sample (Wible et al. 2021), its absence in AMNH 261241 is likely an issue of preservation.

As apparent in Figure 20, the petrosal has a complex series of facets where it abuts it neighbors, including the basisphenoid, alisphenoid, squamosal, parietal, basioccipital, and exoccipital, all of them already reported in Wible (2003), although not illustrated. One contact not illustrated in Figure 20 but reported by Wible (2003) is between the rostral tympanic process and posterior crus of the ectotympanic, as the latter bone is not preserved in AMNH 261241 and does not leave a facet on the petrosal.

There are differences related to the course of the sigmoid sinus between AMNH 261241 and CM 5024. Both have a well-developed sulcus posterior and medial to the subarcuate fossa (Fig. 20E), but CM 5024 had two places on this sulcus where the sinus passes through a foramen and a canal; the sulcus is entirely open in AMNH 261241.

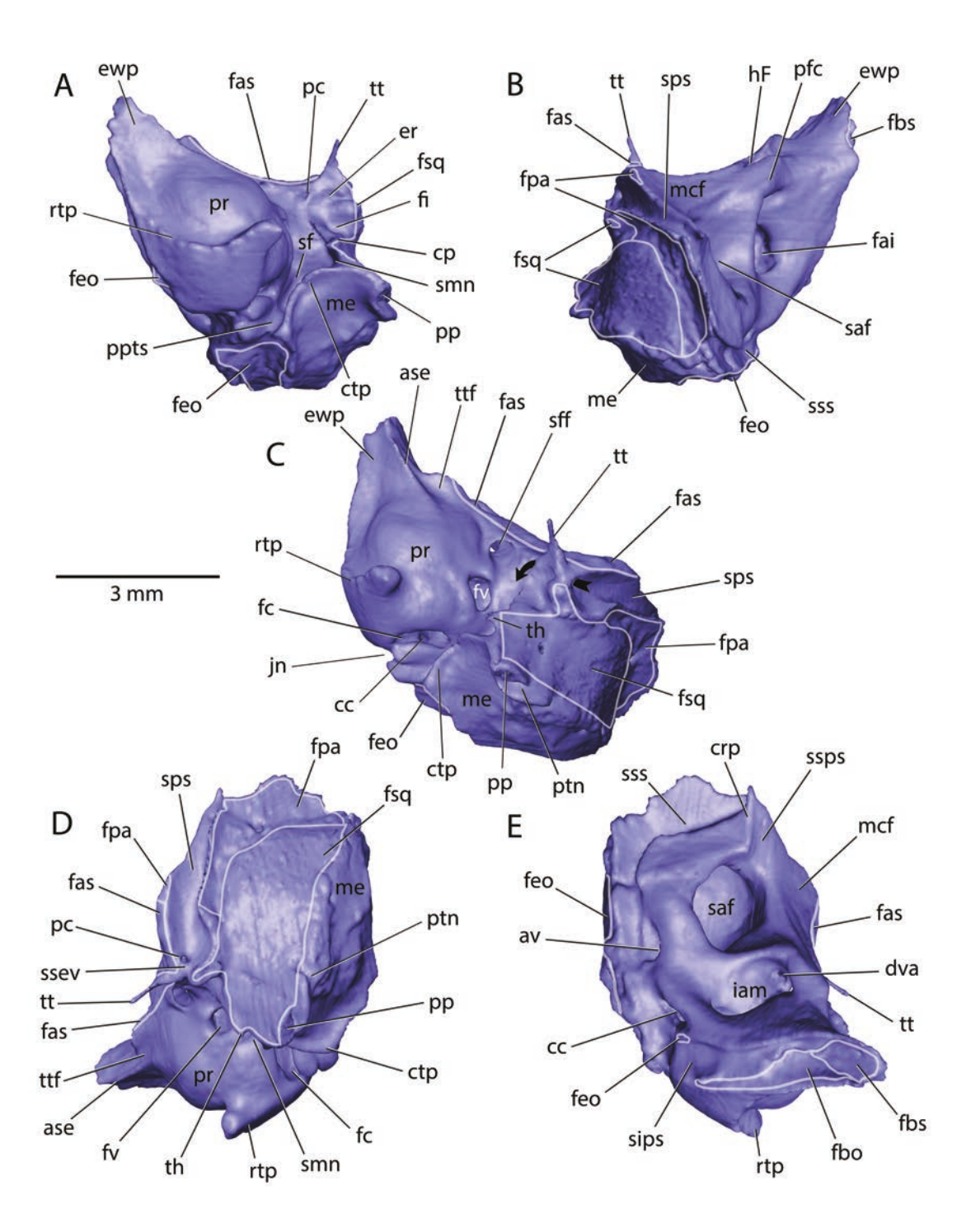


Fig. 20.—Monodelphis domestica, AMNH 261241, isosurface of left petrosal rendered from CT scans. A, ventral view (anterior to the top); B, dorsal view (anterior to the top); C, oblique ventral view (anterior to the top); D, posterior view (dorsal to the top); E, anterior view (dorsal to the top). Abbreviations: ase, anterior septum; av, aqueductus vestibuli; cc, cochlear canaliculus; cp, crista parotica; crp, crista petrosa; ctp, caudal tympanic process; dva, dorsal vestibular area; er, epitympanic recess; ewp, epitympanic wing of petrosal; fai, foramen acusticum inferius; fas, facet for alisphenoid; fbo, facet for basioccipital; fbs, facet for basisphenoid; fc, fenestra cochleae; feo, facet for exoccipital; fi, fossa incudis; fpa, facet for parietal; fsq, facet for squamosal; fv, fenestra vestibuli; hF, hiatus Fallopii; iam, internal acoustic meatus; jn, jugular notch; mcf, middle cranial fossa; me, mastoid exposure; pc, protic canal; pfc, prefacial commissure; pp, paroccipital process; ppts, postpromontorial tympanic sinus; pr, promontorium; ptn, posttemporal notch; rtp, rostral tympanic process; saf, subarcuate fossa; sf, stapedius fossa; sips, sulcus for inferior petrosal sinus; smn, stylomastoid notch; sps, sulcus for prootic sinus; ssev, sulcus for sphenoparietal emissary vein; sss, sulcus for sigmoid sinus; th, tympanohyal; tt, tegmen tympani; ttf, tensor tympani fossa.

Occipital Complex

In M. arlindoi, CM 52729, the specimen illustrated in Wible (2003), a single large bone surrounds the foramen magnum, forms the bulk of the occiput and nuchal crest, and extends onto the posterior braincase roof. Developmentally (Toeplitz 1920; Clark and Smith 1993), this single bone is comprised of five separate elements: the unpaired basioccipital, supraoccipital, and interparietal, and the paired exoccipitals. In M. domestica, AMNH 261241, rather than a single bone, there are two: a ventral one composed of the basioccipital and exoccipitals and a dorsal one composed of the supraoccipital and interparietal. Aspects of these ventral and dorsal bones are visible in all views of the hemi-cranium in Figures 1-3. The basioccipital and exoccipitals are treated as separate bones here as there are CM juveniles of M. domestica that show the entire suture between these elements (e.g., CM 80019, 80020, and 80033). Regarding the suture between the supraoccipital and interparietal, CM 80019 and 80020 have a small segment of the suture but no CM juveniles preserves the entirety. Consequently, the supraoccipital and interparietal are described together.

Basioccipital

In AMNH 261241, the unpaired basioccipital is a midline element set between the pars cochlearis of the left and right petrosals and is fused posterolaterally with the paired exoccipitals (Figs. 2B, 21A-C). Anteriorly, the basioccipital has a facet for the basisphenoid (Fig. 21C) and posteriorly it ends at the odontoid notch of the foramen magnum (Figs. 21A-B). Based on juveniles (e.g., CM 80019, 80020, and 80033), the oblique suture with the exoccipital begins rostrally anterior to the foramen for the inferior petrosal sinus and angles posteromedially (Figs. 21A, C). The anterior half of the ventral surface of the basioccipital has a raised midline crest delimiting weak bilateral muscular depressions (Fig. 21A). The dorsal surface of the basioccipital is relatively featureless beyond a weak, longitudinal midline depression (Figs. 21B–C), reflecting the relatively flat ventral surface of the hindbrain (Macrini et al. 2007). The lateral margin of the basioccipital has facets for the pars cochlearis of the petrosal anteriorly and a sulcus for the inferior petrosal sinus posteriorly (Figs. 21A–C).

Exoccipital

The paired exoccipitals have a horizontal portion on the skull base fused anteromedially with the unpaired basioccipital and a vertical portion on the occiput (Figs. 1B, 2B). The occipital condyle spans both portions and is therefore visible in ventral (Fig. 21A) and posterior (Fig. 21D) views. The anterolateral margin of the horizontal portion, which faces the pars canalicularis of the petrosal (Fig. 2B), has a medial concavity indicating the location of the foramen for

the inferior petrosal sinus and a lateral concavity indicating the location of the jugular foramen (Figs. 21A, C). Lateral to these concavities is the paracondylar process, which provides attachment for the digastric muscle based on D. marsupialis (Turnbull 1970). The dorsal surface of the horizontal portion is featureless beyond its two hypoglossal foramina (Fig. 21C), which are also visible on the ventral surface (Fig. 21A). Lateral to the hypoglossal foramina on the ventral surface is a small nutrient foramen that does not penetrate to the endocranial surface. There is no condyloid canal, an absence that Wible (2003) found in only one CM Monodelphis, M. touan, CM 76730; the remaining CM taxa had bilateral condyloid canals or on one side only. The primary features on the vertical portion are facets on the anterolateral surface for the pars canalicularis of the petrosal and on the dorsal surface for the supraoccipital (Fig. 21C).

Supraoccipital and Interparietal

AMNH 261241 has no indication of a suture between these two bones (Figs. 21D–F). The small part of the suture preserved between them in available *M. domestica* juveniles (i.e., CM 80019 and 80020) shows that the nuchal crest is entirely on the interparietal, that is, the suture is located on the occiput and not on the braincase roof. AMNH 261241 has a midline foramen below the nuchal crest on the occiput (Fig. 21D), which the CT scans reveals opens into a diploic space extending anteriorly into the braincase roof. There are paired foramina representing the anterior egress for this diploic space in the interparietal near the suture with the parietal (Fig. 21E). It seems likely that this diploic space and its foramina are entirely within the interparietal, which provides some indication of the extent of the interparietal on the occiput (Fig. 21D).

The ventral margin of the supraoccipital has three concavities (Fig. 21D): a midline one that forms the dorsal border of the foramen magnum, and left and right ones that have facets for the paired vertical portions of the exoccipitals (Fig. 21F). The anterior margin of the interparietal has a tongue in groove relationship with the paired parietal bones, with a more extensive facet on the dorsal aspect of the tongue than on the ventral (cf. Figs. 21E and F). The only other noteworthy feature is a large central depression on the inner surface that is an impression for the vermis of the cerebellum (Fig. 21F). Although on both bones, the impression is primarily on the interparietal.

COMMENTS Internal Nasal Skeleton Floor

The one topic that I address in more detail here concerns the floor of the internal nasal skeleton and the fused structure in *M. domestica*, AMNH 261241, that stretches from the premaxillae anteriorly to the pre- and orbitosphenoids posteriorly, with the vomer as the central element (Fig. 14). Because the vomer is largely relegated to the confines of

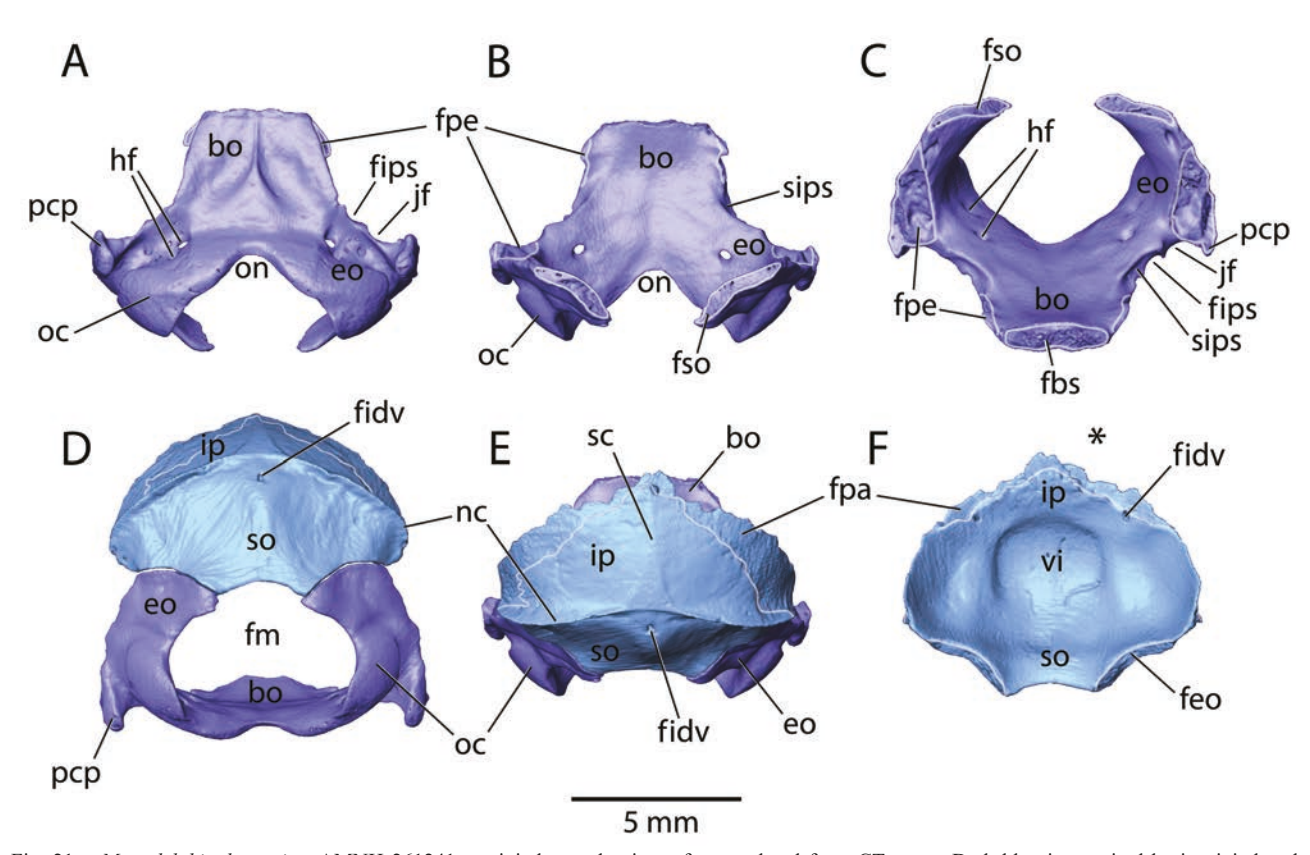


Fig. 21.—Monodelphis domestica, AMNH 261241, occipital complex isosurface rendered from CT scans. Dark blue is unpaired basioccipital and paired exoccipitals; light blue is unpaired supraoccipital and interparietal. A, ventral view (anterior to the top); B, dorsal view (anterior to the top); C, oblique anterior view; D, posterior view; E, dorsal view (anterior to the top); F, ventral view (anterior to the top). Abbreviations: bo, basioccipital; eo, exoccipital; feo, facet for exoccipital; fips, location of foramen for inferior petrosal sinus; fm, foramen magnum; fpa, facet for parietal; fpe, facet for petrosal; fso, facet for supraoccipital; hf, hypoglossal foramen; ip, interparietal; jf, location of jugular foramen; nc, nuchal crest; oc, occipital condyle; on, odontoid notch; pcp, paracondylar process; sc, sagittal crest; sips, sulcus for inferior petrosal sinus; so, supraoccipital; vi, vermiform impression.

the nasal cavity in mammals, it is perhaps one of the least studied cranial bones. I provide a general overview of this bone in mammals and address the unusual features present in *M. domestica*. For discussion of the broader homologies of the mammalian vomer, see Wible et al. (2018) and Wible (2022).

The mammalian vomer generally forms from a single midline ossification ventral to the cartilaginous nasal septum and, therefore, is considered an unpaired dermal element (De Beer 1929, 1937; Moore 1980; Wible 2022). There are exceptions where two centers are described, including *M. domestica* as reported by Rowe et al. (2005), although Clark and Smith (1993) found only one. Among marsupials, left and right centers are also noted in the didelphid *Caluromys philander* (Linnaeus, 1758) (Terry 1909; Denison and Terry 1921) and the diprotodontians *Macropus rufogrisea* (= *Notomacropus rufogriseus* (Desmarest, 1817)) (Müller 1986) and *Macropus eugenii* (= *Notomacropus eugenii* (Desmarest, 1817)) (Clark and Smith 1993). Nevertheless, I follow the standard usage (e.g., De Beer

1937; Evans and Christensen 1993; NAV) and consider the vomer as unpaired. Rowe et al. (2005: 315) wrote that "Each [paired] vomer ossifies from a single perichondral center that arises as a thin sheet of bone appressed to the medial and ventral surfaces of the embryonic paraseptal cartilage." There are two issues with their characterization. First, a perichondral origin for the vomer from the paraseptal cartilage would be a unique circumstance for the vomer in mammals (see, for example, Eloff 1952), which is invariably reported as a dermal bone (De Beer 1937: Moore 1980). Second, the vomer lies posterior to (unconnected with) the paraseptal cartilages in pouch young M. domestica (Freyer 1993), along with D. marsupialis (Toeplitz 1920), Perameles obesula (= Isoodon obesulus (Shaw, 1787)) (Esdaile 1916), Perameles sp. (Cords 1915; Fig. 22), and Notomacropus rufogriseus (Müller 1986), rendering Rowe et al.'s (2005) scenario unlikely. I follow Clark and Smith (1993) who reported the vomer as a dermal bone in M. domestica.

In early ontogenetic stages, the mammalian vomer is a

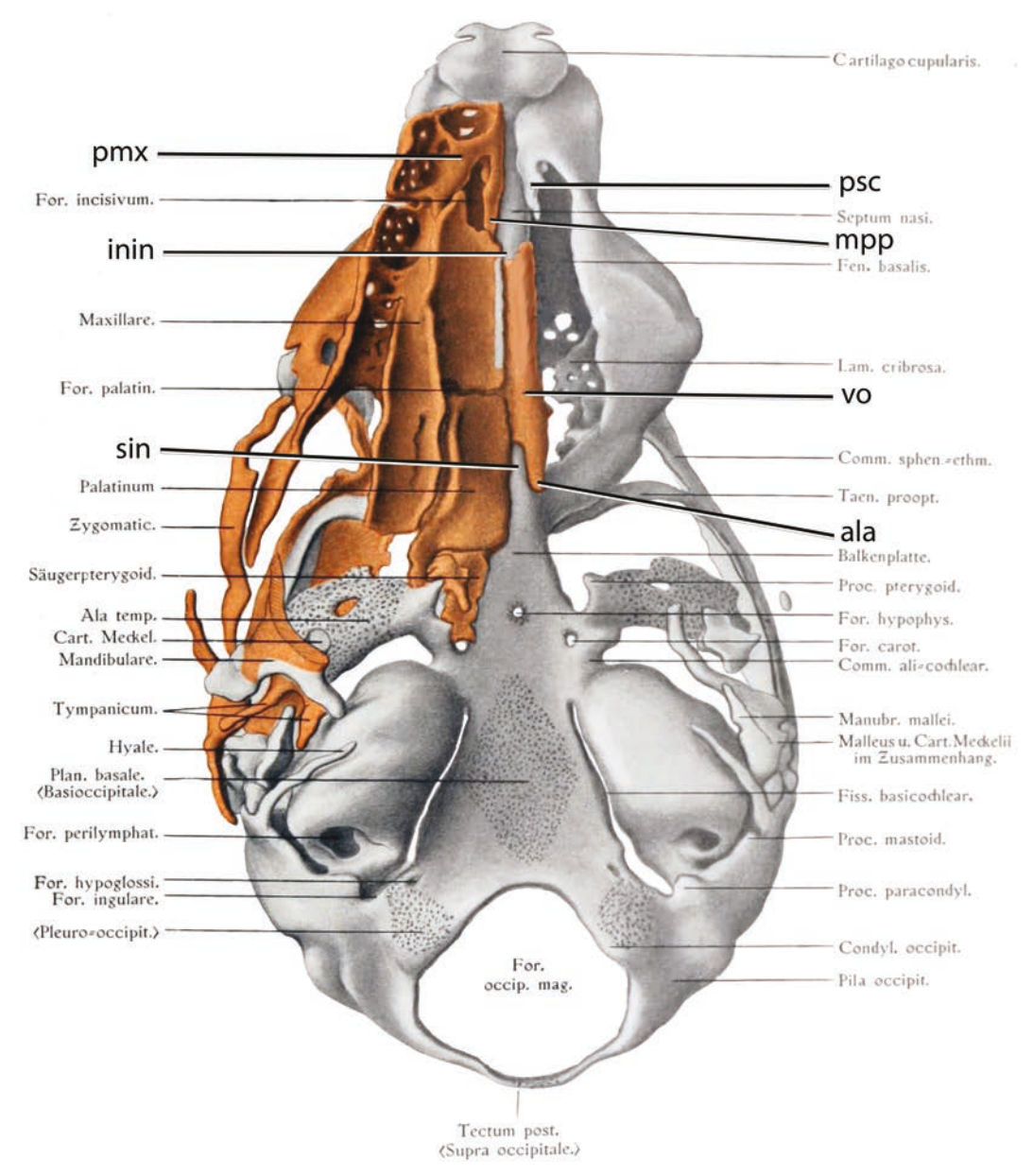


Fig. 22.—Perameles sp., 42 mm long pouch young, cranium in ventral view, modified from Cords (1915: tafel 2, fig. 2). Chondrocranium is in gray; stipple in chondrocranium is ossification center; orange is dermal bone. Paired dermal bones are illustrated only on specimen's right side; only the left side of the unpaired vomer is visible. Anterior to the top. Abbreviations: ala, ala vomeris; inin, incisive incisure; mpp, medial palatine process of premaxilla; pmx, premaxilla; psc, paraseptal cartilage; sin, sphenoidal incisure; vo, vomer.

sleeve, U-shaped in cross section, beneath the nasal septum, which often has a pair of prongs of varying lengths at its anterior and posterior ends (Fig. 22). When present, the anterior prongs contact the medial palatine processes of the premaxillae, and the gap between them is the incisive incisure; the posterior prongs are the wings or ala vomeris, and the gap between them is the sphenoidal incisure (Evans and Christensen 1993). An extreme example of

elongated alae is found in the cat embryo studied by Terry (1917), where the alae are much longer than the midline component of the vomer and rostral prongs are absent (Fig. 23). This foreshadows the adult cat condition, where the alae extend into the basipharyngeal passage (Fig. 24). Among the few pouch young marsupials where details of the vomer are provided, the long-nosed bandicoot, *Perameles* sp., reported by Cords (1915) has both anterior and

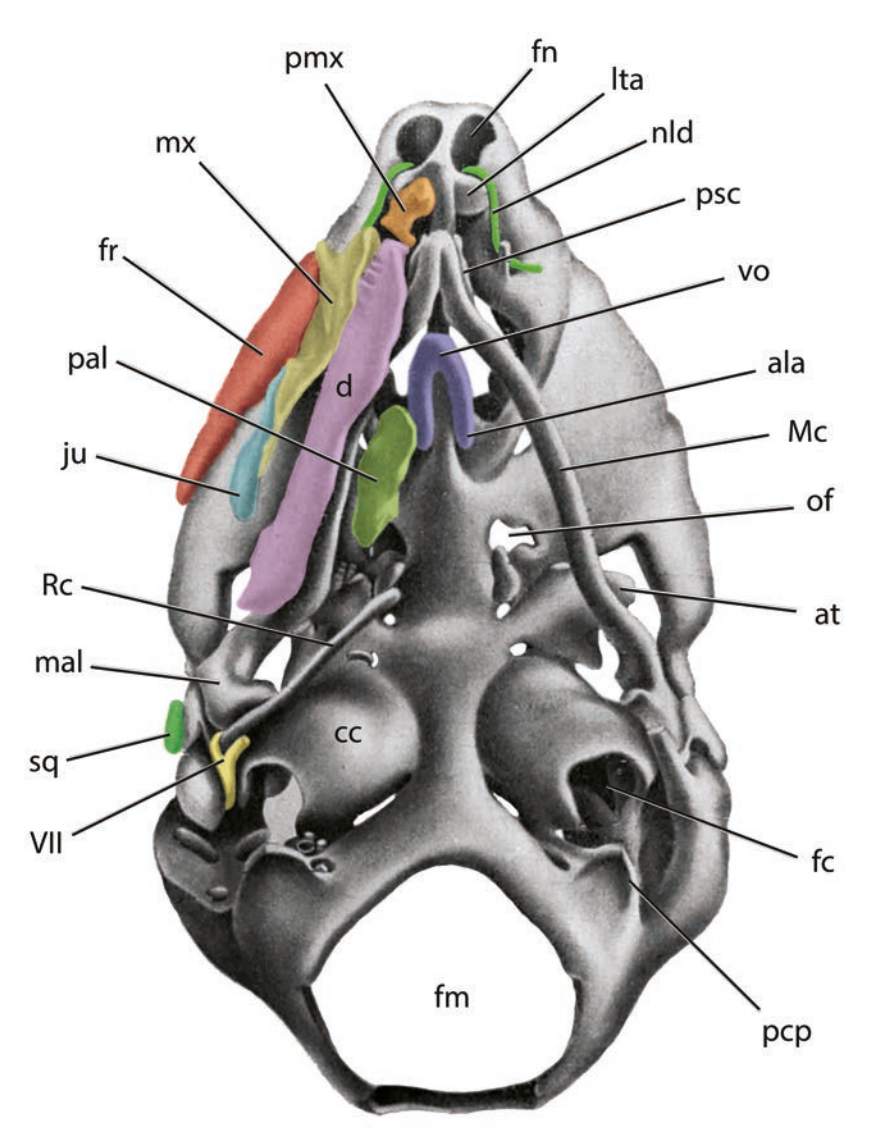


Fig. 23.—Felis domestica, 23.1 mm long embryo, skull in ventral view, modified from Terry (1917: plate 2). Cartilage is in gray; dermal bones are in color; paired dermal bones are illustrated only on specimen's right side. Anterior to the top. Abbreviations: ala, ala vomeris; at, ala temporalis; cc, co-chlear capsule; d, dentary; fc, fenestra cochleae; fm, foramen magnum; fn, fenestra narina; fr, frontal; ju, jugal; lta, lamina transversalis anterior; mal, malleus; Mc, Meckel's cartilage; mx, maxilla; nld, nasolacrimal duct; of, optic foramen; pal, palatine; pcp, paracondylar process; pmx, premaxilla; psc, paraseptal cartilage (largely hidden by Meckel's cartilage); Rc, Reichert's cartilage; sq, squamosal; VII, facial nerve; vo, vomer.

posterior prongs (Fig. 22), whereas the *D. marsupialis* studied by Toeplitz (1920) has only the posterior pair, that is, the vomerine alae. The midline vomer component of *M. domestica*, AMNH 261241, resembles that of the pouch young *Perameles* sp. with a pair of short anterior prongs and longer posterior ones (Fig. 14C).

Rowe et al. (2005) were the first to describe in adult *M. domestica* the extensive lateral shelf of the vomer that runs for more than half the length of the midline component of the vomer and fuses posteriorly with the ethmoid to form the transverse lamina (Fig. 14). They coined two

terms for this shelf; the anterior part attached to the midline component is their paraseptal shelf of the vomer, and the part posterior to the midline component is their choanal process. Having two terms for what is a continuous shelf is misleading, especially without knowledge of how these structures develop. The anterior part of the shelf is on either side of the osseous nasal septum, so that paraseptal is an appropriate descriptor. However, the term paraseptal cartilage is already ensconced in the literature and there is no association between that structure and the shelf on the vomer. To avoid confusion with the paraseptal cartilage,

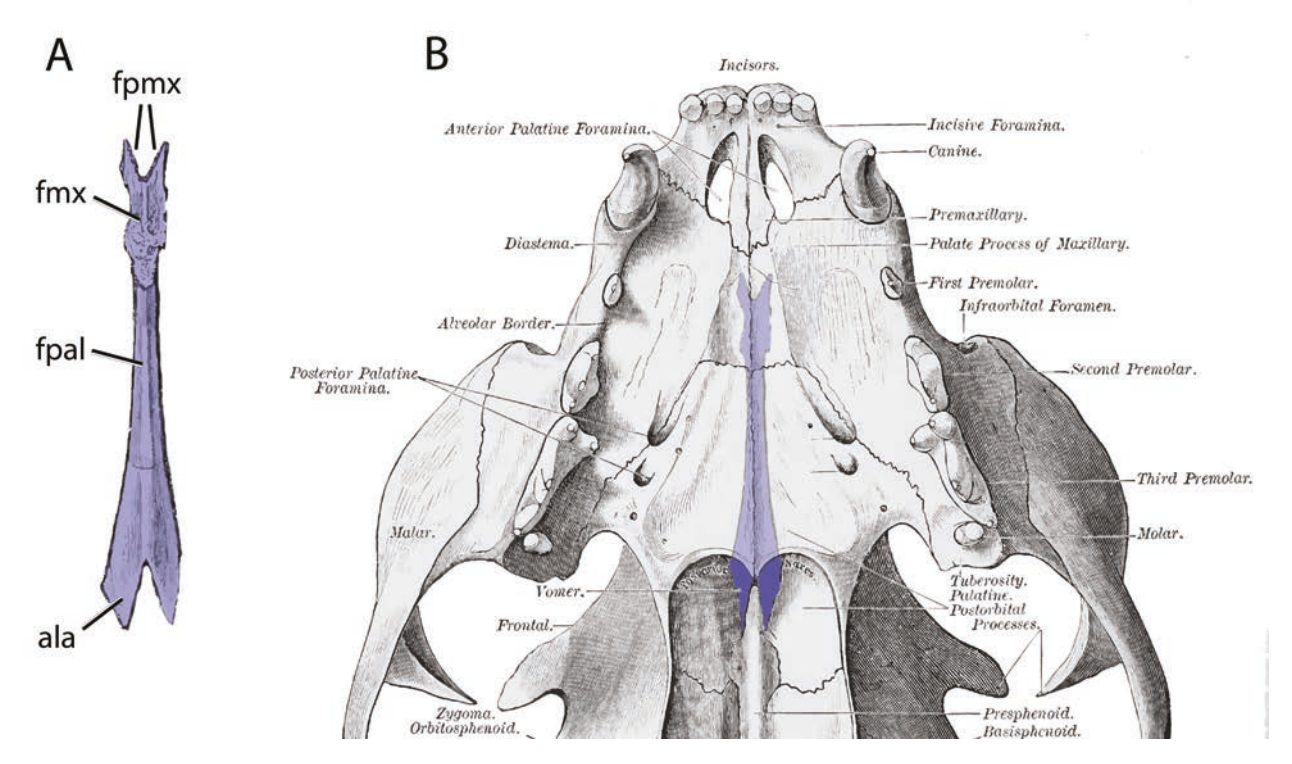


Fig. 24.—Felis domestica, adult. **A,** vomer in ventral view, modified from Jayne (1898: fig. 217); **B,** palate in ventral view, with the position of the vomer dorsal to the palate highlighted in blue, modified from Jayne (1898: fig. 251). Anterior palatine foramina = incisive foramina; posterior palatine foramina = major palatine foramina. Abbreviations: **ala,** ala vomeris; **fmx,** facet for maxilla; **fpal,** facet for palatine; **fpmx,** facet for premaxilla.

I propose the term paraseptal shelf of the vomer be abandoned. On the other hand, I accept the term paraseptal shelf of the premaxilla (Figs. 5C–D, 7A) coined by Rowe et al. (2005) because this part of the medial palatine process houses the paraseptal cartilage and vomeronasal organ (Freyer 1999; Sánchez-Villagra and Forasiepi 2017). Rowe et al.'s (2005) term choanal process for the posterior part of the vomerine shelf is unnecessary as there is already a term widely used in the literature, including NAV, the ala vomeris or vomerine wing. In fact, given the continuity of the anterior and posterior parts of the lateral shelf, I propose using vomerine wing for the entire structure. If detailed ontogenetic study reveals separate origins for parts of this continuous shelf, then perhaps different terms may be useful.

Macrini (2012) studied the distribution of features of the internal nasal skeleton based on CT scans in a sampling of extant marsupials from all seven orders (29 genera distributed as follows: three didelphimorphians, one paucituberculatan, one microbiotherian, four dasyuromorphians, one notoryctemorphian, two peramelemorphians, and 17 diprotodontians). One of the features investigated was the presence of a paraseptal shelf of the vomer (his character #28) sampled rostral to the vomerine contribution to the transverse lamina. As reported here, this character is the rostral extension of the vomerine wing. Macrini (2012)

found a rostrally extended wing in 25 of 29 marsupial genera, with the four absences in some diprotodontians (i.e., *Tarsipes*, *Pseudocheirus*, *Phascolarctos*, and *Vombatus*). He also assessed from CT scans the incidence of the rostrally extended wing in the monotremes *Ornithorhynchus* and *Tachyglossus* and three placentals (*Erinaceus*, *Mus*, and *Pteropus*). Of these five marsupial outgroups, Macrini (2012) reported the wing to be present in *Tachyglossus* and *Erinaceus* and absent in the others.

The incidence of the rostrally extended vomerine wing outside of Marsupialia intrigued me. To assess it, I located on MorphoSource.org the CT scans of *Tachyglossus aculeatus*, AMNH 154457, the same specimen reported by Macrini (2012). Also, on that website, I found *Erinaceus europaeus*, LACM mammals:058376; Macrini (2012) observed *Erinaceus* sp. in Timothy Rowe's personal collection.

The vomer in *Tachyglossus aculeatus*, AMNH 154457, is set off ventrally by sutures from the maxilla (Fig. 25A) and palatine (Figs. 25B–C); the echidna lacks a medial palatine process of the premaxilla and, therefore, has no contact between the vomer and premaxilla. Rostral prongs are not present on the vomer in the adult or the ontogenetic stages studied by Gaupp (1908) and Kuhn (1971), or in adult *Zaglossus* Gill, 1877 (Simon 2013). The rear of the vomer in early ontogeny has a short pair of posterior prongs (Gaupp 1908) but comes to a midline point in later stages (Kuhn

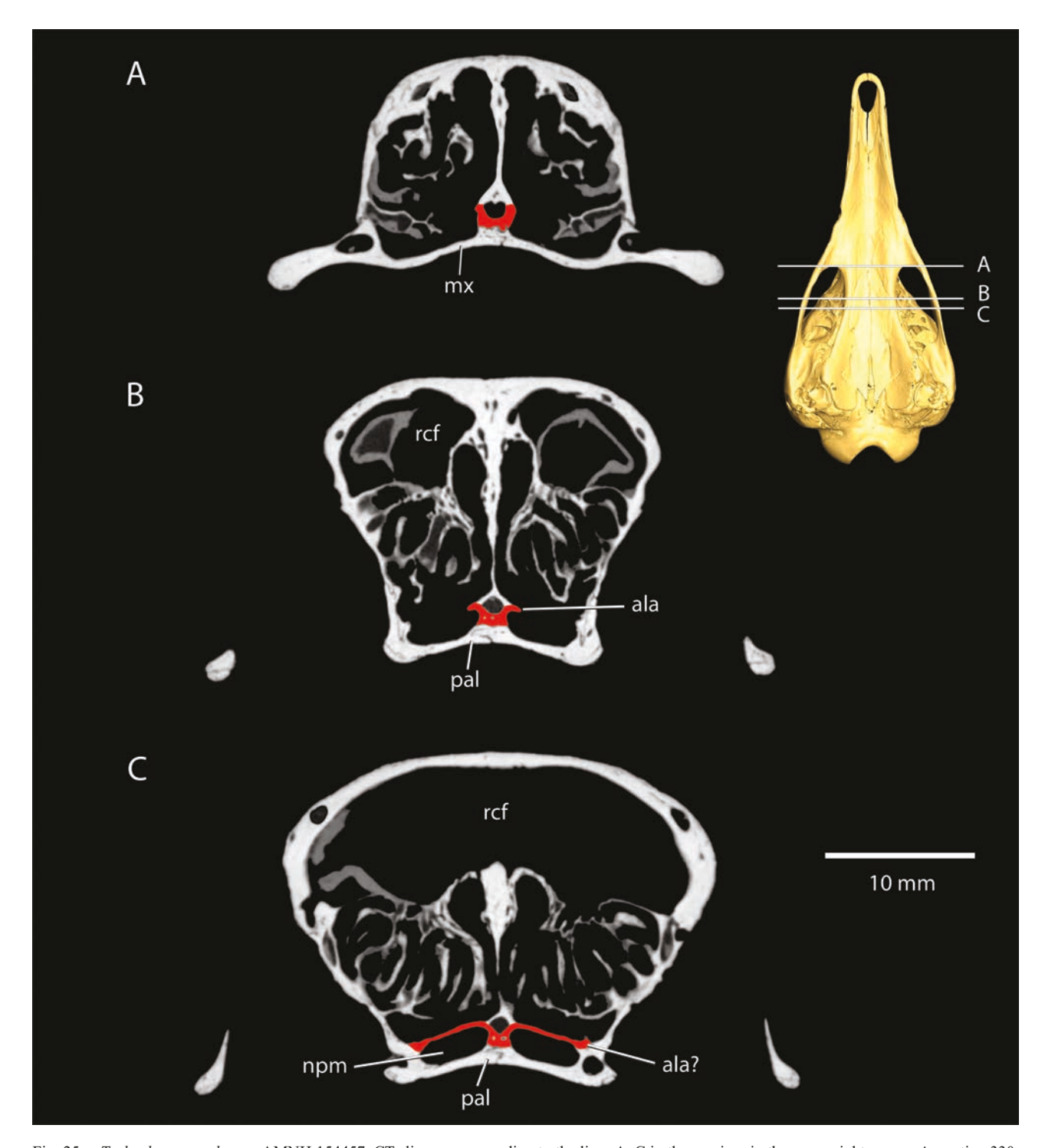


Fig. 25.—*Tachyglossus aculeatus*, AMNH 154457, CT slices corresponding to the lines A–C in the cranium in the upper right corner. **A**, section 330; **B**, section 384; **C**, section 409. Vomer is in red. In C, alae are fused with ethmoid to form the transverse lamina. Abbreviations: **ala**, ala vomeris; **mx**, maxilla; **npm**, nasopharyngeal meatus; **pal**, palatine; **rcf**, rostral cranial fossa.

1971). Sutures delimiting the vomer from the ossified nasal septum in AMNH 154457 are less clear, but are present in some sections. For most of its length, the vomer is U-shaped

with erect lateral laminae (Fig. 25A). Posteriorly, as the vomer approaches the nasopharyngeal meatus, the dorsal aspect of the lateral lamina bends laterally as the ala (Fig.

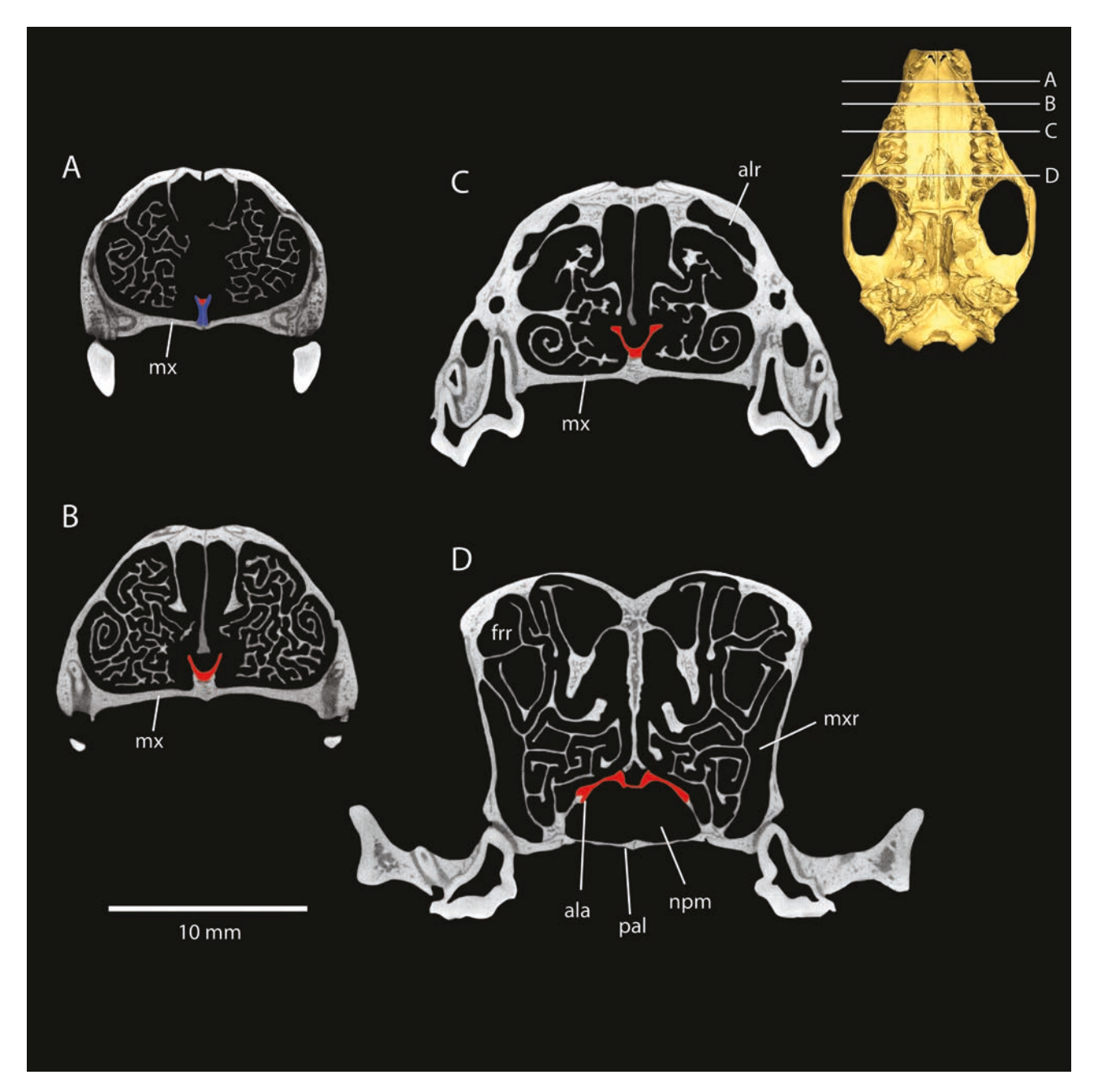


Fig. 26.—*Erinaceus europaeus*, LACM mammals:058376, CT slices corresponding to the lines A-D in the cranium in the upper right corner. **A**, section 232; **B**, section 403; **C**, section 607; **D**, section 940. Tip of rostrum is missing from CT scans. Medial palatine processes of premaxillae are in blue; vomer is in red. Abbreviations: **ala**, ala vomeris; **alr**, anterolateral recess; **frr**, frontal recess; **mx**, maxilla; **mxr**, maxillary recess; **npm**, nasopharyngeal meatus; **pal**, palatine.

25B). At the nasopharyngeal meatus (Fig. 25C), the roof of that passageway is formed by bone that is continuous anteriorly with the bent lateral lamina and posteriorly with the ethmoid. Because of this continuity, whether this roofing bone is vomer or ethmoid is uncertain; it does have sutural contact laterally with the palatine.

The vomer in Erinaceus europaeus, LACM mammals:

058376, appears anteriorly at the level of the canine as a midline prong between the vertical medial palatine processes of the premaxillae, which lack paraseptal shelves (Fig. 26A). The single anterior prong of the vomer transitions into a U-shaped midline component with obliquely oriented lateral laminae (Fig. 26B) that extends to the level of the protocone of the second molar. The ventral surface

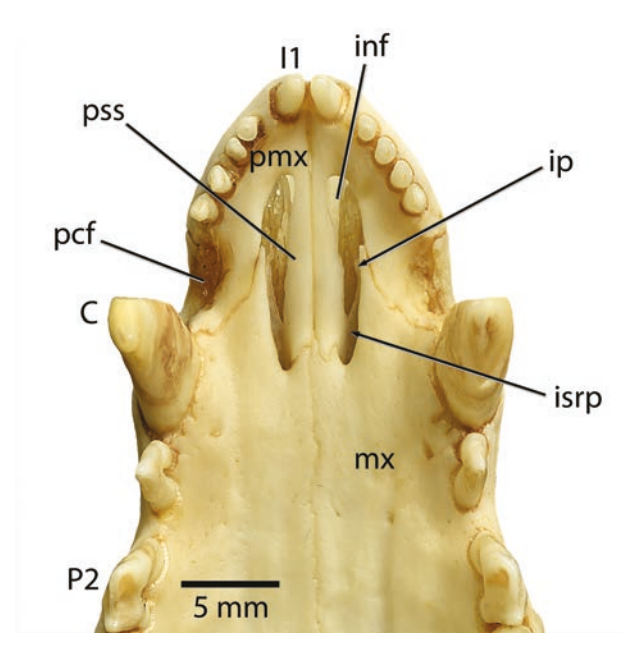


Fig. 27.—Didelphis albiventris, CM 80007, anterior rostrum in ventral view. The paired bone visible through the incisive foramen dorsal to the paraseptal shelf of the premaxilla is the maxilloturbinal. Abbreviations: C, upper canine; I1, upper first incisor; inf, incisive foramen; ip, incisive process; isrp, inferior septal ridge process; mx, maxilla; P2, upper second premolar; pcf, paracanine fossa; pmx, premaxilla; pss, paraseptal shelf of premaxilla.

of the midline component contacts the maxillae up to the level of the protocone of the first molar; posterior to that, the vomer is separated from the hard palate by the nasopharyngeal meatus. At the level of the protocone of the ultimate premolar, the dorsal tip of the lateral lamina swells to a foot-like process, the ala (Fig. 26C). The ala increases in width posteriorly, and at the level of the protocone of the second molar joins (and then fuses with) the ethmoid to form the transverse lamina (Fig. 26D). The long ala present in the adult is foreshadowed in the embryonic appearance of the vomer reported in prenatal specimen by Parker (1885) and Fawcett (1918), which generally resembles the vomer in the cat embryo (Fig. 23).

The ala vomeris in *Tachyglossus aculeatus* (Fig. 25B) and *Erinaceus europaeus* (Fig. 26C) is not as long anteroposteriorly or as wide mediolaterally as the ala vomeris in *M. domestica* (Figs. 5C, 14A, C). Moreover, the ala arises differently from the midline component: from the dorsal tip of the lateral lamina in *Tachyglossus* (Fig. 25B) and *Erinaceus* (Fig. 26C), but from the ventrolateral aspect of the lamina in *M. domestica* (Fig. 5C). I do not consider these differences sufficient to exclude the homology of structure. Yet, to equate these three with the same character state as done by Macrini (2012) does not sufficiently capture the extreme differences evident here. Macrini (2012) has taken the first steps by recognizing the structure as variable and including it in a phylogenetic analysis. How-

ever, refinement of the character description is needed to account for the differences. Without investigating a greater range of taxa and morphologies, I am loathe to recommend amendments here.

The other unexpected result of the CT scans of M. domestica, AMNH 261241, concerns the medial palatine process of the premaxilla, with its extensive inferior septal ridge process and elongate incisive process (Figs. 5A–B, 7). As noted above, Broom (1896) described the inferior septal ridge as a mucosal fold over the paraseptal cartilage in various pouch young marsupials. Freyer (1999), in his study of nasal cartilage structures in pouch young marsupials, considered the inferior septal ridge to be in the marsupial ground plan, but he did not document the contribution of a process on the premaxilla to the formation of the mucosal fold. The incidence of inferior septal ridge and incisive processes may be visible in museum osteological specimens as shown in Didelphis albiventris Lund, 1840, CM 80007, in Figure 27. However, these structures may not be visible in direct ventral view, they may be hidden by tissue and/or the bone around the incisive foramina, and they are delicate and easily damaged. Survey of the didelphids in the CM collection reveals incidence of both the inferior septal ridge process and incisive process in all species represented (genera Caluromys, Chironectes, Didelphis, Gracilianus, Lutreolina, Marmosa, Marmosops, Metachirus, Monodelphis, Philander, and Thylamys).

Sampling the morphology of the vomer and medial palatine process of the premaxilla more widely in marsupials would benefit from additional CT scanned specimens beyond the scope of this study. Here, I make observations on only one specimen, the microbiotherian Dromiciops bozinovici, CM 40621, which was recently CT scanned. It has structures of the vomer and premaxillae reminiscent of those in M. domestica along with some noteworthy differences. As in M. domestica, AMNH 261241, the vomer and medial palatine processes are fused, although with some unossified areas between them, and the alae of the vomer and ethmoid are fused to form the transverse laminae (Figs. 28A–B). However, posteriorly the alae extend into the basipharyngeal passage in Dromiciops bozinovici and are separated by sutures from the palatines and pterygoids. The maxillopalatine fenestrae are much larger in Dromiciops bozinovici and expose the vomerine wings along with the ethmoturbinals within the nasal cavity. There is not a constricted sub-alar recess. The alae develop a sizeable midline crest (Figs. 28A, D) that approaches the underlying palatines to separate left and right nasopharyngeal meatuses at the choanae (Fig. 28B). On the medial palatine process of the premaxilla, in dorsal view (Fig. 28C), is a prominent septal process and a concave paraseptal shelf that is primarily situated posterior to the incisive foramen (Fig. 28B). Posterior to the paraseptal shelf is a narrow flat section that is angled dorsolaterally, the inferior septal ridge process (Fig. 28C). The inferior septal ridge process and vomerine ala are connected laterally by bony threads but lie in different planes, the former more ventral than the

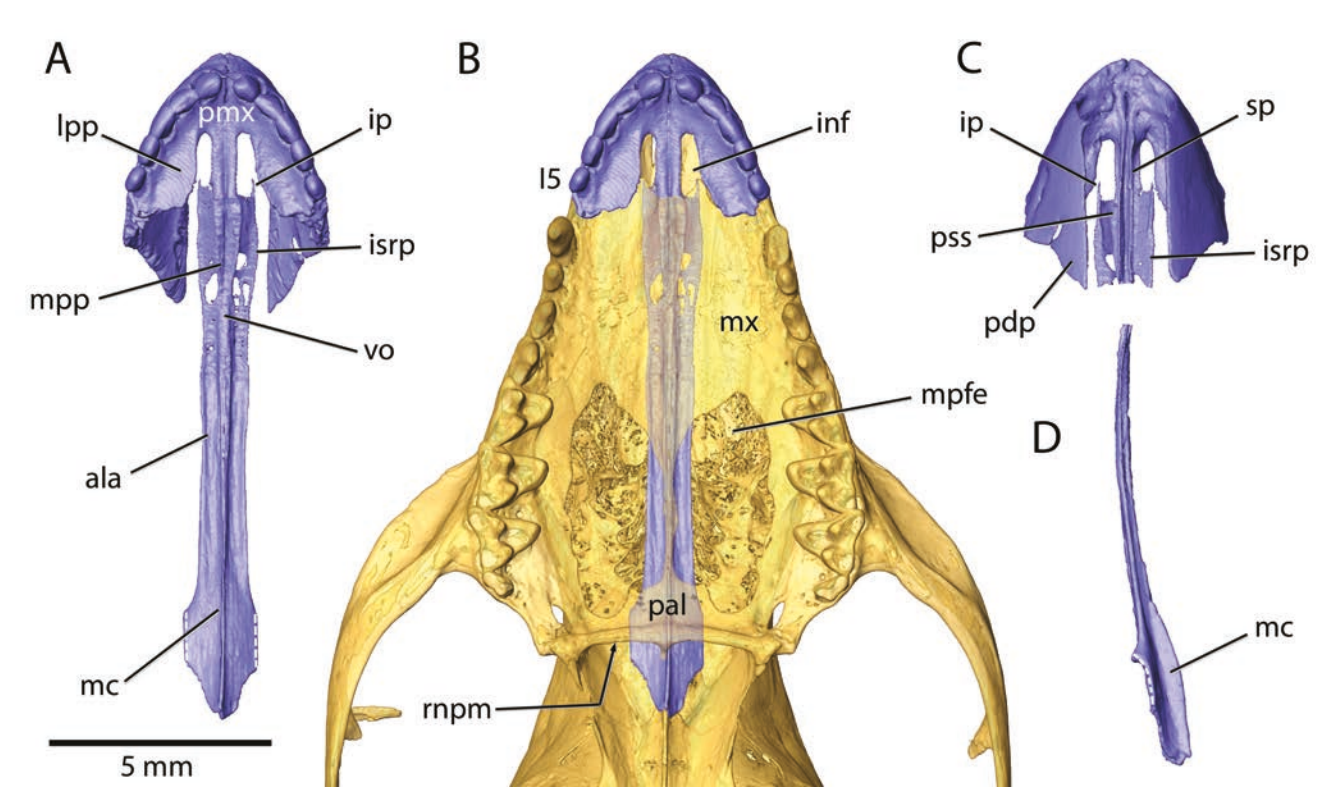


Fig. 28.—Dromiciops bozinovici, CM 40621, isosurfaces rendered from CT scans. **A,** fused premaxilla and vomer in right lateral view; **B,** palate in ventral view with transparency to show fused premaxilla and vomer; **C,** separated premaxilla in dorsal view; **D,** separated vomer in right lateral view. Separation between premaxillae and vomer was made at posterior end of septal processes of the former. Alae of vomer are fused posterolaterally with ethmoid to form the transverse lamina; dashed white lines in A and D indicate cut edge on the transverse lamina. Abbreviations: **ala,** ala vomeris; **15,** upper fifth incisor; **ip,** incisive process; **isrp,** inferior septal ridge process; **lpp,** lateral palatine process of premaxilla; **mc,** midline crest on vomer; **mpfe,** maxillopalatine fenestra; **mpp,** medial palatine process of premaxilla; **pal,** palatine; **pdp,** posterodorsal process of premaxilla; **pmx,** premaxilla; **psp,** paraseptal shelf of premaxilla; **rnpm,** right nasopharyngeal meatus; **sp,** septal process of premaxilla; **vo,** vomer.

latter. The dorsolateral margin of the inferior septal ridge process and paraseptal shelf have a thickened ridge that extends forwards a slight distance as an incisive process, the left one longer than the right.

In the future, I hope to address how the internal nasal floor skeleton is formed in other marsupials and in placentals in order to pose hypotheses of why the morphology is so diverse in the few mammals that have been studied in sufficient detail.

ACKNOWLEDGMENTS

I am grateful to MorphoSource.org for organizing the online repositories for CT scanned data that made this study possible. The CT scanning of *Dromiciops bozinovici*, CM 40621, was completed at the Center for Quantitative Imaging at The Pennsylvania State University, and I thank Odette Mina and Tim Stecko for their assistance and expertise. Paul Bowden added details of facets and cut edges to figures derived from the CT scans. I acknowledge the curators of the American Museum of Natural History, the Department of Biological Anthropology and Anatomy, Duke University, and the Natural History Museum of Los Angeles County for making CT scans of their specimens available for research.

The manuscript benefitted from comments from Robin Beck, Guillermo Rougier, Sarah Shelley, and Timothy Smith. Funding for this project is from National Science Foundation Grant DEB 1654949, the Carnegie Museum of Natural History, and the R.K. Mellon North American Mammal Research.

LITERATURE CITED

BECK, R.M.D., R.S. Voss, AND S.A. Jansa. 2022. Craniodental morphology and phylogeny of marsupials. Bulletin of the American Museum of Natural History, 457:1–355.

Broom, R. 1896. On the comparative anatomy of the organ of Jacobson in marsupials. Proceedings of the Linnean Society of New South Wales, 21:591–623.

BURNETT, G.T. 1830. Illustrations of the Quadrupeda, or quadrupeds, being the arrangement of the true four-footed beasts indicated in outline. Quarterly Journal of Science, Literature and Art, 1829:336–353.

CLARK, C.T., AND K.K. SMITH. 1993. Cranial osteogenesis in *Monodelphis domestica* (Didelphidae) and *Macropus eugenii* (Macropodidae). Journal of Morphology, 215:119–149.

DE BEER, G.R. 1929. The development of the skull of the shrew. Philosophical Transactions of the Royal Society, Series B, 217:411–480.

- . 1937. The Development of the Vertebrate Skull. Clarendon Press, Oxford. 554 pp., 143 pl.
- DENISON, W., AND R.J. TERRY. 1921. The chondrocranium of *Caluromys*. Washington University Studies, Scientific Series, 8(2):161–181.
- DESMAREST, A.G. 1817. Nouveau dictionnaire d'histoire naturelle, appliquèe aux art, principalement à l'agriculture et à l'economie rurale et domestique; par une société de naturalistes. Nouvelle edition, presqu'entierement refondue et considerablement augmentee, tome 17. Deterville, Paris.
- Dom, R., B.L. FISHER, AND G.F. MARTIN. 1970. The venous system of the head and neck of the opossum (*Didelphis virginiana*). Journal of Morphology, 132(4):487–496.
- DOUTT, J.K. 1938. Two new mammals from South America. Journal of Mammalogy, 19:100–101.
- EKDALE, E.G. 2010. Ontogenetic variation in the bony labyrinth of *Monodelphis domestica* (Mammalia: Marsupialia) following ossification of the inner ear cavities. The Anatomical Record, 293:1896–1912.
- ELOFF, F.C. 1952. On the relations of the human vomer to the anterior paraseptal processes. Journal of Anatomy, 86:16–19.
- FAWCETT, E. 1918. The primordial cranium of *Erinaceus europaeus*. Journal of Anatomy, 52:211–250.
- ERXLEBEN, I.C.P. 1777. Systema regni animalis per classes, ordines, genera, species, varietates, cum synonymia et historia animalium. Classis I, Mammalia. Impensis Weygandianis, Leipzig.
- EVANS, H.E., AND G.C. CHRISTENSEN. 1993. Miller's Anatomy of the Dog. Second edition. W.B. Saunders Company, Philadelphia. 1181 pp.
- FREYER, C. 1999. Die Regio ethmoidalis in der Ontogenese von Monodelphis domestica (Didelphidae: Marsupialia): ein Beitrag zur Rekonstruktion des Grundplanes der Marsupialia mit Befunden zur Regio ethmoidalis in Einzelstadien von Didelphis marsupialis (Didelphidae: Marsupialia) und Thylacinus cynocephalus (Thylacinidae: Marsupialia). Diplomarbeit, Humboldt Universität, Berlin.
- GAUPP, E. 1908. Zur Entwicklungsgeschichte und vergleichenden Morphologie des Schädels von Echidna aculeata var. typica. Semon's Zoologische Forschungsreisen in Australien und dem malayischen Archipel (3/2). Denkschriften der medicinisch-naturwissenschaftlichen Gesellschaft zu Jena, 6:539–788.
- GELDEREN, C. VAN. 1924. Die Morphologie der Sinus durae matris. Zweiter Teil. Die vergleichende Ontogenie der neurokraniellen Venen der Vögel und Säugetiere. Zeitschrift für Anatomie und Entwickelungsgeschichte, 74:432–508.
- GILL, T. 1877. P. 171, in Annual Record of Science and Industry for 1876 (S.F. Baird, ed.). Harper & Brothers, New York.
- HIIEMAE, K., AND F.A. JENKINS, JR. 1969. The anatomy and internal architecture of the muscles of mastication in *Didelphis marsupialis*. Postilla, 140:1–49.
- JAYNE, H. 1898. Mammalian Anatomy, A Preparation for Human and Comparative Anatomy. Part 1. The Skeleton of the Cat, Its Muscular Attachments, Growth, and Variations Compared with the Skeleton of Man. J.B. Lippincott Company, Philadelphia. 816 pp.
- KERR, R. 1792. The Animal Kingdom, or Zoological System of the Celebrated Sir Charles Linnaeus; Class I. Mammalia. A. Strahan and T. Cadell, London; W. Creech, Edinburgh.
- KUHN, H.-J. 1971. Die Entwicklung und Morphologie des Schädels von Tachyglossus aculeatus. Abhandlungen der Senckenbergischen Naturforschenden Gesellschaft, 523:1–224.
- Kuhn, H.-J., And U. Zeller. 1987. The cavum epiptericum in monotremes and therian mammals. Pp. 51–70, *in* Morphogenesis of the Mammalian Skull (H.-J. Kuhn and U. Zeller, eds.). Mammalia depicta, 13. Verlag Paul Parey, Hamburg.
- LINNAEUS, C. 1758. Systema Naturae per regna tria naturae, secundum classis, ordines, genera, species cum characteribus, differentiis, synonymis, locis. Tenth ed., Vol. 1. Laurentii Salvii, Stockholm. 824 pp.
- LUND, P.W. 1841. Blik paa Brasiliens Dyreverden f\u00f6r sidste Jordomvaeltning. Tredie Afhandling: Fortsaettelse af Pattedyrene.

- Konigelige Danske Videnskabernes Selskabs Afhandlinger, Kjöbenhavn, 8:219–272, pls. 14–24.
- MACRINI, T.E. 2012. Comparative morphology of the internal nasal skeleton of adult marsupials based on x-ray computer tomography. Bulletin of the American Museum of Natural History, 365:1–91.
- 2014. Development of the ethmoid in *Caluromys philander* (Didelphidae, Marsupialia) with a discussion of the homology of the turbinal elements in marsupials. The Anatomical Record, 297:207–217.
- MACRINI, T.E., T. ROWE, AND J.L. VANDEBERG. 2007. Cranial endocasts from a growth series of *Monodelphis domestica* (Didelphidae, Marsupialia): a study of individual and ontogenetic variation. Journal of Morphology, 268:844–865.
- MAGA, A.M. 2008. Systematic paleontological investigation of the metatherian fauna from the Paleogene Uzunçarşıdere Formation, central Turkey. Ph.D. dissertation, The University of Texas at Austin. 309 pp.
- MAIER W. 1993. Cranial morphology of the therian common ancestor, as suggested by adaptations of neonate marsupials. Pp. 165–181, in Mammal Phylogeny: Mesozoic Differentiation, Multituberculates, Monotremes, Early Therians, and Marsupials (F.S. Szalay, M.J. Novacek, and M.C. McKenna, eds.). Springer Verlag, New York.
- MOORE, W.J. 1980. The Mammalian Skull. Cambridge University Press, Cambridge. 369 pp.
- MÜLLER, U. 1986. Zur Morphologie der Ethmoidal- und Orbitotemporalregion bei *Wallabia rufogrisea* (Marsupialia). Inauguraldissertation, Johann Wofgang Goethe-Universität, Frankfurt am Main.
- Nomina Anatomica Veterinaria, Sixth Edition. 2017. Editorial Committee Hanover (Germany), Ghent (Belgium), Columbia, MO (U.S.A.), Rio de Janeiro (Brazil).
- Nummela, S., G. Aguirre-Fernández, K.K. Smith, and M.R. Sánchez-Villagra. 2022. Growth pattern of the middle ear in the gray short-tailed opossum, *Monodelphis domestica*. Vertebrate Zoology, 72:487–494.
- PARKER, W.K. 1885. Structure and development of the skull in the Mammalia. —Part III. Insectivora. Philosophical Transactions of the Royal Society 176: 124–275.
- PAVAN, S.E. 2019. A revision of the *Monodelphis glirina* group (Didelphidae: Marmosini), with a description of a new species from Roraima, Brazil. Journal of Mammalogy, 100:103–117.
- PAVAN, S.E., R.V. ROSSI, AND H. SCHNEIDER. 2012. Species diversity in the *Monodelphis brevicaudata* complex (Didelphimorphia: Didelphidae) inferred from molecular and morphological data, with the description of a new species. Zoological Journal of the Linnean Society, 165:190–223.
- PAVAN, S.E., AND R.S. Voss. 2016. A revised subgeneric classification of short-tailed opossums (Didelphidae: Monodelphis). American Museum Novitates, 3868: 1–44.
- PORAN, N.S. 1998. Vomeronasal organ and its associated structures in the opossum *Monodelphis domestica*. Microscopy Research and Technique, 43:500–510.
- QUINTERO-GALVIS, J.F., P. SAENZ-AGUDELO, G.C. AMICO, S. VAZQUEZ, A.B.A. SHAFER, AND R.F. NESPOLO. 2022. Genomic diversity and demographic history of the *Dromiciops* genus (Marsupialia: Microbiotheriidae). Molecular Phylogenetics and Evolution, 168:107405.
- Rossie, J.B. 2006. Ontogeny and homology of the paranasal sinuses in Platyrrhini (Mammalia: Primates). Journal of Morphology, 267:1–40.
- ROUGIER, G.W., AND J.R. WIBLE. 2006. Major changes in the mammalian ear region and basicranium. Pp. 269–311, *in* Amniote Paleobiology: Perspectives on the Evolution of Mammals, Birds, and Reptiles (M.T. Carrano, T.J. Gaudin, R.W. Blob, and J.R. Wible, eds.). University of Chicago Press, Chicago.
- Rowe T.B., T.P. EITING, T.E. MACRINI, AND R.A. KETCHAM. 2005. Organization of the olfactory and respiratory skeleton in the nose of the gray short-tailed opossum *Monodelphis domestica*. Journal of Mammalian Evolution, 12:303–336.

- SANCHÉZ-VILLAGRA, M.R. 2002. The cerebellar paraflocculus and the subarcuate fossa in *Monodelphis domestica* and other marsupial mammals ontogeny and phylogeny of a brain-skull interaction. Acta Theriologica, 47:1–14.
- SÁNCHEZ-VILLAGRA, M.R., AND A.M. FORASIEPI. 2017. On the development of the chondrocranium and the histological anatomy of the head in perinatal stages of marsupial mammals. Zoological Letters, 3·1
- SHAW, G (1792) Myrmecophaga aculeata. The porcupine ant-eater. Naturalists' Miscellany 3(36). [unnumbered]
- . 1800. General Zoology or Systematic Natural History. G. Kearsley, London.
- SIMON, R.V. 2013. The cranial osteology of the long-beaked echidna and the definition, diagnosis, and origin of Monotremata and its subclades. Master's thesis, University of Texas, Austin. 348 pp.
- SMITH, T.D., T.P. EITING, AND J.B. ROSSIE. 2011. Distribution of olfactory and nonolfactory surface area in the nasal fossa of *Microcebus murinus*: implications for microcomputed tomography and airflow studies. The Anatomical Record, 294:1217–1225.
- SMITH T.D., AND J.B. ROSSIE. 2008. The nasal fossa of mouse and dwarf lemurs (Primates, Cheirogaleidae). The Anatomical Record, 291:895–915.
- TATE, G.H.H. 1934. New generic names for two South American marsupials. Journal of Mammalogy, 15:154.
- Terry, R.J. 1909. An observation in the development of the mammalian vomer. The Anatomical Record, 3(10):525–529.
- . 1917. The primordial cranium of the cat. Journal of Morphology, 29(2):281–433.
- 1942. Osteology. Pp. 77–265, in Morris's Human Anatomy, A Complete Systemic Treatise, 10th ed. (J.P. Schaeffer, ed.). The Blakiston Company, Philadelphia.
- TOEPLITZ, C. 1920. Bau und Entwicklung des Knorpelschädels von *Didelphis marsupialis*. Zoologica, Stuttgart, 27:1–84.
- TURNBULL, W.D. 1970. Mammalian masticatory apparatus. Fieldiana, Geology, 18:149–356.
- VOSS, R.S., AND S.A. JANSA. 2003. Phylogenetic studies on didelphid marsupials II. Nonmolecular data and new IRBP sequences: separate and combined analyses of didelphine relationships with denser

- taxon sampling. Bulletin of the American Museum of Natural History, 276:1–82.
- 2009. Phylogenetic relationships and classification of didelphid marsupials, an extant radiation of New World metatherian mammals. Bulletin of the American Museum of Natural History, 322:1–177.
- WAGNER, A. 1842. Diagnosen neuer Arten brasilischer Säugthiere. Archiv für Naturgeschichte, 8:356–362.
- WAGNER, J.A. 1847. Beiträge zur Kenntniss der Säugthiere Amerika's.
 Abhandlungen der mathematisch-physikalischen Klasse der Königlich Bayerischen Akademie der Wissenschaften, 5:121–208.
- Wible, J.R. 2003. On the cranial osteology of the short-tailed opossum *Monodelphis brevicaudata* (Didelphidae, Marsupialia). Annals of Carnegie Museum, 72(3):137–202.
- 2008. On the cranial osteology of the Hispaniolan solenodon, *Solenodon paradoxus* Brandt, 1833 (Mammalia, Lipotyphla, Solenodontidae). Annals of Carnegie Museum, 77(3): 321–402.
- 2022. The history and homology of the os paradoxum or dumb-bell-shaped bone of *Ornithorhynchus anatinus* (Mammalia, Monotremata). Vertebrate Zoology, 72:143–158.
- WIBLE, J.R., AND S.L. SHELLEY. 2020. Anatomy of the petrosal and middle ear of the brown rat, *Rattus norvegicus* (Berkenhout, 1769) (Rodentia, Muridae). Annals of Carnegie Museum, 86(1):1–35.
- Wible, J.R., S.L. Shelley, AND C. Belz. 2021. The element of Paaw in marsupials and the middle ear of *Philander opossum* (Linnaeus, 1758) (Didelphimorphia, Didelphidae). Annals of Carnegie Museum, 87(1):1–35.
- WIBLE, J.R., S.L. SHELLEY, AND G.W. ROUGIER. 2018. The mammalian parasphenoid: its occurrence in marsupials. Annals of Carnegie Museum, 85(2):113–164.
- WIBLE, J.R., AND M. SPAULDING. 2013. On the cranial osteology of the African palm civet, *Nandinia binotata* (Gray, 1830) (Mammalia, Carnivora, Feliformia). Annals of Carnegie Museum, 82(1):1–114.
- WILSON, D.E., AND D.M. REEDER. 2005. Mammal Species of the World: A Taxonomic and Geographic Reference, 3rd Edition. Smithsonian Institution Press, Washington, D.C. 2142 pp.